Submitted to Physical Review D

LBL-7198
Preprint

FURTHER MEASUREMENTS AND REASSESSMENT OF THE MAGNETIC-MONOPOLE CANDIDATE

P. B. Price, E. K. Shirk,
W. Z. Osborne, and L. S. Pinsky

March 1978

Prepared for the U. S. Department of Energy
under Contract W-7405-ENG-48

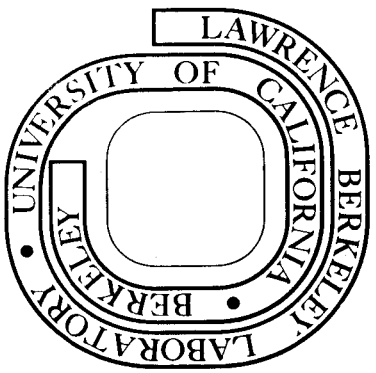

DISCLAIMER

Submitted to Phys. Rev. D

Further Measurements and Reassessment of the Magnetic-Monopole Candidate

P.B. Price
Physics Department and Lawrence Berkeley Laboratory,
Univ. of Calif., Berkeley, CA 94720

and

E.K. Shirk
Physics Department, Univ. of Calif., Berkeley, CA 94720

and

W.Z. Osborne and L.S. Pinsky
Physics Department, Univ. of Houston, Houston, TX 77004

Abstract

Within the stack, consisting of 35 Lexan detectors and of 3 nuclear emulsions, in which the unusual event was found, we have measured tracks of ~200 cosmic ray nuclei with $26 \leq Z \leq 83$, which provide an internal calibration of the response of the detectors. Our measurements in Lexan and in emulsion together show that the unusual particle produced a knockon electron energy distribution incompatible with any known nucleus. The track etch rate and its gradient in Lexan give the quantity $|Z|/\beta$ and, if the particle was a nucleus, a lower limit on its velocity. We found $|Z|/\beta \approx 114$ at each of 66 positions in the Lexan stack extending over a range of ~1.4 g/cm^2. The best fit to the Lexan data alone would be for a hypothetical superheavy element with $Z \approx 108$ to 114 and β such that $Z/\beta \approx 114$. A known nucleus with $90 \leq Z \leq 96$ would also give an acceptable fit to the Lexan data if it fragmented once in the stack

with a loss of about two units of charge, keeping $Z/\beta \approx 114$. A nucleus with $Z < 90$ could maintain $Z/\beta \approx 114$ only by a properly spaced set of fragmentations. A nucleus with β as low as 0.6 could fit the Lexan data only if it fragmented at least 8 times in succession, with a probability $\sim 10^{-17}$. In the 200 μm G-5 emulsion, visual measurements of the track "cores" produced by relatively low-energy electrons ($\lesssim$10 keV) are consistent with the Lexan result that the unusual particle had $|Z|/\beta \approx 114$. However, measurements of the density of silver grains at radial distances greater than ~10 μm show that the particle produced far fewer high-energy ($\gtrsim$50 keV) knockon electrons in each of the three emulsions than would a known nucleus with $Z/\beta = 114$. If it were a known, long-lived nucleus with $Z \leq 96$, and therefore having $0.84 \gtrsim \beta > 0.6$ in order to fit the Lexan data, its signals in the three emulsions imply a very low Z/β of only ~85 instead of 114. The abnormally small production rate of long-range electrons observed in all three emulsions is the essential evidence that we have found a unique particle. A monopole does not provide an acceptable fit to all of the data. A slow particle ($\beta \approx 0.4$) could fit all of the observations, provided its mass were so great ($>10^3$ amu) that it did not slow appreciably in the 1.4 g/cm^2 stack. A fast ($0.7 \lesssim \beta \lesssim 0.9$) antinucleus with $Z/\beta \approx -114$, because of its low Mott cross section for production of high-energy knockon electrons, could fit the data, especially if it fragmented once with loss of one or two units of charge. An ultra-relativistic ($\beta \gtrsim 0.99$) superheavy element with $Z \approx +110$ to $+114$ can also account for the data and is not in conflict with any negative searches. Our knowledge of the Z- and β-dependence of the response of Lexan appears

sufficient to preclude values of $|Z/\beta|$ less than ~110. An explanation of the weak distant energy deposition in terms of fluctuations by a normal nucleus or locally insensitive emulsion regions appears to be unlikely. Freak occurrences such as a 10^{20} eV jet or an upward moving nucleus do not fit the data. Having achieved only an incomplete characterization of a single example of what appears to be a new particle, we emphasize the obvious--that further examples of such particles must be found before its identity can be established.

1. Introduction

In ten years of study of the ultraheavy cosmic rays--those with nuclear charge $Z \gtrsim 70$--one event out of several hundred of these rare particles has stood out as abnormal and quite possibly the first representative of a new class of heavily ionizing particles. In 1975 we mistakenly claimed[1] that the behavior of the particle as it passed through a stack of several types of visual detectors was compatible only with its being a monopole with magnetic charge $g = 137e$ and speed $\beta c \simeq 0.5\ c$.

In the numerous sheets of Lexan in the stack its ionization rate was very high and roughly constant. From experience with previous Lexan detectors we estimated $|Z|/\beta$ to be ~ 137 and $\beta \gtrsim 0.9$ if it were a nuclear particle. However, in a layer of nuclear emulsion it produced an anomalously small number of energetic delta rays such as would be produced by a particle with much lower Z/β. In a fast film supposedly sensitive to Cerenkov light from a heavily ionizing particle with $\beta \gtrsim 0.68$, it produced only a small spot that we interpreted as the ionization from a particle of low velocity, $\beta < 0.68$.

Several errors in the original analysis, together with the publicity and scientific criticisms that followed, have discredited the experiment and obscured the fact that this particle did exhibit a peculiar behavior, outside of any reasonable statistical fluctuations associated with any particle yet seen in the cosmic radiation. We intend here to give a detailed account of the experiment, to show that no previously discovered particle can account for the data, and to show that several hypothetical particles are compatible with the data.

The techniques for particle identification with Lexan detectors are well-known and uncontroversial. They are thoroughly discussed in a monograph[2] but will be reviewed in section 4 for the convenience of the reader. Since the initial report of the monopole candidate[1] we have increased the number of Lexan data points from 58 to 66 for that event and have measured nearly 200 other events with $26 \leq Z \leq 83$ recorded in the same flight, allowing a relation between signal and Z/β to be established for each Lexan sheet. From this internal calibration we find that the average value of $|Z|/\beta$ should be ~114 rather than ~137. Despite this embarrassing change in the value of $|Z|/\beta$, the qualitative claim that our particle was the most penetrating particle with such a high ionization seen to date remains unquestioned.

The techniques of track structure measurement in emulsion developed by one of us (WZO) and used in the initial report[1] had not previously been published, and the interpretation of such measurements depends on the construction of a model of track structure that must be experimentally tested. Criticism[3-6] of the initial paper was directed chiefly at our undocumented claim that the visual measurements of track structure in emulsion, together with a knowledge of Z/β from the Lexan, allowed the particle's velocity to be estimated at $\beta \approx 0.5$ with an absolute upper limit of $\beta = 0.6$. In section 6 of the present paper we take a different point of view that we believe experts on track structure in emulsion will regard as uncontroversial because our conclusion does not depend on the details of the track model used. Instead of claiming that we can measure the particle's velocity, we present several kinds of experimental evidence

(visual measurements of two quantities denoted R_1 and R_2; photographic evidence; and silver grain densities measured with an automated microscopic image dissector) that the energy deposited at large radial distances around the track of the monopole candidate was too low to be compatible with a known, long-lived nucleus with $Z \lesssim 96$, with $Z/\beta \approx 114$, and thus with $0.84 \gtrsim \beta > 0.6$. In the initial paper the 200 μm Ilford G-5 emulsion was examined but the other emulsions were not studied. In the present work the claim of an abnormally low production of high-energy electrons is greatly strengthened by measurements in two independent 10 μm Kodak NTB-3 emulsions as well as in the 200 μm emulsion.

The fast film for recording Cerenkov light emitted by a single heavily ionizing particle is in principle a valuable tool for determining whether the particle's velocity appreciably exceeds the threshold value given by $\beta_{crit} = n^{-1}$. The plastic radiator coupled to our fast film has a refractive index $n = 1.515$, so that $\beta_{crit} = 0.66$. Earlier experiments in which a few heavily ionizing particles were followed through a fast film Cerenkov detector[7,8] into a Lexan stack suggested that particles with $Z \gtrsim 60$ and $\beta \gtrsim 0.68$ would, in that particular film, produce a large region of developed silver grains attributable to the cone of Cerenkov light. Unfortunately, the film prepared by Eastman Kodak for the experiment in which the monopole candidate was found was less sensitive than the earlier film. By etching the plastic radiator above the fast film we have been able to observe, for each particle of interest, an etched track that serves to locate the center of the cluster of developed silver grains. This removes any ambiguity as to the correct spot associated with each event. Despite strenuous

and ongoing efforts to relate the radial distribution of silver grains in these spots to the presence or absence of Cerenkov light, we have not been able to substantiate our earlier claim regarding the speed of the monopole candidate based on the fast film. In the present work we draw only upon measurements made in the Lexan detectors and in the nuclear emulsions.

2. History of the Experiment

In 1969 two of us (WZO and PBP) planned a series of balloon flights in which a stack of Lexan sheets and one or more layers of nuclear emulsion would be used to measure both the charges and velocities of the rare, ultraheavy cosmic rays. An important goal of the experiments was to test the idea of WZO that, over a useful range of velocities, $0.3 \lesssim \beta \lesssim 0.6$, measurements of the radial distribution of silver grains around a track in a single layer of emulsion could be used to estimate both Z and β without the need for Lexan or other detectors.

By the time of our first balloon flight the group included Shirk and Kobetich at Berkeley and Pinsky, Eandi, and Rushing at Houston. Pinsky[8] had built a detector consisting of a layer of plastic radiator coated on both sides with a thin layer of Eastman Kodak's very high speed 2485 film that was to be used to study the possibility of imaging the Cerenkov light emitted by a single heavily ionizing nucleus with $\beta > \beta_{crit}$.

An 18 m^2 array containing a stack of Lexan sheets, a 200 μm emulsion layer, and the fast film Cerenkov detector was launched from Minneapolis on September 4, 1970. Because of failures of the descent mechanisms, it became derelict, but after a 15-day, 5500-mile journey, it landed of its own accord near Regina, Saskatchewan. It spent about

40 h at ~2.8 g/cm^2, ~20 h at ~5.5 g/cm^2, and the remainder of the 15 days at greater depths (largely unknown). The emulsion was dark from the long exposure but usable. About half of the Cerenkov detectors survived the hard landing. All of the emulsion was scanned twice at Houston in a stereomicroscope and visual measurements of the track structure parameters R_1 and R_2 (see Section 6b) were recorded for events thought to be heavier than Fe. The locations, zenith and azimuth angles, and values of R_1 and R_2 were sent to Berkeley, where the various sheets of Lexan were chemically etched in a systematic way to be discussed in section 4. The Z and β determined with the Lexan were taken to be correct, and all events with $Z > 50$ were sought in the fast film Cerenkov detectors. The charge and energy distributions determined with the Lexan detectors have been published.[7] The analysis of the spots containing excess silver grains at the sites traversed by high-Z cosmic rays in the fast film Cerenkov detectors has also been published.[7,8] The measurements of track structure in the emulsions have never been published; they will be discussed in section 6 of the present paper.

In 1973 the present authors constructed a 30 m^2 array shown in Fig. 1, but in three successive launch attempts in spring, 1973, the balloons failed. After a six months' storage in Houston, the array was separated into a 10 m^2 and a 20 m^2 array and successfully launched at Sioux City, Iowa. The 10 m^2 stack was flown for 60 hours at ~3 g/cm^2 beginning September 18, 1973, and the 20 m^2 stack was flown for 60 hours at ~4.5 g/cm^2 beginning September 25, 1973. A shifting mechanism, used to distinguish events at float altitude from events

during ascent, moved the top two Lexan sheets by about 2 cm during the abortive launches in spring, 1973. They were left in a unique shifted position throughout the flights in September, 1973.

The Sioux City array differed in several significant respects from the Minneapolis array. (1) It contained two independent sets of Cerenkov radiator and fast film, each wrapped in light-tight paper. (2) The film, nominally designated as EK-2485, was different from that used in the Minneapolis flight. Eastman Kodak changed the composition so that a more convenient developer could be used, but unfortunately achieved a lower sensitivity than that of the Minneapolis film. (3) In addition to the 200 μm Ilford G-5 emulsion commonly used by cosmic ray experimenters, we included two 10 μm Kodak NTB-3 emulsions on cellulose triacetate backing, each wrapped in light-tight paper. (4) The thickness of light-tight wrapping paper was less for the Sioux City flights than for the Minneapolis flight.

Figure 1 is a more detailed and accurate sketch of the constituents of the stack than was presented in the initial paper.[1] The thickness in g/cm^2 Lexan equivalent, measured normal to the stack, is indicated at several positions in the figure. In the sketch in ref. 1 the thickness of material between Lexan sheet 2 and Lexan sheet 3 was incorrectly labeled. It was taken to be 0.625 g/cm^2 in drawing the figure in ref. 1, whereas it should have been 0.347 g/cm^2. The reader should note that an exploded view of a narrow column through the detector is shown in Fig. 1. The actual stack was ~1 cm thick and 30 m^2 in area.

The 200 μm Ilford emulsion was developed by H.H. Heckman's group at Lawrence Berkeley Laboratory during the period October 16 to

November 2, 1973. The 10 μm Kodak emulsions were developed by the Johnson Spacecraft Center Photographic Technology Division at about the same time. The Lexan was etched in the spring of 1975, after a hiatus of about 18 months during which the Berkeley group analyzed a stack of Lexan exposed on the Skylab orbiting workshop.[9]

Scanners at Houston used stereomicroscopes to locate tracks in the 200 μm emulsion that appeared likely, because of the high density of delta rays, to have been produced by cosmic rays with $Z \gtrsim 40$. A list of these tracks, with their locations, zenith and azimuth angles, and track structure parameters R_1 and R_2, was sent to Berkeley in June, 1975, where the corresponding tracks in the Lexan sheets were to be located and measured. The track of the monopole candidate in the emulsion had not been recognized as unusual. About half of the 68 events later established by Lexan measurements to have $Z \gtrsim 40$ were recorded as having larger halo radii, R_2, than did the monopole candidate. The photomicrographs in Figs. 14 and 15 show that the monopole candidate track had a lower density of high-energy delta rays than did a number of the other events. It was thus completely unexpected when a technician, Walter Wagner, found that the track etch rates in the Lexan sheets indicated that it was an extremely heavy, penetrating particle with apparently no change in ionization rate with depth.

The erroneous identification of this particle as a monopole came about as follows. In the analysis of the Minneapolis flight[7], the Skylab experiment[9], and balloon flights by another group[10], the Lexan stacks had had quite similar responses, with track etch rate v_T going as $\sim(Z/\beta)^{\eta}$, where η was always in the range 3.5 to 4. It was natural,

then, in the preliminary analysis of the Sioux City flight to assume a similar response. Assuming the Sioux City Lexan stack to be identical to the Lexan used on the Skylab, we calculated that the monopole candidate had $Z/\beta \approx 137$ and did not change with depth. Having searched for monopoles in the past, we were well aware of the calculations of Cole and Bauer[11] showing that a monopole of strength g ionizes approximately at a constant rate, independent of β, given by replacing Ze by $g\beta$ in the Bethe-Bloch equation. With Dirac's quantization condition, $ge = n\hbar c/2$, one then expects the ionization rate of a fast monopole to look like that of a minimum ionizing nucleus with $Z = 137n/2$ and $\beta \approx 1$. The association of our particle with a monopole of strength $n = 2$ was obvious. From its weak signal in emulsion and an unpublished track structure model of Osborne, we inferred a low velocity, $\beta \approx 0.5$. Kinematics limits the maximum energy of delta rays to $w_{max} = 2m_e c^2\beta^2\gamma^2$, which for $\beta \approx 0.5$ could, according to the model, account for the small value of the radius R_2 over which delta rays could be seen but would not affect the Lexan signal, which is produced dominantly by very low-energy electrons.

The remarkable coincidence of our estimate of the value of Z/β with the number 137 expected for a monopole, and our belief that the difference between this number and the charge of the heaviest nucleus previously seen in the cosmic rays, $Z = 96$, was far greater than estimated experimental errors, prompted us to publish the Letter[1] before doing the detailed calibrations of the Lexan, emulsion, and Cerenkov detector.

We soon communicated to many colleagues the results of our calibration of the Lexan, showing that Z/β was considerably lower than

137; independently several papers appeared, pointing out that a very heavy nucleus could, by one or more properly spaced fragmentations, maintain a roughly constant ionization rate and account for the observations, provided the emulsion evidence was disregarded.[3-6] The critics were correct. Fragmenting nuclei can fit the Lexan etch rate data, and the event is unique only if evidence for its anomalous nature can be substantiated in the emulsions or Cerenkov film.

Though it is not our purpose here to present a complete case history, we should explain why we did not retract our claim as soon as the Lexan calibration showed that Z/β was only ~114 instead of 137. The reason is that S.P. Ahlen pointed out[12] that the simple, first-order prescription, "Replace Ze by $g\beta$ in the Bethe-Bloch equation," eliminates the β^{-2} factor but retains the logarithmic velocity-dependence, which means that slow monopoles ionize less heavily than fast monopoles. The logarithmic contribution seems to have been overlooked until recently. Ahlen's detailed calculation, including the relativistic density effect, confirms the qualitative correctness of the simple prescription. For one specific model of track formation in a plastic detector--the restricted energy loss model[2]--Ahlen[12] showed that the slower the monopole, the lower the apparent Z of an electrically charged, minimum-ionizing particle with an equivalent signal. His calculations suggested that a slow monopole, if sufficiently massive to traverse the entire stack without significant decrease of velocity, might simulate a fast, electrically charged particle with $Z/\beta \approx 114$. Thus, our view in late 1975 was that the particle was still compatible with a monopole if its velocity was indeed as low as we inferred from its weak signal in

emulsion.[13] In section 4(a), however, we will see that the restricted energy loss model does not give a good fit to available data for charged particles, and in sections 7(b) and 8(a) we will conclude that a slow monopole is not a viable explanation of the event.

In 1976 two new developments made it clear that we could no longer claim that only a monopole could account for both the strong signal in Lexan and the weak signal in emulsion. First, R. Hagstrom, who had independently associated himself with the analysis of the emulsion data and was developing a quantitative model of track structure in emulsion, recognized that a heavy antinucleus, with $|Z| \gtrsim 80$ and $Z/\beta \approx -114$, could fit both the Lexan and the emulsion data better than could its charge conjugate. Hagstrom realized that the abnormally low energy deposition at large radial distances could result from the smaller Mott cross section for scattering of electrons by a negative nucleus than by a positive nucleus. His explanation[14] of the event remains a viable one. Second, given $|Z|/\beta \approx 114$ and the behavior of the Mott cross section, we recognized that an extremely relativistic ($\beta \gtrsim 0.99$) superheavy nucleus, $Z \approx 110$ to 114, might fit both sets of data. Our view since mid-1976 has been that the data are incompatible with a known, positive nucleus but that a monopole is not a good explanation.

3. Known Heavily Ionizing Particles in the Cosmic Rays

The flux of ultraheavy cosmic rays is so low, $\lesssim 1\ m^{-2}\ day^{-1}$, that they have so far been detected in the present-day cosmic radiation only with large arrays of plastic detectors and emulsions. Figure 2 shows the charge distribution of ultraheavy cosmic rays found in two

recent experiments[9,10] using Lexan detectors. Both distributions are roughly consistent with the histogram labeled "r-process abundances," which is the result of a typical calculation of the charge distribution expected if ultraheavy cosmic rays are accelerated from material synthesized by rapid neutron capture, then propagated through an exponential distribution of pathlengths of interstellar gas (with characteristic length $\bar{\lambda} = 5$ g/cm^2) during a time of $\sim 10^7$ years. The main points to note are the so-called "platinum peak" at Z = 76 to 78; the so-called "actinide gap" at Z = 84 to 89; the presence of a few long-lived actinides Z = 90 to 96; and the absence of any events with Z > 100. The resolution in these experiments was usually $\Delta Z \approx \pm 2$. Other experiments, including our Minneapolis flight[7], have given similar results but with poorer statistics. One can see from this distribution why a particle with apparent $Z/\beta \approx 137$ and apparent $\beta \gtrsim 0.9$ would cause a stir. One can also see that a monopole with n = 1, which if relativistic would look like a minimum-ionizing nucleus with Z = 137/2, would be hard to find because of the relatively large background of cosmic rays with $Z \sim 65$ to 70.

We will have occasion later to refer to the "iron-peak." Because of its large binding energy per nucleon, there is a very pronounced abundance peak at Z = 26 which has been thoroughly studied with various cosmic ray detectors. It is very convenient as an internal calibration to use this abundance peak in establishing the response of both Lexan and emulsion. Between Z = 26 and 32 the abundances of cosmic rays decrease by several orders of magnitude and thereafter decline erratically and less rapidly. The abundance ratio of elements with

$Z \gtrsim 65$ to iron is $\sim 10^{-5}$ (ref. 9).

It is useful to list here the area-time factor accumulated in all the ultraheavy cosmic ray experiments. Particles with magnetic rigidity greater than 14.7 GV can penetrate the earth's field at any latitude. The area-time factor for such particles was 1.67 m^2y exclusive of the Sioux City flights and increases to 1.88 m^2y when the Sioux City flights are included. For particles with magnetic rigidity such that they just penetrate the earth's field (and possibly overlying air) at the latitude of South Dakota or Minnesota where many balloon exposures are made, the area-time factor was 0.56 m^2y exclusive of the Sioux City experiment and increases to 0.77 m^2y when the Sioux City experiment is included. It is also useful to list the effective area-time factor, which contains the additional factor $\exp(-x/\lambda)$, where λ is the interaction length of the particle sought and x is the average thickness of overlying material. In a search for a superheavy nucleus, which would have a rather short interaction length, the effective area-time factors are ~ 1.2 m^2y for high-rigidity nuclei and ~ 0.36 m^2y for low-rigidity nuclei when all experiments are considered.

4. Analysis of the Lexan Detectors

For the benefit of the reader who is not interested in the details, we state the results of the analysis of the Lexan data here:

Assuming that the particle was a known or hypothetical nucleus with charge to mass ratio given by the beta-stability line, the best fit to the Lexan data is for $\beta \gtrsim 0.95$, $Z \gtrsim 108$, and average $Z/\beta \approx 114$; a good fit is also obtained for $\beta \approx 0.8$ to 0.84, corresponding to $Z = 92$ to 96, provided it fragments once with loss of one or two units

of charge; with lower β more fragmentations are required to give an acceptable fit; for β as low as 0.6 the number of fragmentations required becomes at least 8, with an overall probability of $\sim 10^{-17}$. The critics[3-6] of the original paper[1] accepted the fact that the Lexan data excluded any nucleus with β lower than ~0.6 to 0.65. Later we will see that this completely non-controversial result is all that is required of the Lexan data to show that the emulsion data are incompatible with any known nucleus.

a. Response of Lexan to heavily ionizing particles

When a heavily ionizing particle passes through Lexan or some other nuclear track-recording solid[2], it can produce a latent, microscopic track of chemically reactive material a few tens of Angstroms in diameter that can be enlarged to visible size by using a chemical reagent that preferentially attacks the reactive material. The shape of the etch pit is conical, with cone half-angle equal to arcsin V_G/V, where V_G is the general rate of etching of unirradiated material and V is the rate of etching along the particle trajectory. If the particle passes through a Lexan sheet an etch pit may be produced at both surfaces.

Etching at a rate greater than V_G occurs only where the energy deposited per unit volume exceeds some very high value. The radius of the region of enhanced etching has been determined[2] directly by electron microscopy and indirectly by electrolytic conductance measurements to be $\lesssim 10^{-6}$ cm. The track etch rate V is an increasing function of the energy density in this narrow region, and particle identification relies upon measuring V and determining how V depends

upon Z and β of the particle.

Track-etch detectors such as Lexan are quite different from other detectors in that they are completely insensitive to energy deposited at distances larger than $\sim 10^{-6}$ cm. This has two important consequences, which can be easily understood by recalling that the cross section for knockon electron production falls off rapidly with energy (e.g., as E^{-2} for close collisions): (1) The resolution is immune to fluctuations in the small number of high-energy knockon electrons, which deposit almost all of their energy outside of this region. (2) The etch rate, V, is related to the production rate of the very numerous electrons of very low energy ($\lesssim 1$ keV) resulting from collisions at large impact parameters ($\gtrsim 10^{-9}$ cm). These electrons have a small CM scattering angle, a small momentum transfer, and a scattering cross section given, in the approximation that they are unbound, by the simple Rutherford formula, which is exactly proportional to Z^2. Thus V will be a function of Z^2, independent of the sign of the charge. For these collisions at large impact parameter, an incompletely stripped nucleus would interact as if it had an effective charge, Z*, less than its nuclear charge. In all experiments to date the following expression[15], based on measurements at energies below ~10 MeV/amu, has been assumed to hold up to relativistic energies:

$$Z^* = Z[1 - \exp(-130\beta/Z^{2/3})] \qquad (1)$$

For $\beta \gtrsim 0.6$ this expression predicts $Z - Z^* \lesssim 2$. Fowler et al.[16] have shown that theoretical cross sections for radiative and non-radiative electron attachment and stripping lead to a qualitatively similar conclusion.

The dependence of the energy density deposited at very small radial distances on the velocity of the incoming particle is complicated. One must take into account the energy deposited both by the primary excitation and by the secondary excitation from knockon electrons.[17] No theoretical expression for the dependence of etch rate on Z and β has been derived. Instead, one assumes that etch rate is a function of the appropriate expression for energy density at small radial distances. A power law relating etch rate to energy density at small radial distances gives an excellent fit to data covering a wide range of etch rates. Several expressions for energy density at small radial distances have been used: (1) Benton[18] and others[19] have assumed that the energy density at small radial distances can be approximated by the restricted energy loss, defined as the energy lost in collisions leading to electrons with kinetic energy less than w_o, where w_o is taken empirically to give the best fit to the data. From studies of ions with $Z \leq 26$ and $\beta \lesssim 0.2$, Benton and co-workers chose $w_o \approx 350$ eV. The restricted energy loss is given by

$$(dE/dx)_{w_o} = (2\pi N_e e^4 Z^{*2}/mc^2\beta^2)[\ell n(w_{max} w_o / I_{adj}^2) - \beta^2 - \delta(\beta)] \qquad (2)$$

where N_e = number of electrons/cm^3 in the detector, $w_{max} = 2m_e c^2\beta^2\gamma^2$ is the maximum electron kinetic energy set by kinematics, I_{adj} is an adjusted mean ionization potential of the detector, and $\delta(\beta)$ is a parameter that takes into account the reduction in ionization rate due to the polarization of the medium at relativistic velocity. This parameter is zero for $\beta \lesssim 0.8$ but represents a significant correction term at greater velocity, nullifying most of the relativistic rise due

to the logarithmic term. In what follows we use the expressions of Sternheimer[20] for $\delta(\beta)$ in a plastic.

$$\delta = \begin{cases} 0 & \text{for } x < 0.14 \\ \ell n(\beta^2\gamma^2) - 3.21 + 0.456(2.0-x)^{2.78} & \text{for } 0.14 \lesssim x \lesssim 2 \\ \ell n(\beta^2\gamma^2) - 3.21 & \text{for } x > 2 \end{cases} \qquad (3)$$

where $x = 0.5 \log_{10} e \ell n(\beta^2\gamma^2)$.

To our knowledge, eq. 2 has been used only for $Z \lesssim 26$ and $\beta \lesssim 0.2$, and no attempt has been made by those who use it to determine whether the data can be fit better with some other expression.

(2) Price and co-workers,[21-24] in some of their early studies of cosmic rays with Z up to ~96 and β up to ~1, rejected the restricted energy loss model as severely underestimating the charges of ultraheavy nuclei at high velocities, and chose a semi-empirical expression of the form

$$J(K) \propto (Z^{*2}/\beta^2)[\ell n(\beta^2\gamma^2) + K - \beta^2 - \delta(\beta)] \qquad (4)$$

where K is a parameter chosen to give the best fit to both accelerator data and to abundance peaks in the cosmic rays at Fe(Z = 26) and at the r-process peak at Z = 76 to 78. In the case of Lexan, for which w_o = 350 eV and I_{adj} = 69.5 eV, the terms in square brackets in eqs. 2 and 4 would become equal if K were chosen to be 11.2, so that the two expressions would then have the same dependence on Z and β. To fit data at high Z and β, it was found necessary to assign a much larger value to K. In their analysis of Ne, Si, Ar, and Ti ions from the Berkeley Hilac and six ultraheavy cosmic rays detected in a

10.2 g/cm^2 stack consisting of 120 Lexan sheets, 9 layers of Ilford G-5 emulsion, and 56 layers of steel absorbers, flown at Sioux Falls, South Dakota, O'Sullivan et al.[21,22] found that eq. 4 with $K \approx 62$ gave the best fit to the data.

(3) In the most recent cosmic ray experiments Shirk et al.[7,9] and Fowler et al.[10] found that the best value of K was sufficiently high as to make the logarithmic dependence negligibly small, and they used the simple expression

$$J(K = \infty) \propto (Z^{*2}/\beta^2). \tag{5}$$

Table 1 summarizes the data used to choose among the three models for energy density at small radial distances, eqs. 2,4, and 5. The method is to compare, in the same Lexan stack, the track etch rates for nuclei of the well-defined Fe peak with etch rates for "standard" nuclei, whose identities have been independently established. The first group of standard particles, from the Berkeley Hilac, had precisely known values of Z and β. The second group had their charges determined, with a fractional standard deviation of ~4%, by photodensitometric measurements of their tracks in nine layers of Ilford G-5 emulsion.[21] The use of emulsion to identify ultraheavy cosmic rays, and the model of track formation in emulsion, are discussed in ref. 16. One of these particles was particularly valuable as a test of the three models because it penetrated the 10.2 g/cm^2 stack of emulsions, Lexan, and steel with no perceptible increase in ionization rate[22], and its velocity was determined to be $\beta > 0.97$ (95% confidence), a value sufficiently high to lead to significantly different charges

predicted by the three models. The third group consisted of 57 events with $70 \leq Z \leq 96$ and $\beta > 0.9$ detected in a Lexan stack[9] flown on Skylab; the fourth group consisted of 58 events with $70 \leq Z \leq 96$ and $\beta > 0.88$ detected in Lexan stacks[10] flown in several balloon flights. Both groups show a strong abundance peak close to the expected position of the "platinum peak" at Z = 76 to 78, a weaker peak attributed to U and Th, and an absence of events at the expected position of the "actinide gap." The evidence from these two groups of data, though dependent upon astrophysical arguments (elucidated in more detail in ref. 9), is valuable because it tests the three models at high β.

For each standard particle, of given Z and β, we find the velocity, and thus Z^*/β, for the Fe nucleus that gives the same etch rate as does the standard particle. Data for the standard particles are given in columns 1 to 4; data for the Fe nuclei are given in columns 5 and 6. We then use eqs. 2,4, and 5, together with the velocities of the Fe and of the standard particle and Z^*/β of the Fe, to calculate Z of the standard particle as predicted by each of the three models. The results are given in columns 7 to 9. Clearly the restricted energy loss model is inferior to the other two models, the discrepancy between the calculated Z and the "known" Z increasing as $|Z - 26|$ increases. At low Z, the calculated charge is too high, by 10% at Z = 10. At high Z the calculated charge is too low; for $Z \approx 76$ to 92 the error is about 10 charges. The information in Table 1 does not permit a choice to be made between the Z^{*2}/β^2 model and the model of eq. 4, with $K \approx 62$. For simplicity, in recent balloon experiments and in this paper, the following expression is assumed to provide a satisfactory

fit to data for $Z \gtrsim 10$ and $0.1 \leq \beta \leq 1.0$,

$$V(\beta,Z) = (Z^*/\zeta\beta)^{\eta} \qquad (6)$$

where the free parameters ζ and η characterize the batch of Lexan and the etching treatment. This equation has been observed to hold over a range of $\sim 10^3$ in V for ultraheavy cosmic rays.[21]

Clearly it would be desirable to test the models of track formation in Lexan with particles of precisely known Z and β extending up to $Z = 92$ and $\beta \gtrsim 0.99$, instead of having to depend upon astrophysical arguments and upon charge identification in Lexan. In about 1980 it is expected that the Lawrence Berkeley Laboratory Bevalac will produce beams of nuclei with $\beta \approx 0.92$ and $Z \gtrsim 82$, which will provide a more direct test. We believe the case against a restricted energy loss model, summarized in Table 1, is quite strong. There is no known way by which the cosmic rays could show an abundance peak at $Z \approx 67$. The abundance patterns of both the cosmic rays and the elements that make up our solar system reflect their thermonuclear origin. Essentially all the elements beyond the Fe peak are made by either slow or rapid neutron-capture. The s-process leads to peaks at $Z = 56$ and 82; the r-process leads to peaks at $Z = 52$ and 76-78. The two sets of peaks at 52-56 and at 76-82 correspond to nuclides with closed neutron shells, $N = 82$ and 126. The rare earths, including $Z = 67$, form an abundance valley between these sets of peaks.

A final argument for the absence of a significant logarithmic rise in track etch rate is that in all velocity intervals studied, from $0 < \beta < 0.6$ to $0.9 < \beta < 1.0$, not only the position of the

r-process peak but also the end point of the charge spectrum, at $Z \approx 96$, are correctly located when eq. 4 or 5 is used for the close energy deposition.

We will return to this discussion in section 8, when we consider whether the monopole candidate could have been a normal nucleus with $\beta \approx 1$ that was misidentified in Lexan because the wrong β-dependence was used in eq. 6. Then we will discuss the last two rows of Table 1.

b. Processing and calibration of Lexan from the Sioux City flights

The 30 m^2 Lexan stack consisted of 296 modules each 30.5 cm x 30.5 cm. The problem faced in processing a stack containing many tracks of particles with a wide range of ionization rates is to try to optimize the etching times of different portions of the stack so that each pair of etch pits associated with a track segment in a sheet is long enough for a measurement of its length with small fractional error to be made but not so long that the pits touch and form a cylindrical hole. We did the processing in three stages: (1) We etched layers 5 and 12 (see Fig. 1) for each module for a very long time (160 hours in the standard solution to be described below) so that etch pits at locations corresponding to the ultraheavy cosmic ray events previously located in the emulsion could easily be seen in a stereomicroscope. (2) We set aside the thin Lexan sheets 1 and 3, and from the remaining sheets in the stack we cut out 5 cm x 5 cm portions of Lexan centered on the trajectories of the particles located in sheets 5 and 12. For each event we etched the 5 cm x 5 cm portion from every fourth sheet for a time that we estimated would give long but not touching etch pits, judging from the appearance of

the pits in sheets 5 and 12. We measured the etch pit lengths in these sheets and constructed curves of track etch rate V as a function of range R for each particle, from which refined etch times for the remaining three-fourths of the stack could be determined. (3) We etched the remaining 5 cm x 5 cm portions for optimized times and used the (V,R) data to calculate Z and β of the particles. In practice the etching times were limited to the values 1, 2, 4, 6, 10, 15, 20, 30, 48, 60, 80, and 160 hours.

As in the past, the etching was done under highly reproducible conditions in polyethylene tanks containing 6.25 normal sodium hydroxide solution titrated by the supplier and specified free of sodium carbonate. To this was added 0.1% Dowfax surfactant. The tank was covered tightly to minimize evaporation, stirred, and held at $40.00 \pm 0.01^\circ$ C. The dissolved products of Lexan are themselves a surfactant; to standardize the etching conditions[25], blank Lexan sheets were etched in a fresh solution until a whitish precipitate first appeared. This solution was then used to etch Lexan sheets from the actual flight. The same solution was used until the concentration of etch products reached ~1 g/liter; then a fresh solution was prepared. If a solution is used for too long, the general surface etch rate of the Lexan, as well as V, may increase.[25] To reduce the danger of possible systematic differences between calibration samples and samples containing events of interest, as many sheets as possible were etched at the same time in the same etching solution.

About 600 events were recorded by scanners at Houston as possibly having $Z \gtrsim 40$. Of these, about 70% were found from observations in

Lexan to have $Z \approx 26$. These all had small zenith angles. Nearly vertical tracks in emulsion look darker than shallow tracks and tend to have their charge overestimated in scanning. Of the remaining events, some passed out of the edge of a module at some point along their trajectory; some could not be found in sheets 5 and 12 because they came to rest before reaching sheet 5 (as was confirmed by etching sheets 1 or 4); and some could not be found because they penetrated the entire stack at Z^*/β too small to produce a visible etch pit. Because surface is etched away at a finite rate, $V_G \approx 0.16$ μm/h, the normal component V secθ must exceed V_G in order for an etch pit to be formed (θ is the zenith angle). For a vertically incident particle, in principle, the minimum detectable Z^*/β was ~65 for the Sioux City Lexan; for a particle at $\theta = 60°$ the minimum detectable Z^*/β was ~74.

Sixty-seven events with $Z \gtrsim 40$ and the monopole candidate were studied in detail and will be described in this paper.

Figure 3 shows smoothed curves of etch rate as a function of distance along the trajectory in the main Lexan stack comprising sheets 4 to 35. Measurement techniques have been thoroughly discussed elsewhere.[2,9] Several events with initial etch rates greater than 6 μm/h, corresponding to slow, very heavy nuclei, were studied; they are off-scale above the top of this graph. Because etch rate is an increasing function of ionization rate, the curves in Fig. 3 are somewhat like Bragg curves. The data for the monopole candidate occur at an approximately constant etch rate of ~2.9 μm/h, far above the other horizontal lines between ~0.3 and ~0.8 μm/h that correspond to minimum-ionizing nuclei with Z up to ~83 that were detected on the flights.

Only particles with steeply rising etch rate curves, corresponding to slowing nuclei of lower velocity, reached etch rates as high as 2.9 μm/h. In none of the experiments prior to the Sioux City flights had events been seen with constant etch rates greater than 1 μm/h. To the experienced observer, the curve for the monopole candidate would excite considerable interest.

Module 104 contained the monopole candidate event. Within 10 cm of its trajectory were one event with $Z = 35$ and $\sim 10^2$ tracks of nuclei with $Z \approx 26$ that were used to calibrate the response of the individual sheets in that module. It was obvious from the appearance of the pits at the monopole candidate track in sheets 5 and 12 that V was very high, so the 5 cm x 5 cm portions of every fourth sheet were etched for only 20 hours. Measurements of etch pits in these portions are labeled as triangles in Fig. 4. We will discuss the determination of errors later. Most of the remaining three-quarters of the cut portions for the monopole candidate were etched for 30 hours in a fresh tank (along with cut portions for other events and larger portions of module 104 in which Fe calibration tracks were to be measured). The data for the 30 hour etch are shown as solid points in Fig. 4. Recognizing that we had found a unique particle, we stored the cut portions of sheets 1, 3, 4 and 35 in the event that a better processing scheme might be developed at a future date. After the criticisms of the monopole paper were made public, it was decided to etch these four sheets. In a fresh solution sheets 1 and 3 (thickness 75 μm) were etched eight hours and sheets 4 and 35 (thickness 250 μm, same as for sheets 2 and 5 to 34) were etched 30 hours. Etch rates for these

sheets are shown as open circles in Fig. 4.

Results of the calibration of the stack are shown in Figs. 5, 6 and 7. Etch pits corresponding to (V,R) points to the right of the scanning cutoff line in Fig. 5 were located in module 104 with a stereomicroscope and measurements of (V,R) were made with a Leitz Ortholux microscope.[2,9] (The identification of the line in Fig. 5 with the position of Fe has recently been verified in a combination electronic + Lexan experiment in which a portion of this same batch of Lexan was used together with electronic detectors to resolve Fe isotopes in cosmic rays.[80]) The data for the 30 hour etch are shown in Fig. 5 in a form simplified for legibility. The actual data for each event with $Z \approx 26$ consist of ~6 to 12 values of (V,R) lying along an approximately straight line of well-defined slope on the log-log plot. No attempt was made in Fig. 5 to identify each event with a separate symbol; closely spaced points were replaced by symbols indicating the number of points in that small area. The line labeled "Curve adopted for Fe" follows the maximum in the distribution and has a slope accurately determined by the alignment of data points for individual events. The precipitous decline in population of points to the right of the line reflects the drop in abundance for $Z > 26$. The decline to the left of the line is less spectacular because of the presence of some elements with $Z < 26$. From the position of the Fe line and use of the range-energy tables of Henke and Benton[26], we determined the constants ζ and η in eq. 6. The result of the calibration for the 30 hour etch is

$$V = (Z^*/92.3\beta)^{5.07} \ \mu m/h \qquad (7)$$

where the (coupled) standard deviations in ζ and η are 1.00 and 0.15, respectively. Data for events with $Z \gtrsim 40$ that came to rest in the

stack, shown in Fig. 6, extended to very high etch rate and provided support for the value $\eta = 5.07 \pm 0.15$ obtained with the Fe data. Note that this value for η is much higher than found for previous batches of Lexan. The batch used on the Sioux City flights differed from previous batches in that it did not have the trace of stabilizer normally added by the manufacturer to retard degradation by ultraviolet light.

Inserting the value 2.86 ± 0.10 μm/h for the average etch rate for the monopole candidate, based on both the 20 hour etch and the 30 hour etch, gives an average value of $Z^*/\beta = 113.6 \pm 0.8$. Taking into account errors in ζ and η increases the error in average Z^*/β to ± 1.5 charges. In the remainder of this paper, for convenience we will usually use the rounded average value

$$Z^*/\beta = 114$$

This determination of Z^*/β does not depend on the assumption of a power law dependence of V on the energy deposition at small radial distances, because we are not extrapolating out of the range of etch rates measured for slowing Fe nuclei. It does, however, depend on our having chosen eq. 5 instead of eq. 2 or 4 for the energy deposition at small radial distances. If we had used eq. 4, with $K = 62$, the value of Z^*/β for the monopole candidate would depend slightly on its velocity through the terms in square brackets in eq. 4. The discrepancy with the result from eq. 5 is greatest for the highest velocity. For $\beta = 1$, the value of Z^*/β drops from 114 to 109.3. If we had used the restricted energy loss model, eq. 2, at $\beta = 1$ the value of Z^*/β would drop to 90. From the evidence summarized in Table 1, we rejected eq. 2 but accepted either eq. 4 or eq. 5 as an adequate representation

of the charge and velocity dependence of track formation in Lexan. Thus, we accept values of Z^*/β from ~109 to ~114, depending on the particle's velocity.

To determine whether the data from the 20 hour etch and from the 30 hour etch of the cut portions for the monopole candidate could be treated as statistically equivalent, we made an intercomparison of Fe data, shown in Fig. 7. We traced five Fe events through cut portions etched 20 and 30 hours. These all passed within ~2 cm of the monopole candidate. The line is the fit for eq. 7 which was derived for 30-hour data. The constant ζ in eq. 6 was varied so as to minimize the square error for the 20-hour data alone. The best value for the 20-hour data agrees to within 2.5% with that for the 30-hour data. Thus, from Fe track measurements there appears to be no significant difference in the etching treatment or sensitivity of the sheets etched for 20 and for 30 hours. For the monopole candidate the average etch rate for the 20-hour data is 2.88 ± 0.08 μm/h and for the 30-hour data is 2.86 ± 0.11 μm/h, where the errors refer to individual etch rate measurements.

The analysis of the 67 events with $Z \gtrsim 40$ involved use of data in the form of etch rate V_i vs depth X_i in the stack and the Henke-Benton range-energy tables. For particles that stopped in the stack, the range R_i is of course directly known at each point. The statistic S used in the analysis of these particles is given by

$$S(Z) = \sum_{i=1}^{N} [V_i/V\{\beta(R_i,Z,A),Z\} - 1]^2 \qquad (8)$$

where $V(\beta,Z)$ is defined by eq. 7, $\beta(R,Z,A)$ is obtained by numerically

inverting the range-energy relations that give $R(\beta,Z,A)$, and the mass number A is taken to be given by the empirical relation for the beta-stability line, $A = 2Z + 0.015\ Z^{1.8}$.

For events that penetrated the stack completely the residual energy E' at exit becomes an additional free parameter, and we use the statistic

$$S(E',Z) = \sum_{i=1}^{N} [V_i/V\{\beta(X_i + R',Z,A),Z\} - 1]^2 \qquad (9)$$

where $R' = R(E',Z,A,)$.

The best estimate of Z is obtained by locating the minimum S_{min}. We obtain 68% confidence interval limits by evaluating

$$S_{lim} = S_{min}\ [1 + p(n-p)^{-1}\ F(p,n - p,\ 0.317)] \qquad (10)$$

where p is the number of free parameters and n is the number of data points.[27] The distribution F(p, n-p), well-known for its application in the F-test, is used because there is no independent method of assigning the error to each measurement of etch rate. Sources of errors will be discussed in subsection (d).

The etch rate data for the 67 events with $Z \geq 40$, several of which are shown in Fig. 8, were used to search for systematic variations in sensitivity of different Lexan sheets. For the "interior" sheets 5 through 34 no systematic variations were found. An occasional high or low etch rate in one sheet was uncorrelated with high or low etch rates in other sheets. The etch rates V_i for the top etch pit in sheet 4 and for the bottom etch pit in sheet 35 were systematically higher than the calculated rates $V\{\beta(X_i + R',Z,A),Z\}$ based on the

data in all the sheets. Examples of these deviations can be seen in Fig. 8. The etch rates for both the top and bottom etch pits in sheet 2 were systematically slightly lower than the calculated rates. For sheets 1 and 3 there was no obvious trend, but the scatter of points was larger than for the data in sheets 5 through 34. This is not surprising, because the sheets are quite thin (75 μm), so that fractional errors in etch rate are large. Further, these 75 μm sheets were manufactured in a different batch from the 250 μm sheets and might be expected to have a different response.

We believe that the conservative approach, in examining the evidence that we have found a unique particle, is to disregard the data from these five sheets. Actually, the conclusions we will draw are not significantly affected by whether we include those data or not, because their error bars will be quite large.

For the interested reader, we summarize the results of the calibration of sheets 1 to 4 and 35 here. Least squares lines through correlation plots of measured versus calculated etch rates for the 67 events led to the following correction factors to apply to etch rates in order to make eq. 7 valid:

Sheet 1: $V_{corr} = (0.92 \pm 0.15)\ V_{meas}$ (11)

Sheet 2: $V_{corr} = (1.06 \pm 0.07)\ V_{meas}$ (12)

Sheet 3: $V_{corr} = (0.96 \pm 0.15)\ V_{meas}$ (13)

Top of sheet 4: $V_{corr} = (0.90 \pm 0.12)\ V_{meas}$ (14)

Bottom of sheet 4: $V_{corr} = (0.96 \pm 0.05)\ V_{meas}$ (15)

Top of sheet 35: $V_{corr} = (0.99 \pm 0.03)\ V_{meas}$ (16)

Bottom of sheet 35: $V_{corr} = (0.95 \pm 0.09)\ V_{meas}$ (17)

An adequate theory of errors in the track-etch process does not exist (see subsection d). The error bars in Fig. 4 were arrived at in the following way. Restricting ourselves to the 28 sheets that needed no correction, we assumed that the deviations of the 56 data points from the true curve were normally distributed. As a working hypothesis we assumed the true curve to be the least squares straight line through these 56 points,

$$V(\mu m/h) = (2.81 \pm 0.0479) + (0.0674 \pm 0.0510)Y \qquad (18)$$

with Y = position in g/cm^2 Lexan equivalent, measured from the top of sheet 1. Requiring that the reduced chi-square $\chi_\nu^2 \equiv 1$ gave a standard deviation for a single point, $\sigma = 0.0972$ μm/h. We determined the σ's for sheets 1, 2, 3, 4, and 35 by adding in quadrature this σ to the appropriate values derived from the errors in eqs. 11 to 17.

c. Fragmentation within the Lexan stack

The published interpretations[3-6] of the monopole candidate as a normal nucleus with $Z \lesssim 96$ required at least one fragmentation, and we now discuss that possibility. It has been assumed since the earliest studies of heavy nuclei in the cosmic rays and has recently been established in Bevalac experiments[28] that, in fragmentation of a fast-moving heavy nucleus with loss of only a few nucleons, the speed and direction of the residual nucleus remain almost unchanged. In the frame of the moving nucleus the parallel components of momentum have a most probable value $\sim -10^2$ MeV/c and both the perpendicular and parallel components have a Gaussian distribution with $\sigma \approx 10^2$ MeV/c.

When a heavy nucleus fragments in a Lexan stack the residual

nucleus often is heavy enough to leave a detectable track and the etch rate data show a discontinuity at the point where fragmentation occurred. To date, only the residual nucleus has been detected in Lexan, the light fragments having too low an ionization rate to be recorded.

Figure 8(a) contains an example of a fragmentation with $\Delta Z = 3$. In the case of a slowing particle with a detectable etch rate gradient, the gradient decreases after the interaction because the residual nucleus, being lighter, has a greater range than the initial nucleus even though its velocity is the same. Thus the portion of the etch rate curve after fragmentation does not exactly map onto an extension of the etch rate curve before fragmentation by a simple upward translation but has a smaller slope as well as magnitude. In practice the decrease in slope may be too small to detect.

Fluctuations in etch rate are sufficiently small that one can usually be certain of detecting fragmentations with $\Delta Z \gtrsim 3$ unless they occur in one of the top two or bottom two sheets of a stack. Fragmentations with $\Delta Z = 1$ or 2 are difficult to distinguish from a series of correlated deviations in etch rate, some of which are not obviously indicative of fragmentation. Figure 8(b) shows examples of such correlated deviations.

Of the 67 particles with $Z \gtrsim 40$, four definite fragmentations with $Z \gtrsim 3$ were observed to occur between sheets 4 and 28. The total pathlength traversed was 25.3 cm and the changes in charge were 3 (shown in Fig. 8a), >8, >16, and 34 (shown in Fig. 8b). From the Skylab experiment[9], in a total pathlength of 68 cm eight interactions

were observed having ΔZ = 3, 3, 4, 5, 10, 17, >16, and 17. Because of the scanning criterion requiring a coincidence between etch pits in widely separated sheets, the number observed on Skylab is probably an underestimate. Nevertheless, in both cases the frequency of detectable fragmentations, ~0.12 to ~0.16 per cm, is quite consistent with the probability of an interaction with $\Delta Z \gtrsim 3$ of nuclei with $40 \leq Z \leq 92$ in Lexan, estimated from the geometric cross section.

At a depth of ~1.1 g/cm^2 in the stack, the data in Fig. 4 show a glitch that has been commented on by critics and cited by one[4] as evidence of an "obvious fragmentation." The magnitude of the discontinuity corresponds to $\Delta Z \leq 2$, which we have said is insufficient proof of a nuclear fragmentation. The slope after the glitch is not smaller, as it should be if the glitch signified a fragmentation, but larger than before the glitch. It may be an example, like those in Fig. 8(b) and (d), of correlated fluctuations of unknown origin, possibly even statistical. If the four low data points immediately following the glitch are removed, one would not notice a glitch; these four points come from cones in only two sheets. The last four points (in sheets 34 and 35) actually lie well below the curve for a fragmenting nucleus, as will be seen in Fig. 9. Our view, and that expressed by other nuclear track experts, is that "the scatter in the data is such that an interaction is by no means demonstrated, but it is certainly not ruled out" (quoted from ref. 6).

d. Large fluctuations in effective charge?

It is necessary to consider whether the monopole candidate can be explained in terms of a chance occurrence whereby a slow, heavy

ion attaches a sufficient number of electrons at the appropriate spatial locations to mimic a more rapidly moving, heavier ion. In principle, an advantage of this atomic mechanism over the nuclear fragmentation mechanism would follow from the relatively large cross sections typical of atomic processes, which might remove the need to invoke very small probabilities of occurrence. For $Z/\beta \approx 114$ and $\beta < 0.6$ the ion slows so rapidly that the required large number of attached electrons is easily ruled out, and we consider only the intermediate velocity regime $\beta \approx 0.6$ to 0.7. Fowler et al.[16], and more recently Wilson[29], have discussed quantitatively the competition between the electron stripping process and the two processes of non-radiative and radiative attachment, as a function of the velocity and charge of the moving nucleus and the charge of the medium traversed. The results of recent measurements of electron attachment cross sections[30], made at the Bevalac, support their conclusion that the radiative process dominates over the nonradiative process at the velocities relevant to the present case. Both theory and the empirical expression in eq. 1 agree that a heavy nucleus with $Z^*/\beta \approx 114$ and $\beta \approx 0.6$ to 0.7 will retain one or possibly both of its K electrons. However, in order to maintain a roughly constant ionization rate through the stack, the number of electrons attached would have to grow to ~10 to 16, which seems far-fetched for two reasons. Though a quantitative theory of attachment and stripping cross sections of L, M,... electrons has not been developed, the qualitative argument of Bohr[31], that an ion retains only those electrons with speed comparable to or greater than the ion's speed, would indicate that electrons less tightly bound than K

electrons to a nucleus with $Z/\beta \approx 114$ and $\beta \gtrsim 0.6$ will not be attached. Further, if numerous electrons in higher than K shells could be readily attached, it would be virtually impossible to identify high-energy heavy nuclei because of the extremely large fluctuations of effective charge. This is in direct contradiction with the large number of measurements of etch rate vs depth in Lexan stacks and with the quite reasonable charge distributions obtained for the ultraheavy cosmic rays.[7,9,10,21] Finally, even if a partially stripped nucleus with β as low as 0.6 could maintain $Z^*/\beta \approx 114$ and account for the Lexan data, its distant energy deposition would be too high to fit the data in the three emulsions. For example, its track structure would look similar to that in Fig. 14(b) of the nucleus with $Z = 75$, $\beta = 0.67$, rather than like that of the monopole candidate in Fig. 14(a).

e. Sources of errors in etch rates

At present, our understanding of Lexan detectors is inadequate for us to discuss errors from first principles. Our discussion must be somewhat phenomenological. For the monopole candidate the etch rates in sheets 5 to 34 appear to be normally distributed about the line in eq. 18 with a fractional standard deviation $\sigma/\bar{V} = 0.0972/2.86 = 0.034$. For the other particles from the Sioux City flights the fractional errors for a single point have a median value of 0.035 and range from 0.018 to 0.074, taken with respect to curves calculated from eq. 7. Half of them fall between 0.027 and 0.04. The magnitude of the fractional error does not appear to correlate with either Z or β. For the Skylab experiment[9] the median value was 0.025. The scatter in the measurements for the monopole candidate appears to be

typical of ultraheavy cosmic ray measurements.

Sources of error include those due to measurement errors and those due to physical and chemical effects.[9] Measurement errors account for a length error of ~0.8 μm, which amounts to a fractional error of only 0.010 for the monopole candidate. Physical effects include statistical fluctuations in the energy deposited by the numerous electrons with energy less than ~ 1 keV; electron capture and loss processes that change Z* abruptly; fragmentations that change Z abruptly; and mechanical deformation of the Lexan stack, which might affect detector response. Statistical fluctuations in the production rate of low-energy electrons contribute a negligible error. For a nucleus in a certain range of energies that depends on Z, capture and loss of electrons results in a variability of Z* by one unit, which could in principle be detected if other contributions were sufficiently small. For capture of an electron by a nucleus with Z = 80, the etch rate would decrease by ~6%. Nuclear fragmentation happens too rarely to explain more than an occasional fluctuation. No obvious mechanical deformation of module 104, containing the monopole candidate track, was observed.

Chemical effects include inherent microscopic variability in structure and composition of the Lexan sheets, variability associated with the etching process, and variability of the chemical environment during and after the balloon flights. The first of these is probably the major source of the uncorrelated errors. This conclusion is supported by recent work[32] in which a more homogeneous plastic than Lexan was found with a response showing a much smaller fractional error than that for Lexan. The second chemical effect is probably

negligible for all sheets etched in the same well-stirred solution. The third probably at least partly explains the systematic errors observed in sheets 1, 2, 3, 4, and 35. We give three examples. (1) Oxygen and other gases dissolved in Lexan are known to play a role in fixation of the latent track.[2] External sheets may be exposed to greater changes in ambient gas composition during the balloon flight than do sheets inside the bolted stack. (2) Over a period of months, mold slowly grows on Lexan and may affect track etch rates of sheets exposed in the storage area. (3) Lexan in contact with adhesive tape or even dissimilar plastic seems to give a larger variability in etch rates than Lexan in contact with other sheets of Lexan.

The Lexan modules were assembled by stacking pieces successively cut from a single roll. The apparently correlated errors in several successive sheets might be explained by systematic variability along the original roll.

5. Tests of Hypothetical Fits to Lexan Data

Not every physicist accepts statistical analyses of experimental data, perhaps partly because of the frequency with which 3- or 4σ effects are claimed and later disappear when the experiment is repeated. The material in this section is included for those who find it useful to have an objective, quantitative comparison of the quality of fits of various hypothetical curves to the Lexan data alone. First we evaluate the goodness of fit of nuclei with various initial charges and velocities that fragment zero or more times with integral loss of charge at arbitrary positions in the stack. Then, following Fleischer and Walker,[6] we estimate the total probability of a particular

scenario occurring in either the Minneapolis, Skylab, or Sioux City flights. The overall figure of merit for a hypothesis will be taken as the product of the confidence level for the fit to the data and the total probability of occurrence of that scenario.

The χ^2 test is very commonly used as a measure of goodness of fit but requires an independent knowledge of the error for each point. The Particle Data Group finds[33] that particle physics experimentalists often underestimate σ. As a rule, when the quantity $\chi^2 = \sum_i (x_i - \bar{x})^2/\sigma_i^2$ is significantly greater than the number of degrees of freedom in a particular experiment, the Particle Data Group multiplies the σ's by a scale factor, typically of order 1.34, so that the reduced χ^2 is of order 1. In effect, we used similar reasoning when we chose $\sigma = 0.0972$ μm/h in order that $\chi^2/\nu = 1$ for the distribution of etch rates about a straight line for the monopole candidate.

The F-test is a better, more conservative way of comparing the variances of two hypothetical curves through a set of data than is the χ^2-test. The statistic F is defined as the ratio of reduced chi-squares for the two curves. If it is known that all points have the same σ, then the F-test does not require σ to be known because its square appears in both numerator and denominator. In our case we use the 56 data points from sheets 5 through 34, which had the same sensitivity, and ignore the data from sheets 1, 2, 3, 4, and 35, which had larger errors, arising from both normalization and inherent errors. Thus F is given simply by the ratio of variances and is independent of the size of the error bars. (Note that the χ^2-test, which requires a knowledge of σ, is a limiting case of the F-test

when one hypothesis has an infinite number of degrees of freedom.) If one wished to force an acceptably high confidence level using the χ^2-test, he could, if they were not independently known, arbitrarily inflate the σ's until some arbitrary, quite unlikely hypothesis gave a reduced $\chi^2 \approx 1$.

We assume, as is customary in statistics[34], that of two hypotheses compared by means of the F-test, the one with the higher confidence level is the more likely. For convenience, we take as the baseline hypothesis the least squares straight line given by eq. 18. Column 4 of Table 2 lists F-test confidence levels for several combinations of β, Z, and types of fragmentations. Figure 9 shows curves for several hypothetical cases that approximately pass through the data. The curves are the results of calculations in which, for a given number of fragmentations, the values of initial β and Z and the positions and ΔZ values of fragmentations were calculated to minimize the square error. It is interesting that a lower square error is achieved for a single fragmentation that occurs near the middle of the stack rather than at the glitch at 1.1 g/cm^2. The conclusions in Table 2 are insensitive to the precise positions of the fragmentations.

Note that the number of fragmentations required to fit the data at a specified confidence level increases rapidly as the assumed initial velocity decreases. For a fixed number of fragmentations the confidence level decreases rapidly as the initial velocity decreases.

If, instead of the F-test, one uses the χ^2-test with the σ's chosen so that $\chi_\nu^2 \approx 1$ for the least squares straight line, then the confidence levels for the various nuclei are considerably lower, typically by a factor $\sim$10 for $\beta \lesssim 0.8$.

Column 5 of Table 2 gives the integrated probability for finding, in some flight, an event of the type described. It is equal to the

product of the total number of similar tracks of nuclei in a suitable range of Z and β seen in all experiments times the probability of occurrence of that number of fragmentations by a single nucleus. We took for the pool of nuclei those seen in the Minneapolis, Skylab, and Sioux City flights with initial etch rates greater than those corresponding to $Z^*/\beta = 100$ and gradients less than those corresponding to $\beta = 0.65$. In the Minneapolis experiment[7] four such particles were seen. Their initial values of Z and β were 90, 0.7; 74, 0.72; 80, 0.76; and 82, 0.74. None of these nuclei fragmented, so their etch rate curves rose steeply with depth in the stack. In the Skylab experiment one nucleus was detected with $Z = 82$, $\beta = 0.68$, and Z/β increasing from 121 to 153 through the stack. In the Sioux City experiment, in addition to the monopole candidate there were four events with initial $Z^*/\beta > 100$ and $\beta \gtrsim 0.65$. The total number of observed particles that might fragment such as to mimic a particle with a constant, very high ionization rate implying an apparent $Z \gtrsim 110$ is taken conservatively to be ten.

To calculate the probability of a single interaction of appropriate type in the ~ 0.9 g/cm^2 of Lexan between sheets 5 and 34, we assumed the same fragmentation mean free path as did Fleischer and Walker[6] as modified in their footnote 14. We assumed that $\Delta Z = 1$ or 2 at any interaction would give an acceptable fit for any of the fragmentations in Table 2, so that $\lambda \approx 29$ g/cm^2. Following Fleischer and Walker, as a rough estimate of the probability of an optimum spacing of the interactions within the stack, we included the additional factor $n!/n^n$, where n is the number of interactions to be put into n separate compartments.

Column 6 of Table 2 gives the figure of merit for each hypothesis, defined as the product of column 4 and column 5.

One could apply additional tests to the data; for example, the "run test" examines the hypothesis that the data are randomly distributed above and below a particular curve. We believe it is sufficient, however, to end this section by stating the following two non-controversial conclusions: (1) In the absence of information from other detectors, the monopole candidate would be perfectly consistent with a once-fragmenting nucleus with Z = 90, 92, 94, or 96. (2) If the particle was a nucleus, the confidence level that its velocity was as low as 0.6 c is vanishingly small.

6. Analysis of the Nuclear Emulsions

a. General

For the benefit of the reader who is not interested in the details, we state here the main result of the analysis of the emulsion data: Outside of the cylindrical region of very heavily developed grains a few microns in radius, the energy deposited by energetic knockon electrons was much lower for the monopole candidate than expected for a known, long-lived nucleus with $Z \lesssim 96$, $Z/\beta \approx 114$, and $0.84 \gtrsim \beta \gtrsim 0.6$, and appears to be similar to that expected for a nucleus with $Z/\beta \approx 85$ and $\beta \gtrsim 0.6$.

The response of nuclear emulsion to a charged particle is, in a sense, complementary to the response of Lexan. The track etch rate in Lexan depends on energy deposited in a cylinder of radius $\lesssim 10^{-6}$ cm predominantly by very low-energy electrons and is completely insensitive to energy deposited at large radial distances. The density of developed silver grains in electron-sensitive emulsion such as we used is a measure of the density of energy deposited primarily by knockon elec-

trons. Within a radial distance of ~2 to ~6 μm the grain density for a very heavily ionizing particle is too high to give quantitative information. At greater distances the radial distribution of silver grains gives a useful measure of the knockon electron energy spectrum. Lexan responds to very low-energy electrons produced in distant encounters, giving an accurate measure of $|Z|/\beta$, whereas emulsion gives in convoluted form the energy-dependence of the cross section for production of high-energy electrons in close encounters. The Rutherford scattering cross section, though an adequate approximation for distant encounters of a highly charged particle and a free electron, is incorrect for close encounters. The relevant cross section will depend on the particle: for a point nucleus or antinucleus the Mott cross section is relevant;[35] for a monopole the cross section recently calculated by Kazama, Yang, and Goldhaber is relevant;[36] and for an extended particle with arbitrary charge distribution a still different cross section dependent on the form factor would apply.

A quantitatively correct relationship between the silver grain density as a function of position in the emulsion and the Z, β, and zenith angle of the particle would depend on a number of factors, the detailed dependence being still controversial. Three models relating the spatial variation of silver grain density to Z and β exist--the unpublished model of Osborne, based on the calculations of Katz and Kobetich;[37-39] the approximate analytic model of Fowler;[16] and the unpublished, detailed, physical model of Hagstrom[14], which uses a Monte Carlo program. Though these models differ in some of the detailed conclusions regarding the monopole candidate, they agree in the follow-

ing generalizations noted by Hagstrom:[14]

(1) Saturated darkening due to developed silver grains in the so-called core of the emulsion track results from knockon electrons with energies 1 keV $\lesssim$ E $\lesssim$ 50 keV, whereas unsaturated but easily visible darkening in a halo of extent ~10 to ~30 μm from the core results from knockon electrons of energies 25 keV $\lesssim$ E $\lesssim$ 1000 keV.

(2) Given the constraint imposed by the Lexan, $|Z|/\beta = 114$, the energy deposition in the core is virtually independent of Z.

(3) Among the positive nuclei with $Z \lesssim 96$, $\beta \gtrsim 0.6$, and $Z/\beta = 114$, energy deposition in the 10-30 μm halo depends only very weakly on Z.

In the next subsections we present several types of measurements on the three layers of nuclear emulsions showing that the energy deposition in the halo was significantly depleted from that expected for the known, long-lived nuclei with $Z \lesssim 96$, $\beta \gtrsim 0.6$, and $Z/\beta = 114$, thus establishing at a high confidence level that the particle was unique.

b. Visual measurements of R_1 and R_2

The traditional method for inferring the radial distribution of energy deposited around a track has been to use a photodensitometer[16] to measure the attenuation of a pencil of light transmitted through a column of the emulsion defined by a small slit. A disadvantage of this method is that it integrates along a column containing silver grains at varying radial distances from the trajectory. Some years

ago one of us (WZO) began developing a system called AMID (automated microscopic image dissector), which could recognize individual grains, automatically scan the volume of emulsion around a track, record the locations of silver grains, subtract background, and compute the radial distribution of silver grains. Only now has the system begun to be employed on a substantial number of events. Before the system became operative, WZO found that it was possible to make fairly reproducible visual measurements of the radial distances at which two specific levels of darkening occurred, using a calibrated eyepiece reticle in a microscope. These two radial parameters are called R_1, the radius of the core of complete darkening, and R_2, the radial distance at which the halo of partial darkening drops to the background level. The values of R_1 and R_2 were measured for the ultraheavy cosmic ray tracks in the Minneapolis flight but have not previously been published; the values of R_1 and R_2 have been reported for the monopole candidate[1] but not for the other ultraheavy events in the Sioux City flights.

R_1, the radius of the core of saturated darkening near the center of the track, is obtained by using a 53X oil objective with high numerical aperture (NA = 0.95), focusing along the center of the track, and estimating the average radius of the completely dark central region. For very steep tracks R_1 is measured by focussing at the interface between the bottom of the emulsion and the plastic backing. Measurements of R_1 for events from the Minneapolis and Sioux City flights are shown in the left-hand side of Fig. 10 as a function of Z/B. The latter quantity was calculated at the emulsion from the set of measurements made in the Lexan stack <u>after</u> the core radii were measured. Rather

surprisingly, we found no systematic difference in the dependence of R_1 on Z/β for the two flights and so the same symbols are used for both sets of data.

For both R_1 and R_2 (see Fig. 11) we show separately the data for events at low velocity ($\beta < 0.58$) and at high velocity. In accord with track models, we see that R_1 increases approximately linearly with Z/β and does not depend on β alone. The dispersion of points is much greater than that due to measurement error ($\Delta R_1 \approx \pm 0.5$ μm). It was pointed out in the status report on the monopole candidate[13] that R_1 depends rather strongly on zenith angle θ: steep tracks have a larger core width than do shallow tracks with the same Z/β. This is a well-known consequence of distortion during processing of the emulsion. During fixing, the undeveloped silver halide grains are removed, the emulsion shrinks in thickness, and the dense mass of silver grains in the core, being much less compressible than the gelatine, are displaced outward in order to conserve volume.[3,40] The lateral displacement is a maximum for a vertical track and is almost zero for a horizontal track. If one fails to control processing properly and over-develops the emulsion, the silver grains may grow so large that the core becomes a solid wire that punches through the surfaces of the shrinking emulsion rather than deforms with the emulsion.[40] No cases of punch-through were observed for tracks in the emulsions used in the Sioux City flights.

For properly developed emulsion it is straightforward to apply a geometric correction to the measured core radii in order to infer the core radii before shrinkage. The points on the right-hand side

of Fig. 10 have been corrected, assuming a density of silver grains that falls off as $(Z^*/\beta r)^2$, a volume per grain that is a free parameter, and a shrinkage factor, S, defined as the ratio of initial to final emulsion thickness, that is directly measured. For the data in Fig. 10, we chose to normalize the correction so that the core radius for the monopole candidate (with $\theta = 10^\circ$) would be unchanged. The essence of our calculation of corrected core radii can be reproduced by a simple one-parameter model involving only the shrinkage factor, the zenith angle θ, and the assumption of a deformable, incompressible fluid whose initial radius R_{l_i} is related to its final radius R_{l_f} as follows:

$$R_{l_i} = R_{l_f} (\sin^2\theta + S^{-2} \cos^2\theta)^{1/4} \qquad (19)$$

Of course, θ is the true zenith angle, which we determined by measurements in the Lexan stack.

After correction, the dispersion is much reduced and is consistent with measurement error alone. Though the corrected core radius is rather insensitive to the identity of the particle, one can say from the position of the data point for the monopole candidate that both the Lexan and the core radii agree that the particle behaved in its close energy deposition like a particle with $|Z|/\beta \simeq 114$. Hagstrom has pointed out that the tightness of the correlation provides strong evidence that the cylindrical region of emulsion of radius $\sim$6 μm traversed by the monopole candidate had closely the same sensitivity as the other emulsions. If, for example, we were to propose that the

deficiency of silver grains at large radial distances (to be presented below) was caused by passage of a normal nucleus with $Z/\beta = 114$ through a very insensitive region of emulsion, then the corrected core radius would also have to reflect a deficiency of silver grains, i.e., it would lie well below the population of points for emulsion of normal sensitivity. Measurements of Fe tracks, to be presented later, show that over dimensions of many centimeters the sensitivity of the emulsion in module 104, containing the monopole candidate, was indistinguishable from the sensitivity of the emulsion in the other modules. Figure 10 shows that the sensitivity of the emulsion was normal within a few microns of the region in which the energy deposition was observed to be abnormally low.

Next we discuss R_2, which is a visual measure of the distant energy deposition. At low magnification, ~80X, the eye perceives that the darkening resulting from energetic knockon electrons decreases with radial distance and becomes indistinguishable from background at some distance we call R_2. It is impossible to describe quantitatively how the eye evaluates R_2, and this is a serious drawback to the use of data for R_2 as evidence for a unique particle. The measurements shown in Fig. 11 were made at Houston by WZO before the events were located in Lexan and assigned values of Z and β. Events for both the Minneapolis and Sioux City flights are included, and data for low and high velocities are plotted separately.

In contrast to the situation in Fig. 10, where the energy deposition at distances of only a few microns depends only on Z/β, not on β, in Fig. 11 we see that the energy deposition at large distances

(tens of microns) can depend both on Z/β and β. For the ordinary nuclei, denoted by black points, R_2 correlates well with Z/β for values of $\beta \gtrsim 0.58$, in accord with track structure models. The generally lower values of R_2 at a given Z/β for ordinary nuclei with low velocity are expected because of kinematic effects such as the cutoff in the electron energy spectrum at $w_{max} = 2m_e c^2\beta^2\gamma^2$. The models differ so much in the quantitative details of how the energy deposition depends on β and radial distance for low-velocity particles that we make no attempt here, as we had earlier, to infer the velocity of the monopole candidate from the measurements.

The reader cannot fail to note that the point for the monopole candidate, labeled X, does not seem to be a member of the population of events with $\beta \gtrsim 0.58$. Instead of having a halo radius of nearly 100 μm, as did the several fast particles with $Z/\beta \approx 110$ to 120, it had a halo radius of only 55 μm, like fast particles with $Z/\beta \approx 80$. In the right-hand side of Fig. 11 one sees that the point for the monopole candidate is bracketed by data for particles known to have $\beta < 0.58$. Endowing the particle with a low velocity is one way to account for the anomalously small value of R_2, provided its mass is made large enough so that its constant ionization rate in the Lexan stack can be understood. We will see later that the required mass would be so large ($\gtrsim 10^3$ amu) that nuclei are excluded.

c. Photodensitometry; relative sensitivity of emulsions

Using a Perkin-Elmer PDS Microdensitometer Model 1010A in the Astronomy Department at Berkeley, we have made two sets of measurements of tracks in the Ilford G-5 emulsion from the Sioux City flight.

With P.H. Fowler and D.L. Henshaw of the University of Bristol, we have found[41] that measurements of optical density as a function of lateral distance from tracks in emulsion made with the PDS and with the Bristol densitometer on the same events give extremely good agreement. A separate paper[41] describes the PDS and the techniques of track densitometry.

In the first set of measurements we wanted to see if the visual quantity R_2, which might be subject to error due to peculiarities in the physiology of vision, was closely correlated with the darkening of the emulsion around a track as measured by its optical density relative to background.

Figure 12 compares measurements of R_2 with photodensitometric measurements for the same set of tracks from the Sioux City flights. (No PDS measurements were made on the Minneapolis tracks.) The abscissa, K_{rms}, is a measure of the optical density[41], obtained by minimizing the sum

$$\chi^2(K) = \sum_x [D(x) - \bar{P}(K,x,t,\theta)]^2 \qquad (20)$$

where $D(x)$ is the optical density measured at a lateral distance x from the projection of the track axis and $\bar{P}$ is a theoretical expression[16] for the average projected density of silver grains in a column at distance x sampled by a long, narrow slit of length $\Delta y = fL \sin\theta$ and width $\Delta x \ll \Delta y$ (rewritten in our nomenclature):

$$\bar{P}(K,x,t,\theta) = \frac{2K^2\csc\theta}{fx}\left\{\frac{1+f}{2}\arctan\left[\frac{(1+f)t\sin\theta}{2x}\right] - \frac{1-f}{2}\arctan\left[\frac{(1-f)t\sin\theta}{2x}\right] - \frac{x}{2t\sin\theta}\ln\left[\frac{1+(1+f)^2t^2\sin^2\theta/4x^2}{1+(1-f)^2t^2\sin^2\theta/4x^2}\right]\right\} \qquad (21)$$

Here t is the emulsion thickness, L sinθ is the projected length of the track and the slit length was set for each track to be 20, 60, or 100 μm such that $f \lesssim 0.8$ in order to exclude the portions of the track nearest the two surfaces, where transition effects are large. The slit width was $\Delta x = 5$ μm and readings of D(x) were taken automatically every 2 μm. The sum in eq. 20 is over data for $|x| = 4$ to 100 μm and for which the density is more than 2σ above background. The values of D(x) were taken relative to a background level given by the average density in two strips at x = -150 to -130 μm and x = 130 to 150 μm.

K includes all the physics of grain sensitization, the chemistry of development, and the optics of observation. When χ^2 is minimized, the value of K_{rms} is found[41], in accord with track models, to increase roughly linearly with Z/β for high-velocity particles and to show a velocity dependence for particles with $\beta \lesssim 0.6$. Data showing the dependence of K_{rms} on Z, β, and θ are presented in ref. 41.

The good correlation between R_2 and K_{rms} in Fig. 12 for velocities ranging from 0.36 to 0.98 c suggests that physiological effects such as the difficulty of seeing gradual spatial variations in brightness do not seriously impair the usefulness of R_2 as an indicator of the magnitude of energy deposition at several tens of microns.

The results in Fig. 12 strengthen our confidence in the significance of the discrepancy for the monopole candidate, shown by the X in Fig. 11. It is unfortunate that we cannot report reliable densitometric measurements of the monopole candidate track itself. During intensive microscopic study and photography of the event by R. Hagstrom, the emulsion was exposed to illumination so intense that the track

was distorted into a C-shape. Straightforward corrections for the distortion (discussed in ref. 40), utilizing neighboring tracks of relativistic alpha particles, allow one to reconstruct the positions of the grains to within a few microns. This makes feasible the determination of the radial distribution of grain density with AMID. Fortunately a set of photomicrographs at about 40 positions along the track, including the micrograph in Fig. 14(a), were completed before the damage occurred.

The second set of measurements was designed to search for possible systematic variations in sensitivity within the Ilford emulsion in module 104 and from module to module. If, for example, it turned out that the emulsion in module 104 was much less sensitive than the other emulsions, due perhaps to an accident in manufacture or in development, then the low density of grains at large radial distances for the monopole candidate would have a trivial explanation.

Variations in response of emulsion can be caused by variations in its initial chemical or physical state; variations in its history prior, during or after exposure, and variations in the degree and type of development. Previous studies of emulsion sensitivity have included, inter alia, counts of blob density along tracks of minimum-ionizing protons[40], photodensitometric measurements of the magnitude of fluctuations in the optical density of the emulsion as a function of position[16], and photodensitometric measurements of tracks of Fe nuclei.[16] The latter method, though laborious, is the best because it measures most directly the relevant quantity, the production of silver grains due to energetic knockon electrons.

In addition to module 104, which contained the monopole candidate track, we chose seven modules containing tracks of ultraheavy cosmic rays with zenith angles or Z/β similar to those of the monopole candidate. One of the modules, no. 76, contained an event with $Z/\beta = 112$, $\theta = 14°$ (photographed in Fig. 14(b)), nearly identical to the values for the monopole candidate. We first compared the average background optical densities of the eight emulsions, correcting for differences in thickness. We determined the thickness of emulsion in the vicinity of an ultraheavy cosmic ray track by measuring the projected length of that track and of several nearby Fe tracks, assuming only vertical shrinkage without shear, and determining the true zenith angles of these tracks from measurements in the Lexan stack adjacent to the emulsion. All of the emulsions had average optical densities per unit thickness that agreed within ~1%, indicating a high degree of uniformity of initial sensitivity and of degree of development.

Next, from measurements in the Lexan we selected 56 tracks of nuclei identified as having $Z = 26$ and with similar zenith angles, 35° to 45°, and similar Z/β, 59 to 68, at the emulsion. Twenty-one of the tracks were distributed throughout module 104. The first set of data were obtained at 2 μm intervals for $|x| \gtrsim 4$ μm in the same way as the measurements were made for the heavier nuclei. For each track we calculated K_{rms} as described earlier. Assuming an approximate proportionality to (Z/β),

$$K_{rms} = C_1(Z/\beta) \tag{22}$$

we found for the entire sample, $C_1 = 0.153 \pm 0.015$, and for the 21 tracks from module 104, $C_1 = 0.152 \pm 0.020$. These results show that

the average sensitivity of the region of emulsion in module 104 is indistinguishable from the average sensitivity of the emulsion in the other seven modules. For the sample of Fe tracks Z, β, and Z/β are known quite accurately because each event was traced to the end of its range in the Lexan stack and several measurements of etch rate were made at known residual ranges. If one were to use these emulsions to determine Z/β for unknown particles with about the same ionization rate as in the sample, one could determine Z/β with a fractional error of ~10%. Although calibration particles with a higher Z/β are not yet available, we expect the fractional error for the ultraheavy cosmic ray tracks to be considerably smaller because of the greater signal.

The density of silver grains around Fe tracks is considerably lower than that for the ultraheavy cosmic ray tracks. To get a greater signal for the sample of Fe tracks we made a second set of measurements, with a slit of width $\Delta x = 5$ μm and length $\Delta y = 100$ μm centered on the track core. Figure 13 shows the data. At the track axis the gradient of light across the width of the slit is particularly large, and the central density does not respond linearly to silver grain density. Denoting the central density by D_c, we utilize the relation determined empirically by Fowler et al.[16]

$$D_c = C_2(Z/\beta)^{1.34} \tag{23}$$

which accounts approximately for the non-linear response. A least squares fit of all of the data to eq. 23, shown by the line in Fig. 13, gives a value $C_2 = 1.91 \pm 0.11$, and a least squares fit to the data in module 104 alone gives a value $C_2 = 1.94 \pm 0.11$. Thus, both the central densities and the densities at $|x| \gtrsim 4$ μm in module 104

have average values that are indistinguishable from the overall averages. The standard deviation in C_2 corresponds to an ability to determine Z/β of an unknown particle with a fractional error of about 4%.

We believe that these results for Fe tracks, together with the results for core radii in Fig. 10, constitute strong evidence that the abnormally low density of silver grains for the monopole candidate is due to a property of the particle and not to a low sensitivity of that emulsion relative to the other emulsions.

d. Photomicrographic evidence

The abnormally low density of silver grains around the monopole candidate track is quite easily seen in a microscope by even an inexperienced observer and is quite obvious in a photomicrograph. From the complete sample of ultraheavy cosmic ray tracks we selected those with zenith angles nearly the same as that of the monopole candidate ($\theta = 10°$), so that the effects of obscuration by out-of-focus grains and transition effects at the surfaces would be comparable. The photomicrographs in both Figs. 14 and 15 were taken at equal magnifications, about one-third of the way down each track. A 53X oil objective with a high numerical aperture (0.95) was used, which means that only grains within a micron or so of the focal plane are in focus. Figure 14 compares the silver grain distributions around the tracks of the monopole candidate and of a nucleus with $Z = 75$, $\beta = 0.67$, $Z/\beta = 112$, and $\theta = 14°$. It is fortunate that this event with almost identical Z/β and θ to those of the monopole candidate occurred on the Sioux City flight. The eye can readily see that over a wide range of distances outside the core the distant energy deposition is much lower for the

monopole candidate than for a normal nucleus with $Z/\beta = 112$. The striking difference between the two particles is clear in each of the 40 pairs of micrographs taken at different depths from top to bottom of the emulsion. The large central dark region, which consists of grains in the optical path but not necessarily in focus, obscures the smaller core region in these photographs. The cores of saturated darkening can only be seen by direct microscopic examination. Their radii are about the same, ~6 μm, as seen in Fig. 10. We reiterate that the distortion of the monopole candidate track caused by intensive optical examination occurred after these photographs were made.

Figure 15 compares these two tracks with all other steep tracks having $8° \lesssim \theta \lesssim 14°$, $Z/\beta > 70$, and $Z > 40$. The values of Z, β, and θ for the nine events are given in Table 3. The values of Z/β are labeled in the figure. The micrographs are arranged in a sequence of increasing size of the region of intense darkening, going from top to bottom and from left to right. Note that with two exceptions the size of the dark region, a rough measure of the density of silver grains at radial distances ~15 to ~40 μm, increases with Z/β. The first exception is the monopole candidate, whose photograph looks similar to that for a normal fast nucleus with $Z/\beta \approx 80$. The second exception is the very slow event in the upper right, which has $Z/\beta = 120$ but has a dark region smaller than that for the fast nucleus with $Z/\beta = 106$. The small size of the dark region is a result of kinematics, which cuts off the knockon electron spectrum at a maximum energy of ~160 keV for a nucleus with $\beta = 0.37$.

The photomicrographs show clearly that far fewer silver grains were produced around the monopole candidate track than around the track of event 76-1, the fast nucleus with $Z/\beta = 112$. In the absence of a large set of micrographs of tracks of nuclei with all possible combinations of Z and β giving $Z/\beta \simeq 114$, we have to utilize models of track structure to predict how the grain density will vary with Z and β and how fluctuations in the energy deposition can affect track structure. We will do this in section 7(a). We point out explicitly here that the difference in grain densities in Fig. 14(a) and (b) cannot be attributed to an abnormality in event 76-1. The emulsion in module 76 had a sensitivity indistinguishable from the sensitivity of the emulsion in module 104. Moreover, there were several other events in the flight with $Z/\beta > 112$ and higher silver grain densities which we did not show in photographs because of the difficulty of making visual comparisons of tracks with quite different zenith angles. To show that event 76-1 did not have an abnormally high grain density, in Fig. 16 we compare that event with others of lesser, comparable, and greater values of Z/β and zenith angles between 8° and 14°. Event 76-1 appears at the top of the middle column. Our events 156-113 and 191-1 are at the middle and bottom of the first column. The other six events are from emulsion exposed by the Bristol and Dublin groups.[10] All nine photomicrographs were taken under identical conditions in P.H. Fowler's laboratory. The events in the first column have Z/β between 79 and 87 and are similar in appearance to event 104-121, our monopole candidate. The events in the second column have Z/β between 112 and 118 and are illustrative of the appearance the track of event

104-121 should have if it were a normal ($Z \lesssim 96$) fast nucleus with $Z/\beta = 114$. The events in the third column have $Z/\beta \gtrsim 125$ and are illustrative of steep tracks with considerably higher silver grain density than the track of event 76-1. Even though, because of their different histories, the tracks in the Bristol/Dublin emulsions should not be compared quantitatively with the tracks in our emulsions, the qualitative trends in growth of silver grain content of tracks in all the emulsions are similar and support the contention that event 76-1 was not at the extreme upper end of the distribution of track sizes for ultraheavy cosmic rays.

e. Quantitative studies of the Kodak NTB-3 emulsions with AMID

The two layers of 10 μm Kodak NTB-3 emulsion, each coated on a 200 μm thick cellulose triacetate base and independently wrapped in opaque paper, provide independent evidence for the deficiency of silver grains around the monopole candidate track. The appearance of tracks in thin emulsion is quite different from that of tracks in Ilford 200 μm emulsion. The thin emulsion can be thought of in first approximation as an infinitesimally thin detector of energetic electrons generated in the low-Z material above and below it by the ultraheavy cosmic ray. Fewer knockon electrons per unit volume are produced in the low-Z material than in the emulsion. Those that are produced do not scatter as frequently as they would in emulsion; they stream to a greater radial distance before reaching the end of their range. The silver grain density is lower and individual delta rays can be more readily recognized and followed than in thick emulsion.

After development the Kodak emulsion is only ~6 μm thick, and the number of silver grains per event is small. Considerable effort is

required to find each event with an optical microscope, but once an event is located, the silver grain distribution can be quite readily determined with the AMID system developed at Houston. For events 76-1 and 104-121, we etched the plastic backing of the thin emulsions and confirmed that the events had been correctly located. For the other events, we found several Fe tracks near each ultraheavy event that could be traced through the thin and thick emulsions and that confirmed the correctness of the location. All events with $\theta < 20^\circ$ and $Z/\beta \gtrsim 80$ in both sets of thin emulsions were selected for measurements. In addition, we selected 104-117, with $\theta = 0^\circ$ and $Z/\beta = 66$, because it was within 8 cm of event 104-121, and we selected a random sample of four additional events with $\theta < 20^\circ$ and $60 < Z/\beta < 80$ to extend coverage over a wide range of values of Z/β. An event is first centered on the microscope stage and focused by hand at a particular depth in the emulsion. An image dissector divides the image into cells of size 0.25 μm x 0.25 μm and an integral minicomputer determines whether each cell is or is not within a developed silver blob. The blob recognition algorithm yields results independent of absolute illumination level over a wide range, and variation of integration time to achieve constant total signal for each cell assures a constant signal to noise ratio. The total number of cells within blobs is thus a measure of the amount of developed silver within the focal depth for that particular field of view.

After one scan is complete the operator focuses the stage at a different depth and starts a new scan. For the thin emulsions essentially all of the silver blobs could be recorded with scans at only

two vertical positions of the stage. A computer program sums the filled cells at a given radial distance, subtracts a background reading, and generates a quantity proportional to silver density above background as a function of radial distance from the trajectory. For the thin emulsions we defined the background density as the average density of filled cells in an annulus from 40 to 80 μm. The total number of silver blobs per event in the thin emulsions is too low to warrant using the radial distributions, but provides quite significant information when we sum the signal cells within a cylinder of radius 30 μm centered on the track.

Figure 17 shows the density of filled cells within a circle of radius 30 μm, after background subtraction, as a function of Z/β. Data for the upper and lower Kodak emulsions are indicated by open and closed circles respectively. Repeated measurements on the same tracks have shown that the standard deviation of the measurements is 2%. One open circle in Fig. 17 has no corresponding closed circle; the track in that emulsion was obscured by a general blackening due to a mechanical deformation of that region. The important result of these measurements is that for both emulsions the point for the monopole candidate lies well below a least squares line through the remainder of the data.

Assuming no systematic errors and a normal distribution of errors due to the statistics of δ-ray production and of grain development in the thin emulsion, we can assess the significance of the departure of the measurements for the monopole candidate from the value expected for a normal nucleus. Let S_{30} denote the density of filled cells

within the circle of 30 μm radius. Because the δ-rays contributing to S_{30} are produced and are scattered both in the thin emulsion and in the surrounding low-Z medium, the dependence of S_{30} on Z/β may be more complicated than it would be for the thick emulsion. For convenience we have calculated errors and confidence levels assuming a linear and a quadratic dependence on Z/β. On the assumption $S_{30} = a + b(Z/\beta)$, the measured values of S_{30} for the monopole candidate in the top and bottom emulsions lie 3.38 σ and 2.07 σ below the least squares line in Fig. 17, and the product of the confidence levels for the two measurements to be part of a normal distribution about the line is 7.1×10^{-6}. If S_{30} is assumed to vary as $S_{30} = a + b(Z/\beta)^2$, then the product of confidence levels for the two points is 2.9×10^{-6}. For either a linear or quadratic dependence on Z/β, the thin emulsions provide strong supporting evidence for an abnormally small density of energy deposited by the monopole candidate in close collisions. From an examination of photomicrographs of the tracks in the thin emulsions, we believe that the large fluctuations of the values of S_{30} in Fig. 17 are entirely consistent with the statistics of a thin detector having a limited number of developable silver grains.

A word of caution is in order. This is the first time that Kodak's thin emulsion has been used in a quantitative study of highly charged particles, and our experience with its response is rather limited. Because of the small total number of silver grains produced per particle, it was not feasible for us to calibrate the sensitivity of individual emulsions by measurements of Fe tracks, as we did with the Ilford G-5 emulsions.

Projecting the points for the monopole candidate sideways to the least squares line, we see that in the top emulsion its silver grain density was like that of a particle with $Z/\beta \approx 80$ and in the bottom emulsion its silver grain density was like that of a particle with $Z/\beta \approx 94$. These results are consistent with the photographic evidence and the visual measurements of R_2 for the 200 μm emulsion.

Measurements of the radial distribution of silver blobs around tracks in the 200 μm emulsions with the AMID system are more laborious than measurements in the thin emulsions, because of the much greater information content. Considerable progress has been made with these measurements, and it is now clear that they support the visual and photographic evidence to the effect that the monopole candidate has a track structure similar to that for an ordinary nucleus with $Z/\beta \approx 90$ and $0.6 \lesssim \beta \lesssim 0.95$, but grossly different from that for an ordinary nucleus with $Z/\beta = 114$, $Z \lesssim 96$, and $\beta \gtrsim 0.6$. These measurements, after correction for distortion, may make it possible to eliminate some of the now acceptable interpretations. When completed, these results will be reported in a detailed paper on measurements and calculations of track structure.

7. Particles Compatible with Both the Lexan Data and the Emulsion Data

a. Track structure calculations

Some important qualitative features of track structure can be inferred from Fig. 18, which shows the ratio of the exact Mott cross section[35] to the Rutherford cross section for the process in which an electron at rest in emulsion is scattered by a nucleus or

antinucleus with $|Z|/\beta = 114$. The abscissa gives the lab kinetic energy, as well as the true range, of the scattered electron. (Because of multiple Coulomb scattering, the radial distance diffused from the trajectory of the incoming particle will be much smaller than the electron range.) For tracks in Lexan the relevant electron energies are less than ~1 keV; for the saturated core in emulsion (R_1), the electron energies are ~1 to ~50 keV; and for the halo (R_2) or photographically detectable region of darkening in emulsion, the electron energies are ~25 to ~1000 keV. One sees from the figure that the cross section ratios for producing electrons with energies ~50 to a few hundred keV are smallest for an antinucleus, intermediate for an ultrarelativistic superheavy nucleus, and greatest for long-lived nuclei with $Z \approx 75$ to 96.

We now want to utilize non-controversial features common to all models of track structure to account for the two facts: (1) the particle had an average value of $|Z|/\beta$ that did not substantially change from ~114 in passing through ~1.4 g/cm^2 Lexan equivalent; and (2) it produced energetic knockon electrons at a rate similar to that of a fast normal nucleus with $|Z|/\beta \approx 85$.

We begin by assuming that the silver grain density at a particular radial distance r from a track in emulsion is a measure of the energy per unit volume deposited by δ-rays at that point. A linear relationship is reasonable at radial distances ($r \gtrsim 10$ μm) where the proportion of grains developed is low enough that individual grains can be counted. We are thus interested in an expression for $\varepsilon_v(r)$, the energy deposited per unit volume at radial distance r from a short

segment of track in an emulsion of finite thickness $t \approx 200$ μm, sandwiched between plastic or paper of low Z.

Let us first discuss the case of an infinitely thick emulsion considered by Fowler and by Osborne. To find $\varepsilon_v(r)$ we need an expression for the energy spectrum of knockon electrons produced per unit length of track segment and a way of accounting for the spatial dependence of the rate of energy loss of the electrons as they undergo multiple Coulomb scattering and straggling from their most probable range. It is useful pedagogically to outline Fowler's model because it leads to a simple analytic expression for $\varepsilon_v(r)$. (Several aspects of this model are wrong in detail, but it reproduces quite well many of the features of energy transport by the δ-rays.) In order to arrive at an integrable expression, Fowler[16] uses the simple Rutherford scattering cross section which leads to the expression for the number of δ-rays per cm

$$dN \approx 2\pi N_e Z^2 r_e^2 \frac{m_e c^2}{\beta^2} \frac{dw}{w^2} \text{ cm}^{-1} \tag{24}$$

for

$$w < w_{max} = 2m_e c^2 \beta^2 \gamma^2. \tag{25}$$

N_e is the number of electrons/cm^3 in the emulsion and $r_e = e^2/m_e c^2$. Fowler then assumes that, independent of initial direction, multiple Coulomb scattering is so intense that electrons of energy w emitted from a line source <u>diffuse</u> isotropically,

$$\frac{dP(r)}{dw} = \frac{w dN/dw}{2\pi\sigma^2(w)} \exp\left(-\frac{r^2}{2\sigma^2(w)}\right) \text{ erg cm}^{-3} \tag{26}$$

with a diffusion distance $\sigma(w) \approx 0.22\ R(w)$, where the true range $R(w)$ is approximated by a power-law relation

$$R(w) = kw^n, \quad n \approx 1.54 \tag{27}$$

He finds that the energy deposited in a thin cylindrical shell is given approximately by

$$dE/dr = wR^{-1}f(r/R) \tag{28}$$

with $f(r/R)$ independent of w. Integrating along the track and over the knockon spectrum (eq. 24), he obtains the simple expression

$$\varepsilon_v(r) \approx \frac{2.2Z^2}{\beta^2 r^2} \exp\left(-\frac{r^2}{2\sigma_{max}^2}\right)\ \text{eV}/\mu\text{m}^3 \tag{29}$$

where $\sigma_{max} = 0.22\ R_{max}$.

Consider now the dependence of ε_v on β for particles with fixed Z/β. We must consider the behavior of the exponential factor for values of r less than ~100 μm where the density of silver grains is still large enough to measure. For $r < 100$ μm and large diffusion distance, corresponding to a large kinematic cutoff and large β, the exponential factor is essentially unity and $\varepsilon_v(r)$ does not depend on β for particles with fixed Z/β. The thin-down regime where the depletion of silver grains becomes detectable corresponds to a β small enough that $r \gtrsim 0.3\ R_{max}$. Both this simple analytic model and the experience of Fowler and co-workers[42] indicate that $\beta \approx 0.45$ is the practical limit above which one cannot conclusively determine the velocity of an ultraheavy cosmic ray by photodensitometric measurements.

Among the defects of the model, the most serious are the failure

to use the exact Mott cross section and neglect of the initial direction of the emitted electrons. Failure to use the Mott cross section (which would necessitate numerical integration) means that (1) the model does not distinguish nuclei from their conjugate anti-nuclei, (2) the cross section is seriously underestimated in many cases for ordinary nuclei, and (3) the decrease in cross section for $Z/\beta \gtrsim 100$ as β increases toward 1 is not described. Neglect of the initial direction of the emitted electrons led to the simple conclusion that the only difference in ε_v for different values of β is caused by δ-rays with energies between w_{max} for one β and w_{max} for another β. Naturally as $\beta \to 1$ these differences vanish. However, it is well known that the dependence of the initial direction of an electron on its energy w and on β of the particle can have an important effect on ε_v. The lab angle θ_{lab} of emission of an electron of energy w is given by

$$\theta_{lab}(w) = \arctan \left(\frac{2m_e(w_{max}-w)}{w(w_{max}+2m_e)}\right)^{\frac{1}{2}} \qquad (30)$$

when we neglect initial binding of the electron.

On the average, a δ-ray path is roughly straight for about the first 25% of its range, so that a δ-ray is transported to $r \approx 0.25\ R\sin\theta_{lab}$ away from the particle's trajectory before it becomes "randomized." At fixed Z/β, as β increases, the δ-rays of any fixed energy $w_o \lesssim w_{max}(\beta)$ are ejected at steadily increasing angles, which leads to a systematic increase of ε_v at large r that is not taken into account in eq. 29. Inclusion of this effect should increase somewhat the range of velo-

cities that can be detected by measurements of $\varepsilon_v(r)$.

Application of Fowler's model to the behavior of $\varepsilon_v(r)$ for low velocities leads to the conclusion that $\varepsilon_v(r)$ for a particle with $Z/\beta = +114$ and $\beta \approx 0.4$ will be similar, at $20 \lesssim r \lesssim 40$ μm, to $\varepsilon_v(r)$ for a fast nucleus with $Z/\beta = +85$, $\beta > 0.6$. Fowler's model cannot be used to compare quantitatively the track structure of various fast particles with $|Z|/\beta = 114$, because of his failure to use the Mott cross section. (In their analysis of tracks of ultraheavy cosmic rays in emulsion, Fowler et al.[16] measured the optical density at a fixed distance from the track core and crudely corrected the model by multiplying the value of ε_v at the fixed distance by the ratio of Mott cross section to Rutherford cross section for electrons of some average energy believed to be most effective at that fixed distance.)

Osborne's model is an extension of the track structure model of Katz and Kobetich[37] and their electron energy deposition algorithm.[38] His expression for the energy spectrum of knockon electrons produced per unit length of track segment differs from eq. 24 in that he uses the Mott cross section instead of the Rutherford cross section. His computer program that calculates $\varepsilon_v(r)$ as a function of r, Z, and β contains a table of Mott cross sections calculated by L.V. Spencer[43] for values of Z from -110 to +110, for β from 0.2 to 0.99, and for center-of-momentum scattering angles θ from 0 to 180°. The relation between θ, w, and w_{max} is simply

$$w = w_{max} \sin^2(\theta/2) \tag{31}$$

Osborne follows the Kobetich and Katz approximate treatment of electron energy transport.[38] He has taken two approaches with respect to $\theta_{lab}(w)$, the angular distribution of electrons. The first approach uses the value of θ_{lab} given by kinematics and overestimates the effect of initial direction of the electrons. The second approach uses $\theta_{lab} = \pi/2$ for all electron energies and ignores the effect of initial directions. The real situation should lie between these extremes. Although the problem has cylindrical symmetry, Kobetich and Katz make a one-dimensional approximation that enables them to use an algorithm for electron energy dissipation fitted to experimental data and to the calculations of Spencer[44] for monoenergetic electrons normally incident on flat slabs. They assume that the energy dissipation at radial distance r of electrons ejected at angle θ_{lab} is equal to the energy dissipation of these electrons normally incident on a slab of thickness $t = r/\sin\theta_{lab}$, and that the effect of electrons that scatter so as to interact with too little material compared to a slab is compensated by those that encounter too much material. They express the energy density on the cylinder in terms of the energy flux through the cylinder, F:

$$\varepsilon_v(r) = -(2\pi r)^{-1} dF/dr \tag{32}$$

and write dF/dr as

$$dF/dr = \int_{w_1-I}^{w_2-I} \frac{d}{dt} \{W(r,w-I,\theta_{lab})\eta(r,w-I,\theta_{lab}) \frac{dN}{dw}\} dw \tag{33}$$

where w_1-I and w_2-I are the kinetic energies of δ-rays that just reach the cylinder of radius $r = t \sin\theta_{lab}$; I is an average ionization poten-

tial for emulsion; dN/dw is the δ-ray energy spectrum given by the Mott cross section; W is the residual kinetic energy of an electron of initial kinetic energy w-I that penetrates a slab of thickness t; and η is the probability of transmission through the slab. The reader is referred to refs. 37-39 for the details of the calculation of ε_v for the simple case in which dN/dw is given by eq. 24.

Osborne's model, with its use of the Mott cross section, correctly predicts large differences in $\varepsilon_v(r)$ for nuclei and anti-nuclei with the same $|Z|/\beta$. Like Fowler's model, Osborne's model predicts that for a fixed $|Z|/\beta$ the major changes in $\varepsilon_v(r)$ at $r < 100$ μm will occur for small β. However, in Osborne's model changes in $\varepsilon_v(r)$ can be seen for large Z/β ($\gtrsim 100$) as β increases from 0.9 to 1.0, and changes in $\varepsilon_v(r)$ in the low-velocity regime can still be seen at β up to roughly 0.6. The changes in the high-velocity regime occur because the effective cross section must decrease to the Rutherford cross section as β approaches unity. Both models predict, for large β, that $\varepsilon_v(r)$ decreases approximately as r^{-2}.

In Osborne's model three classes of hypothetical particles could have energy deposition rates ε_v similar to that of a fast nucleus with $Z/\beta \approx 85$ to 95 at radial distances $20 \lesssim r \lesssim 40$ μm: an extremely relativistic ($\beta \gtrsim 0.99$) superheavy nucleus ($Z \approx 114$), a fast anti-nucleus with $Z/\beta \approx -114$, and a slow particle with $Z/\beta \approx +114$ and $\beta \approx 0.45$ to 0.5. With θ_{lab} given by kinematics, the ratio of ε_v for particles with $Z/\beta = +114$ to ε_v for a fast nucleus with $Z/\beta = +85$ increases as β increases until it reaches a maximum at $\beta \approx 0.85$ and then decreases as β approaches 1. At $r = 30$ μm the ratio is ~2 for

values of β between 0.6 and 0.84, corresponding to nuclei up to Z = 96, whereas for $\beta \gtrsim 0.99$ the ratio is 1.25. For a hypothetical nucleus with $Z/\beta = +110$ and $\beta \gtrsim 0.99$, which will be of interest to us in later sections, the ratio is only 1.13. With θ_{lab} fixed at $\pi/2$, the ratio is ~1.85 for $Z/\beta = +114$ and $0.6 \lesssim \beta \lesssim 0.84$ and drops to 1.40 for $\beta \gtrsim 0.99$. For $Z/\beta = +110$ and $\beta \gtrsim 0.99$ the ratio is ~1.30. For either choice of θ_{lab}, Osborne's model shows that the track structure for an ultrarelativistic superheavy nucleus, $Z \approx 110$ to 114, is significantly smaller than that for $Z/\beta = +114$ and $0.6 \lesssim \beta \lesssim 0.84$ and close to that for $Z/\beta = +85$.

In principle, Hagstrom's model[14] overcomes the drawbacks of Fowler's and Osborne's models. It was designed to describe both expectations and fluctuations in energy deposition in emulsion. Hagstrom used a Monte Carlo program to calculate $\varepsilon_v(r)$ for a track segment perpendicular to an emulsion of thickness 200 μm surrounded by a vacuum. For our event, with zenith angle ~10°, this is a good approximation; the calculation is easily extended to arbitrary zenith angle. He used a table of Mott cross sections for particles with $-110 \leq Z \leq +110$, $0.2 \leq \beta \leq 0.99$, and center-of-mass scattering angles $0° \leq \theta \leq 180°$. To keep the duration of the calculation for an individual event at a reasonable level, he followed the production of primary electrons only of energies greater than 25 keV. A 25 keV electron travels a radial distance no more than ~5 μm from the particle's trajectory. The omission of electrons with $w \lesssim 25$ keV thus invalidates the calculation only in the core region of the track. For each trial particle of a given Z and β the Monte Carlo program

generated a spectrum of primary knockon electrons with $w \geq 25$ keV along a line of length equal to the thickness of the emulsion before development (200 μm). Each primary electron was followed as it scattered and transferred energy to bound electrons in the medium. All collisions were treated rigorously, using exact forms both for the multiple small-angle scatters and the large-angle scatters and taking shielding into account. The Berger-Selzer range-energy relation for electrons was used[45], and range-straggling of the electrons was included. An electron that reached the surface of the emulsion was considered to be lost. (The probability of being back-scattered into the emulsion from the low-Z plastic or paper in contact with the emulsion was taken to be zero.) The emulsion was described as a mixture, not as a single element. Granularity was ignored; this is quite a safe approximation at radial distances greater than ~1 μm. The model contains no fitting parameters.

Hagstrom found that his model reproduces remarkable well the shapes and absolute magnitudes of the appropriate calculations of Spencer[44] for point isotropic and plane perpendicular sources of monoenergetic electrons.

Hagstrom has published a summary of some of his findings[14] and has supplied us with numerous graphs of $\varepsilon_v(r)$ for various combinations of Z and β. Because he has not published his study, we restrict ourselves to qualitative statements about his findings regarding energy deposition by particles with $|Z|/\beta \approx 114$ in the 200 μm emulsion at radial distances $10 \lesssim r \lesssim 50$ μm where good measurements of grain density or optical density can be made. Note that his results are not

precisely comparable with our emulsion measurements because he summed over the entire 200 μm emulsion thickness, whereas in our visual, photographic, and AMID measurements we ignored the regions near the top and bottom of the emulsion where the transition effects are large.

We make the following inferences from the Monte Carlo Calculations:

(1) All positive nuclei with $Z/\beta \approx +114$ and $0.6 \lesssim \beta \lesssim 0.95$ have statistically indistinguishable energy deposition curves, $\varepsilon_v(r)$, which are decisively higher than the curves for positive nuclei with $Z/\beta = +85$ and $0.6 \lesssim \beta \lesssim 0.95$.

(2) The energy deposition curve for a hypothetical nucleus with $Z/\beta = +110$ and $\beta \gtrsim 0.99$, which will be of interest to us in later sections, is considerably lower than the curves for $Z/\beta \approx +114$ and $0.6 \lesssim \beta \lesssim 0.95$. It lies about halfway between the curves for those nuclei and the curves for nuclei with $Z/\beta = +85$ and $0.6 \lesssim \beta \lesssim 0.95$.

(3) Antinuclei with $Z/\beta \approx -109$ to -114 and $0.65 \lesssim \beta \lesssim 0.85$, which fit the Lexan data, have energy deposition curves at radial distances $20 \lesssim r \lesssim 100$ μm that are quite similar to that for a fast normal nucleus with $Z/\beta = 85$.

(4) A slow particle with $Z/\beta = 114$ and $\beta \approx 0.4$ has an energy deposition curve that is steeper than the curve for the nucleus with $Z/\beta = 85$ but has a similar magnitude at intermediate radial distances, ~20 to ~40 μm. It deposits essentially no energy beyond ~50 μm.

(5) From several hundred Monte Carlo simulations, Hagstrom found that all curves of $\varepsilon_v(r)$ for nuclei with $Z/\beta = +114$ and $0.6 \lesssim \beta \lesssim 0.95$ lay well above all curves for fast nuclei with $Z/\beta = +85$ and well above

all curves for fast antinuclei with $Z/\beta = -114$.

The rigorous approach of Hagstrom is superior in principle to that of Fowler and of Osborne, and the excellent fits to the extensive calculations of electron beam energy dissipation reported by Spencer[44], together with a wide range of energy dissipation measurements, provide strong evidence for the essential correctness of the treatment. We hope that further Monte Carlo calculations can be done in which $\varepsilon_v(r)$ is evaluated for the region of emulsion about midway between the two surfaces, for the resulting curves would be directly comparable with experimental observations.

Despite quantitative differences in the details of the energy deposition curves, we believe that the two models that use the exact Mott cross section allow us to draw the same qualitative conclusion: The small distant energy deposition in the emulsion is satisfactorily accounted for by the highly relativistic superheavy element with $Z/\beta \approx 110$ to 114, by the fast antinucleus, and by the slow, supermassive particle.

b. Compatibility of the three candidates with the Lexan data

Hagstrom has pointed out[14] that a fast antinucleus with $Z/\beta \approx -114$ not only fits the emulsion data but fits the Lexan data better than would a nucleus with the same velocity and opposite charge. Because of the lower Mott cross section, dE/dx for the antinucleus would be considerably less than for the nucleus, making it a more penetrating particle with a smaller loss of speed in passing through the stack. For $|Z|/\beta \approx 114$ and $\beta > 0.6$ Hagstrom calculated that the stopping power of an antinucleus would be 15% to 25% lower than the

stopping power of its charge conjugate.[14] This result can easily be verified using the analytic expression of Ahlen.[46] This difference in dE/dx gives rise to an etch rate vs range curve with reduced positive slope. For an antinucleus in the pertinent charge regime $-96 \lesssim Z \lesssim -76$ the etch rate vs range curve is similar to that of the positive nucleus with the same initial $|Z|/\beta$ and about three charges higher. (Note that the etch rate at a given $|Z|/\beta$ is the same for Z and $\bar{Z}$; it is only the rate of increase of etch rate with depth that differs for Z and $\bar{Z}$.) Thus, if in Table 2 we admit that positive nuclei, with possible fragmentations allowed for, with initial charges between ~76 and ~96 can fit the Lexan data, then antinuclei with the same fragmentation sequence and charges -73 to -93 would have comparable fits, and antinuclei with charges -76 to -96 would fit the data better.

Hagstrom has argued[14] that fragmentation with small loss of charge in a peripheral collision would be more likely for an antinucleus than for a positive nucleus. Thus, an antinucleus with $|Z| \gtrsim 76$ and average $Z/\beta = -114$, possibly fragmenting, is compatible with all the data in our Sioux City experiment. We will comment on its compatibility with negative searches by previous experimenters in section 8.

All of the track structure models agree that the distant energy deposition by a <u>slow</u> particle with $|Z|/\beta \approx 114$ would be small enough to be compatible with the visual and photographic evidence. The best estimate of the necessary velocity is $\beta \approx 0.4$. But we have seen in section 5 that the rate of change of etch rate through the Lexan stack would be ridiculously high for a nucleus with any ratio of Z/A compatible with particle stability and β as low as 0.6. Only if the

mass were enormously large would the rate of slowing, $d\beta/dx$, be low enough to give an etch rate vs range curve compatible with the Lexan data. It is easy to see approximately how large the mass of the slow particle would have to be if we take dE/dx as approximately proportional to Z^2/β^2 and write

$$\frac{dE}{dx} = \frac{dE}{d\gamma}\,\frac{d\gamma}{d\beta}\,\frac{d\beta}{dx} = \frac{\beta_i A_i m_p c^2}{(1-\beta_i^2)^{3/2}}\,\frac{d\beta_i}{dx} \approx C\,\frac{Z_i^2}{\beta_i^2} = (114)^2\,C \qquad (34)$$

As an example, $d\beta/dx$ for a supermassive particle with $\beta = 0.4$ and $Z/\beta = 114$ will equal $d\beta/dx$ for a nucleus with $Z = 92$, $A = 238$, $\beta = 0.81$ (such that $Z/\beta = 114$) provided the supermassive particle has a mass of ~1840 amu. However, the fit for a uranium nucleus is unacceptably poor unless it fragments once. If the slow particle is to give an acceptable fit to the data without fragmenting, it must have $d\beta/dx$ comparable to that for a hypothetical nucleus with $Z \approx 108$, $\beta \approx 0.95$. Its mass must then be ~56 times greater than the mass of the nucleus with $Z = 108$, or about 16,000 amu, and its mass to charge ratio would be ~350. Hypothetical charged particles with huge mass and huge A/Z ratio have been discussed in several contexts in the literature.[47-50] We will include them in our discussion in section 8.

Assuming the applicability of the restricted energy loss model of track formation in Lexan, Ahlen showed[12] that a monopole of charge $g = 137e$ and low speed, $\beta \approx 0.3$, could account for the Lexan data, provided its mass were sufficiently great to give a nearly zero value of $d\beta/dx$ and thus a nearly zero value of dV/dR. The slope dV/dR would be small enough to be compatible with the Lexan data if, for $\beta = 0.3$, the mass were at least 3400 amu. Kinematics alone ensures that for

$\beta \approx 0.3$ the distant energy deposition by a monopole with g = 137e would be quite low, perhaps even compatible with the visual and photographic data for the 200 μm emulsion. We will discuss the difficulties of the monopole interpretation in section 8.

A hypothetical superheavy nucleus, $Z \approx 110$ to 114, $\beta \approx 1$, gives an excellent fit to the Lexan data. In discussing the response of Lexan, we showed that either eq. 4 (with $K \approx 62$) or eq. 5 gave an adequate representation of the energy deposition at small radial distances. The last two rows of Table 1 show the charges predicted by these two models, along with the charge predicted by the unsatisfactory model in which restricted energy loss is used as the criterion for track formation. An Fe nucleus with a speed $\beta = 0.22$ has $Z^*/\beta = 114$ and an etch rate identical to the average rate for the monopole candidate. If the particle were a nucleus with $\beta \approx 1$, the two acceptable models predict Z = 114 and 109; if it were a nucleus with $\beta \approx 0.98$, the two models predict Z = 112 and 108. These values are quite consistent with the range of charges of hypothetical superheavy nuclides calculated to have long half-lives. We regard a nucleus with Z = 110 to 114, $\beta \gtrsim 0.99$, and $Z/\beta \approx 110$ to 115 as compatible with the etch rate data in Lexan and with the distant energy deposition in emulsion. We will include this hypothetical superheavy nucleus in our discussion in section 8.

A hypothetical particle with $Z/\beta \approx 114$ and a diffuse charge distribution extending to a radial distance of $\sim 10^2$ fermis could in principle account for the small number of high-energy δ-rays in emulsion. We will not consider such a hypothetical particle because we want to

focus discussion in this paper on particles that not only fit the data but have been predicted to exist.

8. Discussion

Table 4 summarizes the status of the evidence. The first five columns, which relate to our own experiment, simply recapitulate what has been said in sections 4 through 7. Assuming that an entry represents a positive observation of a particular particle, column 6 indicates whether it constitutes a serious discrepancy with searches by other experimenters.

a. Was the event a normal nucleus?

The entries in the first three rows of Table 4 refer to normal nuclei known or expected to exist in the cosmic rays ($Z \leq 96$). If we accept the constraint from the Lexan data that $|Z/\beta| \approx 110$ to 115, then nuclei with $\beta \lesssim 0.6$ fail to fit the Lexan data and nuclei with $\beta > 0.5$ fail to fit the emulsion data. There is thus no velocity for which a normal nucleus would fit both the Lexan data and the emulsion data. Even if we admit the possibility that the nucleus underwent an abnormally large number of properly spaced nuclear fragmentations or attached an unusually large number of atomic electrons so as to match the Lexan data, it would, in order to penetrate the Lexan stack, have too high a velocity to fit the emulsion data.

We now consider whether unexpectedly large systematic errors might allow a normal nucleus to fit both the Lexan data and the emulsion data. Again accepting the constraint from the Lexan data that $|Z/\beta| \approx 110$ to 115, we would have to make the ad hoc hypothesis of some unexplained failure in response of all three emulsions. The

statistics of δ-ray production along the track in the two emulsions are poorer than for the track in the thick emulsion, and fewer events have been studied in the thin emulsions than in the thick emulsion. Nevertheless, using the fluctuations of the data in Fig. 17 as a measure of δ-ray statistics and of reproducibility of response of the thin emulsions makes it appear quite unlikely that the event was a normal nucleus. Consideration of the visual and photographic data for the thick emulsion, together with the AMID data for the thin emulsions, makes the case against a normal nucleus very much stronger than if data were available only for the thick emulsion or the two thin emulsions.

Finally, we consider the strength of the constraint from the Lexan data that $|Z/\beta| \approx 110$ to 115. Referring to the last two rows of Table 1, we see that an ultrarelativistic nucleus with $Z \approx 89$ to 90, $\beta \approx 0.98$ to 1, and $Z^*/\beta \approx 89$ to 92 could produce the same track etch rate as an Fe nucleus with $Z^*/\beta \approx 114$ if the restricted energy loss model (eq. 2) were an adequate representation of the energy deposition at small radial distances. The distant energy deposition by such an ultrarelativistic nucleus would probably be compatible with the track structure in the emulsion. However, the evidence in Table 1 shows that the restricted energy loss model does not fit the available data. Lest one think that a discrepancy of one charge at $Z = 10$ is not significant, we point out that, because the track etch rate increases roughly as the fourth or fifth power of Z, a 10% error in charge amounts to at least a 50% error in etch rate. At $Z \approx 77$ to 92 the discrepancy is about ten charges. Thus, both the low- and high-

charge measurements of standard particles summarized in Table 1 are incompatible with a restricted energy loss model. By using eq. 4 instead of the restricted energy loss model and arbitrarily dropping the value of K from 62 to about 15 or 20, one could somewhat reduce the discrepancy with the low- and high-charge measurements in Table 1 and allow a nucleus with $Z = 96$ and $\beta \approx 1$ to produce a track like that of an Fe nucleus with $Z^*/\beta = 114$. With this choice of K, the cosmic ray abundance peak would move to $Z \approx 70$ instead of 67, and the ions with $Z = 10$ would have charges calculated to be $Z \approx 10.7$ instead of 11. Even this "optimum" choice of energy deposition equation could, we believe, be reconciled with the data in Table 1 only by rejecting the astrophysical evidence for r-process nucleosynthesis and an end of the charge spectrum at $Z \approx 92$ to 96. Choosing a value of K between 20 and 62 does not help, because there is no known long-lived nuclide with $Z > 96$.

It is true that we have no direct measurement of the velocity dependence of the track etch rate at very high Lorentz factor. One might hypothesize that at high γ the etch rate might increase enough that a nucleus with $Z \approx 90$ to 96 could mimic a nucleus with low γ and $Z/\beta \approx 114$. However, the density effect is known to prevent an increase of the energy loss due to distant collisions at high γ in a condensed medium, whereas it does not affect the close collisions. Regardless of whether eq. 2, 4, or 5 represents track formation in Lexan better, it is clear that the density effect will prevent a relativistic rise in the etch rate because etched tracks result from energy deposited at small radial distances.

We conclude that a normal nucleus cannot account for the event unless we invoke large downward fluctuations in the distant energy deposition or in the response of all three emulsions.

b. Was the event a fast, heavy antinucleus?

As row 4 of Table 4 points out, an antinucleus with suitable charge, velocity, and possible fragmentations is compatible with the data in Lexan and in the emulsions. We consider now the theoretical expectations, previous searches, and indirect negative astrophysical evidence for antinuclei in nature. The positron, the antiproton, and numerous other antiparticles up to anti-^{3}He in mass have been produced in accelerators, and even the most conservative physicists would agree that highly charged antinuclei are not excluded by the laws of physics. In fact, the symmetry between particles and their charge conjugate antiparticles is quite well established, whereas the symmetry between electric and magnetic charge remains only a theoretical possibility.

The question of whether the present universe could be baryon-symmetric is still under debate. Of the theoretical models purporting to explain how large-scale regions of matter and antimatter could separate and survive complete annihilation, the one by Omnes and co-workers[51] has been developed the most quantitatively and has been discussed the most in recent years. Our views and those of a number of astrophysicists are that, though various aspects of the model have been criticized[52], it describes a scenario that might have occurred, and that the question of whether large-scale regions of antimatter exist will have to be answered experimentally.

Gamma-ray measurements from satellites and balloons provide upper limits on the rate of annihilation of matter and antimatter in different regions of space.[52] They suggest that there is very little antimatter in the intergalactic medium, in neighboring galaxies, or in gas in our Galaxy, and that the fraction of antistars in our Galaxy is likely to be less than $\sim 10^{-4}$. However, Stecker[53] has argued that the best explanation of the shape of the energy spectrum of diffuse γ-rays is that they are the products of annihilation integrated back in time to redshifts of ~100. Further, Sofia and Van Horn[54] and Vincent and Thompson[55] have proposed that the much studied γ-ray bursts from space are caused by annihilation of antimatter.

The above evidence is indirect. Measurement of the sign of the nuclear charge of cosmic rays would be direct. Searches with superconducting magnets have yielded only null results.[52] The upper limit on the fractional flux of antinuclei in the cosmic rays is $\sim 10^{-5}$ to $\sim 10^{-4}$ for light antinuclei and $\sim 10^{-3}$ to $\sim 10^{-2}$ for anti-iron. There is, however, no direct negative experimental evidence against the interpretation of our event as an antinucleus with $|Z| \gtrsim 76$, because the total collecting power of all such experiments is about four orders of magnitude smaller than that of Lexan and emulsion experiments. Furthermore, almost all of the previous searching was done at high rigidity, whereas if our particle was an antinucleus it had a rather low rigidity. Even if one assumes locally identical charge spectra and rigidity spectra for positive and negative nuclei, a fractional flux of 10^{-5} to 10^{-4} is not seriously discordant with our observation of one possible antinucleus. A total of $\sim 10^2$ particles with $|Z| \gtrsim 60$ and $\beta \gtrsim 0.6$ have been identified with a Lexan stack and have had their distant energy deposition measured with emulsion. To

have found one antinucleus out of 10^2 normal nuclei would be regarded as lucky but not statistically incompatible with an average ratio a few hundred times lower.

c. Was the event a slow, supermassive particle?

Row 5 of Table 4 indicates that a hypothetical particle with a huge ratio of A/Z could fit the data and does not conflict with previous searches for such particles.

Yock[47] has proposed that hadrons are composed of heavy, highly electrically charged "subnucleons," of which the heaviest stable one would have a mass of order 200 to 2000 amu and electric charge of order 40e. In section 7 we showed that if our event was a slow particle with $\beta = 0.4$ and $Z/\beta = +114$, its charge would be $Z \approx 46$ and its mass would be $\gtrsim 1840$ amu. These numbers are consistent with those for Yock's heaviest subnucleon.

Lipkin[56] has noted that if free quarks exist[57] they should have an attractive interaction with nucleons and should form stable quark-nuclei that might have very large values of Z and A. The quark-nucleus with greatest binding energy per nucleon would have a Z greater than that of iron, the ordinary nucleus with greatest binding energy per nucleon, and A/Z might be considerably larger than for ordinary nuclei.

Several theorists[48-50] have discussed the possibility of an abnormally dense phase of nuclear matter with peculiar properties. The range of masses, charges, and A/Z ratios contemplated in one or another of these papers overlaps with the values required of our particle.

There is still another hypothetical particle to consider. Hawking[58] has suggested that a large number of small black holes, of mass 10^{-5} g upwards, may have been formed as a result of fluctuations

in the early universe. The lower mass limit is a consequence of quantum gravitational effects, which limit the minimum Schwarzschild radius to about the Planck length. Given that the average density of the universe is no greater than $\sim 10^{-29}$ g/cm^3, the flux of black holes of mass $\gtrsim 10^{-5}$ g cannot exceed $\sim 10^{-2}$/m^{2}y. The probability of such a black hole striking one of our detectors is thus small but not impossibly small. However, Hawking[59] has shown that a charged black hole would spontaneously lose charge by pair creation and that even an uncharged black hole would lose mass rapidly by this process if its mass were less than $\sim 10^{15}$ g. Thus, a small black hole would be essentially neutral and could not produce detectable effects in Lexan or emulsion.

The collecting power of Lexan/emulsion stacks so far exceeds that of all other detectors in balloons or satellites that the failure of other groups to detect a supermassive particle such as Yock's subnucleon, Lipkin's quark-nucleus, or an abnormally dense particle at high altitude is perfectly natural. We must consider also the possibility that a slow, supermassive particle might reach sea level without a destructive interaction in the atmosphere. A particle with initial velocity ~ 0.4 c and charge 46e would reach sea level at vertical incidence if its mass exceeded $\sim 2 \times 10^5$ amu and if it interacted only by ionization loss. Such a slow particle would not be accompanied by an electromagnetic shower and could be detected at sea level or greater depths only by a detector sensitive to a single particle of extraordinarily high ionization rate. It would probably have gone unnoticed in one of the giant emulsion or x-ray film arrays exposed at mountain stations on various continents but would have produced a detectable

track in a sea-level Lexan array[60] exposed at the General Electric Research Laboratory with a collecting power of ~20 m^2y. It might also be detected in a large electronic detector. At sea level several such detectors have been installed, following our first paper on the monopole candidate. No results have yet been published. If its mass were as great as ~10^8 amu it might penetrate deep enough underground to produce a large signal in the neutrino detector of Reines and co-workers.[61] Their accumulated total number of events with unusually large signals corresponds to a flux no greater than ~0.02 $m^{-2}y^{-1}$ at a depth of 10^6 g/cm^2. Neither this limit nor that computed from the sea-level Lexan experiment poses a compelling conflict with our observation of a single event. Highly ionizing, electrically charged supermassive particles at a flux of ~1 $m^{-2}y^{-1}$ would appear to have no observable large-scale astrophysical consequences unless their total mass were so great as to contribute significantly to the expansion rate of the universe. This limit, ~10^{-7} g per particle, seems so high as to be uninteresting. We conclude that the interpretation of our event as a slow, electrically charged particle of mass >10^3 - 10^4 amu is not ruled out by theory, previous searches, or astrophysical effects.

d. Was the event a monopole?

Row 6 of Table 4 summarizes the case against a monopole. Ahlen's analysis showed that a slow monopole would have a lower dE/dx and a lower restricted energy loss than a fast monopole, because of the existence of a velocity-dependent log term. However, the restricted energy-loss model does not fit data for heavy charged particles and the two models that do fit the data, eqs. 4 and 5, would have either a

very weak or non-existent velocity dependence when modified to apply to magnetic monopoles. We regard a slow monopole as incompatible with the Lexan data. At a speed $\beta \approx 0.4$ the distant energy deposition by a monopole would be compatible with the emulsion data.

The observation of one monopole in experiments with a total collecting power of $\sim 1\ m^2 y$ would constitute a very large discrepancy with previous negative searches and with astrophysical effects unless its mass were enormous. Ross[62] has summarized the negative searches, several of which had a collecting power $\sim 10^6$ times greater than that of the Lexan/emulsion experiments. The searches for ancient tracks in mica or obsidian[63] were aimed at relativistic monopoles and might not be sensitive to slow monopoles because the thresholds for track-recording in mica and obsidian, though poorly known, are thought to be marginally able to detect a particle with $Z/\beta \approx 137$ but might not be able to detect a particle like ours, with $Z/\beta \approx 114$. Experiments that used strong magnets to extract monopoles from ferromagnetic ocean sediments and direct them through a plastic track detector[64] or electronic detectors[65] would have given null results if the monopoles had masses greater than $\sim 10^4$ amu, because they would have missed the detectors. The collecting power of the lunar experiments of Alvarez and co-workers[66] decreases rapidly for monopoles of large mass, which would bury themselves at great depths instead of in the shallow sub-surface soil. The maximum available center-of-mass energy at the Fermilab and CERN Intersecting Storage Rings accelerators is inadequate to produce monopoles with mass greater than 14 and 30 amu respectively. Searches at those accelerators have given null results.[67]

Through their interactions with the 2.7° K background radiation and with galactic magnetic fields, monopoles might have profound astrophysical effects. Osborne[68] has obtained very restrictive limits on fluxes of monopoles of either galactic or extragalactic origin by considering energetic photons that would originate in inverse Compton scattering of 2.7° K background photons on energetic monopoles. For a monopole mass greater than $\sim 10^6$ amu these limits are no longer restrictive. Parker[69] has shown that the stability of the interstellar magnetic field limits the flux of monopoles residing in the Galaxy to $\sim 3 \times 10^{-5}$ $m^{-2}y^{-1}$; a higher flux would extract energy from the field faster than it could be replenished. The flux of primordial extragalactic monopoles of sufficiently high energy ($\gtrsim 10^{11}$ GeV) is not restricted by the above argument, because they would give energy to the magnetic fields in a galaxy through which they passed as often as they would extract energy.[70] In order to have $\beta \approx 0.4$, such monopoles must have mass $\gtrsim 10^{11}$ amu. Thus, to reconcile the detection of a monopole with a collecting power of only ~ 1 m^2y with both astrophysical constraints and previous negative searches without invoking a huge statistical fluctuation, the monopole must have a mass $\gtrsim 10^{11}$ amu. Such a large mass is not excluded by theory but is perhaps offensive.

We conclude that there is no justification for referring to the particle as a "monopole candidate."

e. Was the event a superheavy nucleus ($Z \approx 110$ to 114)?

Of the three candidates in Table 4 that give more or less

acceptable fits to all the data, the highly relativistic, superheavy nucleus can be accommodated most comfortably within the framework of theory, previous experiments, and astrophysical effects. There is general agreement[71] among nuclear structure theorists that shell closures at Z = 114, N = 184, will give rise to an island of increased stability around Z = 114, A = 298. Though the calculated decay constants for beta decay, alpha decay, and spontaneous fission for nuclides in this island are uncertain by orders of magnitude, there is a fair body of opinion[71] that the lifetime of at least one nuclide may, in its ground state, exceed 10^6 years. In two independent calculations[72,73], the most stable nuclide was found to have Z = 110, A = 294, and a half-life greater than 10^8 years. The doubly magic nuclide, Z = 114, A = 298, was calculated to be beta-stable and to have a longer spontaneous fission lifetime but a much shorter alpha decay lifetime, with an overall half-life of ~1 year. All nuclides with Z < 110 were calculated to have very short half-lives. Time dilation increases the observed half-life of a relativistic nuclide by its Lorentz factor, but the flux of cosmic rays with energy greater than γMc^2 decreases as $\gamma^{-1.5}$, so that it would be unlikely for a nuclide with a half-life in its rest frame less than $\sim 10^5$ years to survive in the cosmic rays.

Some theorists feel it is unlikely that, in the conventional r-process, heavy nuclides capturing neutrons and moving upward in A along a path to the neutron-rich side of the beta-stability line can avoid fission until they reach the island of stability.[71] Even so, it is possible that superheavy elements might be synthesized in a low temperature decompression of neutron star matter by following a path

near the neutron drip line where the fission barrier remains above zero.[74] The calculations involve large extrapolations and are quite uncertain. The issue must in the end be decided experimentally. Experiments with heavy ion accelerators at Berkeley and Dubna have been unsuccessful in producing superheavy elements, but attempts are continuing. The interested reader should consult ref. 71 for recent papers on the subject of superheavy elements.

Anders and co-workers[75] have isolated rare phases in certain meteorites that contain traces of xenon gas with a peculiar isotopic composition. They have interpreted the isotopic distribution as evidence for in-situ decay by spontaneous fission of small quantities of a superheavy element and have attempted to characterize its chemistry. The interpretation is bold and not without its critics. Blake et al.[76] showed that if this indirect evidence is correct, the relative abundance of superheavy elements in the cosmic rays can be estimated, provided several assumptions are made. They estimated an abundance ratio $[Z \gtrsim 110]/[74 \leq Z \leq 87]$ between 0.0002 and 0.006, which does not conflict with our ratio, 0.004, based on one event out of ~250 events with $74 \leq Z \leq 87$ in all Lexan or emulsion experiments to date.

We conclude that an ultrarelativistic nucleus with Z = 110 gives an acceptable fit to the Lexan data; gives a distant energy deposition in acceptable agreement with the emulsion data and substantially lower than that for nuclei with $Z/\beta = +114$, $Z \lesssim 96$, and $0.6 \lesssim \beta \lesssim 0.84$; is predicted by theory to have a long enough life-time $\gamma\tau$ in the laboratory frame to survive in the cosmic rays if made in astrophysical nuclear reactions; and is consistent with the existing, indirect, positive meteoritic evidence.

f. Can the event be explained by a freak occurrence associated with one or more normal nuclei?

Several improbable scenarios have been suggested, none of which account for both the Lexan data and the emulsion data. Hodson[76] has proposed that a closely collimated jet of $\sim 10^4$ relativistic, singly-charged particles resulting from the interaction of a primary cosmic ray with energy $\gtrsim 10^{18}$ eV in the material just above the first Lexan detector might account for the data. We will disregard the fact that the flux of protons of such energy is extraordinarily low and that the probability of interacting within ~1 mm of the top Lexan sheet is also quite low. We will accept Hodson's main argument that because of destructive interference, Cerenkov emission might be suppressed in a sufficiently closely collimated jet consisting of practically equal numbers of positive and negative secondaries. However, the suggestion of a jet must be rejected because it cannot account for the nearly constant etch rates throughout the Lexan stack. The possibility that a jet could produce an etchable track was quantitatively discussed ten years ago[77], and it was shown that such a track could not exceed a few microns in length. The reason is that the spacing of the bundle of particles increases, and the ionization density decreases, with distance from the point of interaction, so that the track etch rate will decrease with depth. About half of the total number of particles in the jet will be included within an angle $\theta \approx (\gamma_{CM})^{-1}$, where γ_{CM} is the Lorentz factor in the center of momentum system. For a primary energy of 10^{18} eV, half of the particles will emerge at angles greater than $\sim 2 \times 10^{-5}$ rad, which in a stack of thickness ~1 cm amounts to

a lateral spread greater than 2000 Å. Compared to a single particle with $Z/\beta \approx 114$, which forms an etchable track by energy deposition mainly inside a cylinder of radius $\lesssim$100 Å, the density of radiation damage by the jet will be reduced by a factor at least $(2000/100)^2 = 400$ at the bottom of the stack. Only in the top sheet of Lexan would the radiation damage density be great enough to form an etchable track.

A similar argument applies to suggestions that the particle might have been a nucleus that fissioned above the stack, a relativistic dust grain, or a relativistic molecule containing many nuclei with charges such that $\Sigma Z_i^2 \approx 114^2$. Scattering of the individual constituents would cause the track etch rate to decrease from top to the bottom of the stack.

A nucleus that passed upward through the stack could explain the reported absence of a Cerenkov signal, because the plastic radiator film was coated only on the bottom with the fast recording film, but it could not explain the combination of data in the Lexan stack and in the three emulsions.

g. Future expanded searches for more particles

To allow for the possibility that the average flux of particles similar to the monopole candidate may be far lower than given by the reciprocal of the overall collecting power of Lexan/emulsion experiments to date, future searches ought to have a vastly greater collecting power. The space shuttle will eventually make it possible to expose passive arrays of detectors up to several hundred m^2 in area above the earth's atmosphere for times of the order of one year. If emulsion were used to measure the distant energy deposition, shielding or a

near equatorial orbit would have to be employed to reduce the background exposure by ionizing particles in the trapped radiation belts. An array of plastic detectors, including a well-shielded emulsion array, could provide a factor $\sim 10^2$ increase in collecting power over the present value of ~ 1 $m^2 y$. The feasibility of such an experiment is under study.

In the summer of 1976 a colleague at Berkeley, M. Salamon, began an exposure of a 1500 m^2 array of Lexan detectors at a sea-level site at Lawrence Livermore Laboratory. The array consists of four layers of Lexan separated by cardboard absorbers giving a total thickness of ~ 0.5 g/cm^2, all double-bagged in waterproof plastic and covered with a light layer of gravel to prevent damage by heat, light and wind. An analysis of the stack after a two-year exposure would give us about a 200-fold increase in collecting power over the General Electric sea-level experiment.[60] It could not detect fast superheavy nuclei or fast antinuclei, both of which would disintegrate high in the atmosphere, but it is a relatively simple way of looking for extremely massive, electrically or magnetically charged particles that might not disintegrate and that might not produce showers or be detectable in other types of monopole experiments.

Further in the future it should be possible to build electronic arrays ten or more square meters in area that would orbit the earth for several years and record both the close energy deposition (thus giving $|Z|/\beta$) and the distant energy deposition by particles such as the one we have detected. As a specific example, instead of searching for heavy antinuclei in space with a superconducting magnet of limited

area, one could use a large plastic scintillator, which responds only to the distant energy deposition[79], together with a detector such as a gas-filled proportional counter, which responds to the total dE/dx, and a detector that measured velocity, such as a Cerenkov detector.

9. Summary and Conclusions

We have presented detailed evidence that the event in module 104, referred to for convenience as the monopole candidate, had the following two characteristics:

(1) Throughout the ~1.4 g/cm^2 thickness of detector stack it had a roughly constant value of $|Z|/\beta \approx 109$ to 114, derived from measurements of track etch rate, which depend on energy deposition at radial distance $\lesssim 10^{-2}$ μm.

(2) Its energy deposition at radial distance $\gtrsim 20$ μm, judged visually and photographically in the Ilford 200 μm G-5 emulsion and measured with an image dissector in two independent Kodak 10 μm NTB-3 emulsions, was consistent with that from nuclei with $Z/\beta \approx 80$ to 90 and $0.6 \lesssim \beta \lesssim 0.9$, and was incompatible with that expected from known cosmic ray nuclei with $Z/\beta = 109$ to 114, $Z \leq 96$, and $0.6 \lesssim \beta \lesssim 0.84$.

If these two characteristics are accepted, calculations of energy deposition that employ the exact (Mott) nucleus-electron scattering cross section show that known cosmic ray nuclei ($Z \leq 96$) are incompatible with the data, even if unlikely fragmentation sequences or effective charges are allowed. A monopole is incompatible with the data. Three classes of hypothetical particles that deposit less energy at large distances than do known nuclei with the same $|Z|/\beta = 109$ to 114 are compatible with the data:

(1) A slow, supermassive particle with $\beta \approx 0.4$, charge ≈ 45 e, and mass $>10^3$-10^4 amu.

(2) A fast antinucleus with $Z/\beta \approx -109$ to -114 and $76 \lesssim |Z| \lesssim 96$ that might fragment with loss of one or two charges.

(3) A very fast nucleus with $Z \approx 110$ to 114 and $\beta \gtrsim 0.99$.

The particle would have been a normal nucleus only if at least one of the above two characteristics can be rejected. Consider the two possibilities:

(1) The interpretation of the Lexan data may be in error. For ultrarelativistic velocities, perhaps Lexan responds not to Z/β but to the restricted energy loss (eq. 2), so that the particle might have been a nucleus with $\beta \approx 1$ and $Z \approx 90$. This is inconsistent with the evidence in Table 1 that the velocity dependence given by eq. 2 does not fit the data at high Z and high β, and we have pointed out that a relativistic rise in energy deposition should occur only for close collisions, not for the distant collisions that lead to chemically etchable tracks.

(2) The interpretation of the emulsion data may be in error. The low energy deposition at large radial distances might be either <u>real</u> but due to a downward fluctuation or <u>apparent</u> and due to local regions of decreased sensitivity around the track. However, we believe that Hagstrom's Monte Carlo calculations[14] show that it is extremely unlikely that fluctuations in distant energy deposition by a normal nucleus can account for the appearance of the track in the 200 μm emulsion. Further, our calibrations of the sensitivity of individual emulsions by measurements of the optical density of Fe tracks of

known β provide evidence that the low density of silver grains around the track of the particle was not caused by an abnormally insensitive region in the 200 μm emulsion. The independent measurements of a small distant energy deposition by the particle in the two thin emulsions provide strong support for our view that neither a downward fluctuation by a normal nucleus nor a locally insensitive region of emulsion can account for the emulsion data.

We have considered several freak occurrences associated with one or more normal nuclei and find that they cannot account for the event.

Although the identity of the particle remains ambiguous, we believe the evidence for a new class of highly ionizing particles is sufficiently strong to justify intensified searches with instruments of increased collecting power.

Acknowledgments

During the prolonged investigation of this controversial event we have been sustained and encouraged by many colleagues. We are indebted for numerous ideas and valuable conversations to S.P. Ahlen, L. Alvarez, B.G. Cartwright, P.A.M. Dirac, P.H. Fowler, A.S. Goldhaber, M. Goldhaber, J.D. Jackson, E.M. McMillan, and G.H. Trilling. We wish to record our indebtedness to R. Hagstrom for the independent role he played in the analysis. We are also indebted to P.H. Fowler for hospitality and assistance in interlaboratory comparisons of photodensitometry and of ultraheavy cosmic ray tracks in emulsions. Research at Berkeley was supported in part by ERDA Contract AT (04-3)-34 and by NASA Grant NGR 05-003-376; research at Houston was supported in part by NSF Grant PHY 76-08374. PBP thanks the Guggenheim Foundation for support and H. Sato at Research Institute for Fundamental Physics, Kyoto, and D. Hovestadt at the Max Planck Institute for Physics and Astrophysics, Garching bei Munchen, for their hospitality while much of the manuscript was written.

References

1. P.B. Price, E.K. Shirk, W.Z. Osborne, and L.S. Pinsky, Phys. Rev. Lett. 35, 487 (1975).
2. R.L. Fleischer, P.B. Price, and R.M. Walker, Nuclear Tracks in Solids: Principles and Applications, Univ. of California Press, Berkeley (1975).
3. M.W. Friedlander, Phys. Rev. Lett. 35, 1167 (1975).
4. L. Alvarez, LBL Report No. 4260 (1975).
5. P.H. Fowler, Proc. 14th Inter. Cosmic Ray Conf., Vol. 12, p. 4049, Munich, 1975.
6. R.L. Fleischer and R.M. Walker, Phys. Rev. Lett. 35, 1412 (1975).
7. E.K. Shirk, P.B. Price, E.J. Kobetich, W.Z. Osborne, L.S. Pinsky, R.D. Eandi, and R.B. Rushing, Phys. Rev. D7, 3220 (1973).
8. L.S. Pinsky, Ph.D. Thesis, available from Johnson Space Center as NASA Report TMX-58102 (1972).
9. P.B. Price and E.K. Shirk, Proc. 14th Inter. Cosmic Ray Conf., Vol. 1, p. 268, Munich, 1975; E.K. Shirk and P.B. Price, Astrophys. J. 220, 719 (1978).
10. P.H. Fowler, C. Alexander, V.M. Clapham, D.L. Henshaw, C. O'Ceallaigh, D. O'Sullivan, and A. Thompson, Nucl. Instr. and Meth. 147, 195 (1977).
11. E. Bauer, Proc. Camb. Phil. Soc. 47, 777 (1951); H.J.D. Cole, Proc. Camb. Phil. Soc. 47, 196 (1951).
12. S.P. Ahlen, Phys. Rev. D14, 2935 (1976); Phys. Rev. D17, 229 (1978).
13. P.B. Price, "Status of the Evidence for a Magnetic Monopole," in New Pathways in High Energy Physics: Magnetic Charge and Other

Fundamental Approaches, Plenum Publ. Co., New York, 1976, pp. 167-214.

14. R. Hagstrom, Phys. Rev. Lett. 38, 729 (1977). Hagstrom's Monte Carlo program for energy deposition in emulsion will be described in detail in a future publication.

15. T.E. Pierce and M. Blann, Phys. Rev. 173, 390 (1968).

16. P.H. Fowler, V.M. Clapham, V.G. Cowen, J.M. Kidd, and R.T. Moses, Proc. Roy. Soc. (London) A318, 1 (1970).

17. A. Chatterjee, H.D. Maccabee and C.A. Tobias, Radiat. Res. 54, 479 (1973).

18. E.V. Benton, U.S. Naval Radiological Defense Lab., Report TR-68-14 (1968).

19. W. Enge, K. Grabisch, L. Dallmeyer, K.P. Bartholomä, and R. Beaujean, Nucl. Instr. and Meth. 127, 125 (1975).

20. R.M. Sternheimer, Phys. Rev. 103, 511 (1956).

21. D. O'Sullivan, P.B. Price, E.K. Shirk, P.H. Fowler, J.M. Kidd, E.J. Kobetich, and R. Thorne, Phys. Rev. Lett. 26, 463 (1971).

22. D. O'Sullivan, E.J. Kobetich, E.K. Shirk, and P.B. Price, Phys. Lett. 34B, 49 (1971).

23. P.B. Price, R.L. Fleischer, D.D. Peterson, C. O'Ceallaigh, D. O'Sullivan, and A. Thompson, Phys. Rev. Lett. 21, 630 (1968).

24. P.B. Price, P.H. Fowler, J.M. Kidd, E.J. Kobetich, R.L. Fleischer, and G.E. Nichols, Phys. Rev. D3, 815 (1971).

25. D.D. Peterson, Rev. Sci. Instr. 41, 1254 (1970).

26. R.P. Henke and E.V. Benton, U.S. Naval Radiological Defense Laboratory Report No. 1102 (1966).

27. D. Cline and P.M.S. Lesser, Nucl. Instr. and Meth. 82, 291 (1970).

28. H.H. Heckman, D.E. Greiner, P.J. Lindstrom, and F.S. Bieser, Phys. Rev. Lett. 28, 926 (1972); D.E. Greiner, P.J. Lindstrom, H.H. Heckman, B. Cork, and F.S. Bieser, Phys. Rev. Lett. 35, 152 (1975).

29. L.W. Wilson, Ph.D. Thesis, University of California, Berkeley, 1978.

30. G.M. Raisbeck, H.J. Crawford, P.J. Lindstrom, D.E. Greiner, F.S. Bieser, and H.H. Heckman, Proc. 15th Inter. Cosmic Ray Conf., Vol. 2, p. 67, Plovdiv, 1977.

31. N. Bohr, "Penetration of Atomic Particles through Matter," Kgl. Danske Videnskab. Selskab Mat-fys. Medd. XVIII, No. 8 (1948).

32. B.G. Cartwright, E.K. Shirk, and P.B. Price, accepted by Nucl. Instr. and Meth.

33. A.H. Rosenfeld, Ann. Rev. Nuc. Sci. 25, 555 (1975).

34. P.R. Bevington, Data Reduction and Error Analysis for the Physical Sciences, McGraw-Hill Book Co., New York, 1969.

35. N.F. Mott, Proc. Roy. Soc. (London) A124, 426 (1929) and A135, 429 (1932).

36. Y. Kazama, C.N. Yang, and A.S. Goldhaber, Phys. Rev. D15, 2287 (1977).

37. R. Katz and E.J. Kobetich, Phys. Rev. 186, 344 (1969).

38. E.J. Kobetich and R. Katz, Nucl. Instr. and Meth. 71, 226 (1969).

39. E.J. Kobetich and R. Katz, Phys. Rev. 170, 391 (1968).

40. W.H. Barkas, Nuclear Research Emulsions, Academic Press, New York, 1963.

41. P.B. Price, E.K. Shirk, W.Z. Osborne, P.H. Fowler, and D.L. Henshaw, "Photodensitometry of Tracks of Highly Ionizing Particles

in Cosmic Rays," submitted to Nucl. Instr. and Meth. (1978).

42. P.H. Fowler, Nucl. Instr. and Meth. 147, 183 (1977).

43. L.V. Spencer, unpublished calculations. These tables are an extension of the earlier tables of J.A. Doggett and L.V. Spencer, Phys. Rev. 103, 1597 (1956).

44. L.V. Spencer, U.S. Nat. Bureau of Standards Monograph 1 (1959).

45. M.J. Berger and S.M. Seltzer, in Studies in Penetration of Charged Particles in Matter, U. Fano, ed., NAS-NRC Publ. 1133 (National Academy of Sciences-National Research Council, Washington, D.C., 1964).

46. S.P. Ahlen, Phys. Rev. A17, 1236 (1978).

47. P.C.M. Yock, Int. J. Theor. Phys. 2, 247 (1969); Annals of Physics 61, 315 (1970); Phys. Rev. D13, 1316 (1976).

48. A.R. Bodmer, Phys. Rev. D4, 1601 (1971).

49. T.D. Lee and G.C. Wick, Phys. Rev. D9, 2291 (1974).

50. A.B. Migdal, G.A. Sorokin, O.A. Markin, and I.N. Mishustin, Sov. Phys. JETP, in press.

51. R. Omnes, Astron. and Astrophys. 10, 228 (1971); Phys. Reports 3C, 1 (1972).

52. G. Steigman, Ann. Rev. Astron. Astrophys. 14, 339 (1976).

53. F.W. Stecker, Astrophys. J. 212, 60 (1977).

54. S. Sofia and H.M. Van Horn, Ap. J. 194, 593 (1974); S. Sofia and R.E. Wilson, Ap. Space Sci. 39, L7 (1976); S. Sofia and H.M. Van Horn, Ann. N.Y. Acad. Sci. 262, 197 (1975).

55. J.R. Vincent and W.B. Thompson, submitted to Nature (1976).

56. H.J. Lipkin, unpublished discussion at International Symposium on Lepton & Photon Interactions at High Energies, Stanford Univ., 1975.

57. G.S. La Rue, W.M. Fairbank, and A.F. Hebard, Phys. Rev. Lett. 38, 1011 (1977).

58. S. Hawking, Mon. Not. Roy. Astron. Soc. (London) 152, 75 (1971).

59. S. Hawking, Comm. Math. Phys. 43, 199 (1975).

60. R.L. Fleischer, H.R. Hart, G.E. Nichols, and P.B. Price, Phys. Rev. D4, 24 (1971).

61. F. Reines, private communication.

62. R.R. Ross, "Experimental Searches for Magnetic Monopoles," in New Pathways in High Energy Physics: Magnetic Charge and Other Fundamental Approaches, Plenum Publ. Co., New York, 1976, pp. 151-165.

63. R.L. Fleischer, P.B. Price, and R.T. Woods, Phys. Rev. 184, 1398 (1969).

64. R.L. Fleischer, I.S. Jacobs, W.M. Schwartz, P.B. Price, and H.G. Goodell, Phys. Rev. 177, 2029 (1969); R.L. Fleischer, H.R. Hart, I.S. Jacobs, P.B. Price, W.M. Schwarz, and F. Aumento, Phys. Rev. 184, 1393 (1969).

65. H.H. Kolm, F. Villa and A. Odian, Phys. Rev. D4, 1285 (1971).

66. P.H. Eberhard, R.R. Ross, L.W. Alvarez, and R.D. Watt, Phys. Rev. D4, 3260 (1971); R.R. Ross, P.H. Eberhard, L.W. Alvarez, and R.D. Watt, Phys. Rev. D8, 698 (1973).

67. R.A. Carrigan, F.Z. Nezrick, and B.P. Strauss, Phys. Rev. D10, 3867 (1974); P.H. Eberhard, R.R. Ross, J.D. Taylor, L.W. Alvarez, and H. Oberlack, Phys. Rev. D11, 3099 (1975).

68. W.Z. Osborne, Phys. Rev. Lett. 24, 1441 (1970).

69. E.N. Parker, Ap. J. 160, 383 (1970).

70. S.A. Bludman and M.A. Ruderman, Phys. Rev. Lett. 36, 840 (1976).

71. J.R. Nix, Ann. Rev. Nuc. Sci. 22, 65 (1972); "Superheavy Elements--Theoretical Predictions and Experimental Generation," Proc. 27th Novel Symposium, Ronneby, Sweden, ed. S.G. Nilsson and N.R. Nilsson, Phys. Scripta 10A, 1-187 (1974).

72. S.G. Nilsson, S.G. Thompson, and C.F. Tsang, Phys. Lett. B28, 458 (1969).

73. J.R. Nix, Phys. Today 25, No. 4, 30 (1972).

74. J.M. Lattimer, J. Mackie, D.G. Ravenhall, and D.N. Schramm, Ap. J. 213, 225 (1977).

75. R.L. Lewis, B. Srinivasan, and E. Anders, Science 190, 1251 (1975); E. Anders, H. Higuchi, J. Gros, H. Takahashi, and J.W. Morgan, Science 190, 1262 (1975).

76. J.B. Blake, K.L. Hainebach, D.N. Schramm, and J.D. Anglin, Astrophys. J. 221, 694 (1978).

77. A.L. Hodson, Proc. 14th Inter. Cosmic Ray Conf., Vol. 12, p. 4065, Munich, 1975.

78. R.L. Fleischer, P.B. Price, R.M. Walker, and M. Maurette, J. Geophys. Res. 72, 331 (1967).

79. S.P. Ahlen, B.G. Cartwright, and G. Tarlé, Nucl. Instr. and Meth. 147, 321 (1977).

80. G. Tarlé, S.P. Ahlen, B.G. Cartwright, and P.B. Price, "Isotopic Composition of Iron Group Nuclei at 320-500 MeV/amu," submitted to Phys. Rev. Letters (1978).

Table 1

Tests of Various Models of Tracks in Lexan, Using Standard Particles

Source	Standard particle Z	Standard particle β	Standard particle Z*/β	Fe nuclei with same etch rate as standard particle β_{Fe}	Fe nuclei with same etch rate as standard particle $(Z^*/\beta)_{Fe}$	Z from Z*/β model	Z from J(K=62) model	Z from $(dE/dx)_{W_o}$ model
	10	.149	66.1	.39	66.5	10.0	10.2	11.0
Accelerator	14	.124	105.9	.24	104.5	13.8	14.0	14.6
(ref. 2,21)	14	.149	90.6	.295	87.0	13.4	13.6	14.3
	18	.149	113.6	.22	113.2	17.9	18.0	18.5
	22	.149	135.1	.18	134.4	21.9	22.0	22.2
	~39	.60	~65	.38	68	41	40	39
Lexan/emulsion	~44	.60	~73	.35	74	44	44	41
stack on Sioux	~50	.69	~72	.34	76	53	52	49
Falls flight	~70	.78	~90	.27	94	73	71	64
(refs. 21,22)	~76	>.97	~77	.32	80	80	78	67
	~92	.65	~139	.17	143	94	92	81
Lexan on Skylab (ref. 9)	peak at Z = 77 (57 events)	>.90 ($\bar{\beta}$=0.95)	~81	~.32	~82	peak at 78	peak at 76	peak at 67
Lexan on other balloon experiments (ref. 10)	peak at Z = 77 (58 events)	>.88 ($\bar{\beta}\approx$0.93)	~83	~.31	~84	peak at 78	peak at 76	peak at 67
Monopole candidate,	?	≡1.0	?	.22	114	114	109	89
if a nucleus	?	≡ .98	?	.22	114	112	108	90

Table 2

Likelihood of Nuclear Fit to Lexan Data for Several Initial Velocities

Initial β	Best initial Z	No. of frags.	Conf. level from F-test	Total prob. in any flight	Likelihood (col.4 x col.5)
>0.99	114*	0	0.6	?	?
0.952	108*	0	1	?	?
0.856	96	1	1	0.3	0.3
0.820	92	1	0.1	0.3	0.03
0.744	82	2	0.005	0.005	2×10^{-5}
0.704	76	2	10^{-5}	0.005	5×10^{-8}
0.600	67	8	0.1	10^{-17}	10^{-18}

*Note that no elements with Z > 96 have been seen before in the cosmic rays and no elements with Z > 106 have been made in accelerators.

Table 3

Events Shown in the Micrographs in Fig. 16

Event* number	Zenith angle	Z	β	Z/β
173-102	9°	69	0.95	73
99-3	8°	52	0.69	75
104-121	10°	?	?	114
191-1	11°	53	0.66	80
156-113	9°	83	0.95	87
121-4	10°	56	0.60	93
83-11	11°	44	0.37	120
119-1	13°	57	0.54	106
76-1	14°	75	0.67	112

*The first number is the module number.

Table 4

Compatibility of Particles with $|Z|/\beta \approx 114$ with the Data and with Other Searches

Type of particle	Properties	Lexan data	Data from 3 emulsions	Lexan + emulsions	Discrepancy with other searches?	Overall compatibility
nucleus	$0.6<\beta\lesssim 0.84$, $Z/\beta=+114$	acceptable, but see Table 1	unacceptable	unacceptable	none	no
nucleus	$0.5<\beta\lesssim 0.6$, $Z/\beta=+114$	unacceptable CL$<10^{-18}$	acceptable if $\beta\approx 0.5$	unacceptable	none	no
nucleus	$0.4\lesssim\beta\lesssim 0.5$, $Z/\beta=+114$	unacceptable CL$<10^{-18}$	acceptable	unacceptable	none	no
antinucleus	$76\lesssim\|Z\|\lesssim 96$, $Z/\beta=-114$	acceptable	acceptable	acceptable	indirect negative evidence	yes
supermassive	$\beta\approx 0.4$, $Z/\beta=+114$, $M>10^3$-10^4 amu	acceptable	acceptable	acceptable	none	yes
magnetic monopole	$\beta\approx 0.4$, g=137e $M>10^3$ amu	unacceptable	acceptable	unacceptable	large discrepancy unless $M\gtrsim 10^{11}$amu	no
nucleus	$\beta\gtrsim 0.99$, $Z\approx 110$	acceptable	acceptable	acceptable	none	yes

Figure Captions

Figure 1. Vertically expanded view of detector array with depths in g/cm^2 Lexan equivalent. The particle traversed the stack at a zenith angle of ~10°. Details of the wrapping and of the shifting mechanism are not shown.

Figure 2. Comparison of measured abundances of ultraheavy cosmic rays with calculated abundances of material with r-process composition and with solar system composition, after distortion resulting from fragmentation and radioactive decay in interstellar space. Corrections to actual counts in top two histograms allow for detector efficiency. (From ref. 9)

Figure 3. Smoothed response curves for the majority of the ultraheavy particles found on the Sioux City balloon flights. A few slow particles with very steep curves are not plotted.

Figure 4. Calibrated Lexan data for the monopole candidate.

Figure 5. Determination of the response to slowing Fe nuclei of the sheets etched 30 hours in Lexan module 104, which contained the monopole candidate.

Figure 6. Etch rate response curves of several stopping ultraheavy nuclei as a function of residual range, along with the curve for Fe from Fig. 5. The parameters in the power law response, eq. 6, were determined from a fit to these data. Note that the curves of Fig. 3 become nearly straight when plotted on a log-log scale with residual range as abscissa.

Figure 7. Evidence that the responses of the sheets etched 20 hours and of the sheets etched 30 hours were the same. (See text)

Figure 8. Etch rate response data for several ultraheavy nuclei, showing examples of fragmentations and small, systematic variations in response of sheets 1, 2, 3, 4, and 35.

Figure 9. Response curves for several combinations of initial Z and β and fragmentations that approximately pass through the data. If the initial β is small, the number of successive fragmentations must be large.

Figure 10. Observed correlation of core radius, R_1, with Z/β for slow ($\beta < 0.58$) and fast ($\beta > 0.58$) particles in the Minneapolis and Sioux City flights. The point for the monopole candidate is labeled X. A geometric correction that takes into account distortion due to shrinkage of the emulsion gives the improved correlation shown on the right.

Figure 11. Observed correlation of halo radius, R_2, with Z/β. The halo radius for the monopole candidate, labeled X, is much less than expected if it were a nucleus with $\beta \gtrsim 0.58$. The data show that slow nuclei ($\beta < 0.58$) tend to have smaller halo radii than fast nuclei with the same Z/β.

Figure 12. Comparison of halo radius, measured visually in the G-5 emulsion, with the quantity K_{rms}, which is a measure of the optical density distribution determined with a photodensitometer. Each point is labeled by the value of β truncated in tenths.

Figure 13. Evidence that the sensitivity of the region of G-5 emulsion near the monopole candidate track was closely the same as the sensitivity of the emulsions traversed by other ultraheavy cosmic rays. The photodensitometric readings with the slit centered on the track axis show the same distribution with Z/β for Fe tracks near the monopole candidate track and in other emulsions.

Figure 14. Photomicrographs in G-5 emulsion of (a) the monopole candidate track, with $Z/\beta = 114$ and zenith angle $\theta = 10°$, and (b) the track of a nucleus with $Z = 75$, $\beta = 0.67$, $Z/\beta = 112$, and $\theta = 14°$. For both tracks the region in focus is about one-third of the way below the top surface of the emulsion.

Figure 15. Photomicrographs of tracks of the events in Table 2, which have similar zenith angles and values of Z/β ranging from 73 to 120. The abnormally small density of silver grains for the monopole candidate track is obvious.

Figure 16. Other tracks at zenith angles similar to those in Fig. 16. In the left column are tracks of particles with Z/β between 79 and 87; in the middle column the Z/β is between 112 and 118; in the right column Z/β is greater than 125.

Figure 17. Density of silver blobs in a cylinder of 30 μm radius around the track in thin emulsion as a function of Z/β for tracks with $\theta \leq 18°$. Reproducibility of measurement at each point is better than the size of the point. In both emulsions the silver grain density for the monopole

candidate (at $Z/\beta = 114$ on the graph) is much lower than expected from the least squares line for normal nuclei.

Figure 18. Radio of exact Mott cross section to Rutherford cross section as a function of kinetic energy or range for an electron initially at rest to be scattered by a fast nucleus or antinucleus with $|Z|/\beta = 114$. Radial diffusion distance of an electron from a track in emulsion is much smaller than the range.

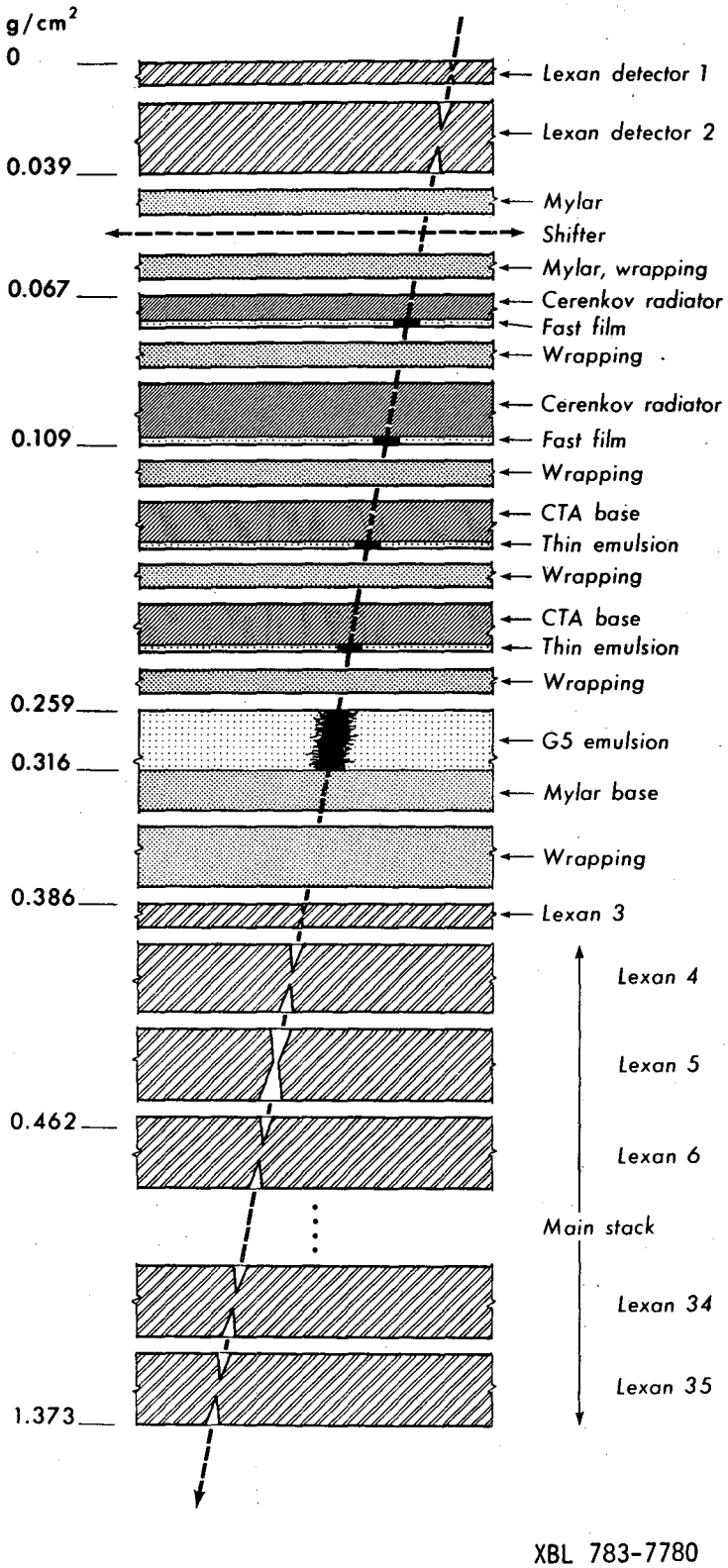
g/cm²
0
0.039
0.067
0.109
0.259
0.316
0.386
0.462
1.373
Lexan detector 1
Lexan detector 2
Mylar
Shifter
Mylar, wrapping
Cerenkov radiator
Fast film
Wrapping
Cerenkov radiator
Fast film
Wrapping
CTA base
Thin emulsion
Wrapping
CTA base
Thin emulsion
Wrapping
G5 emulsion
Mylar base
Wrapping
Lexan 3
Lexan 4
Lexan 5
Lexan 6
Main stack
Lexan 34
Lexan 35
XBL 783-7780

Fig. 1

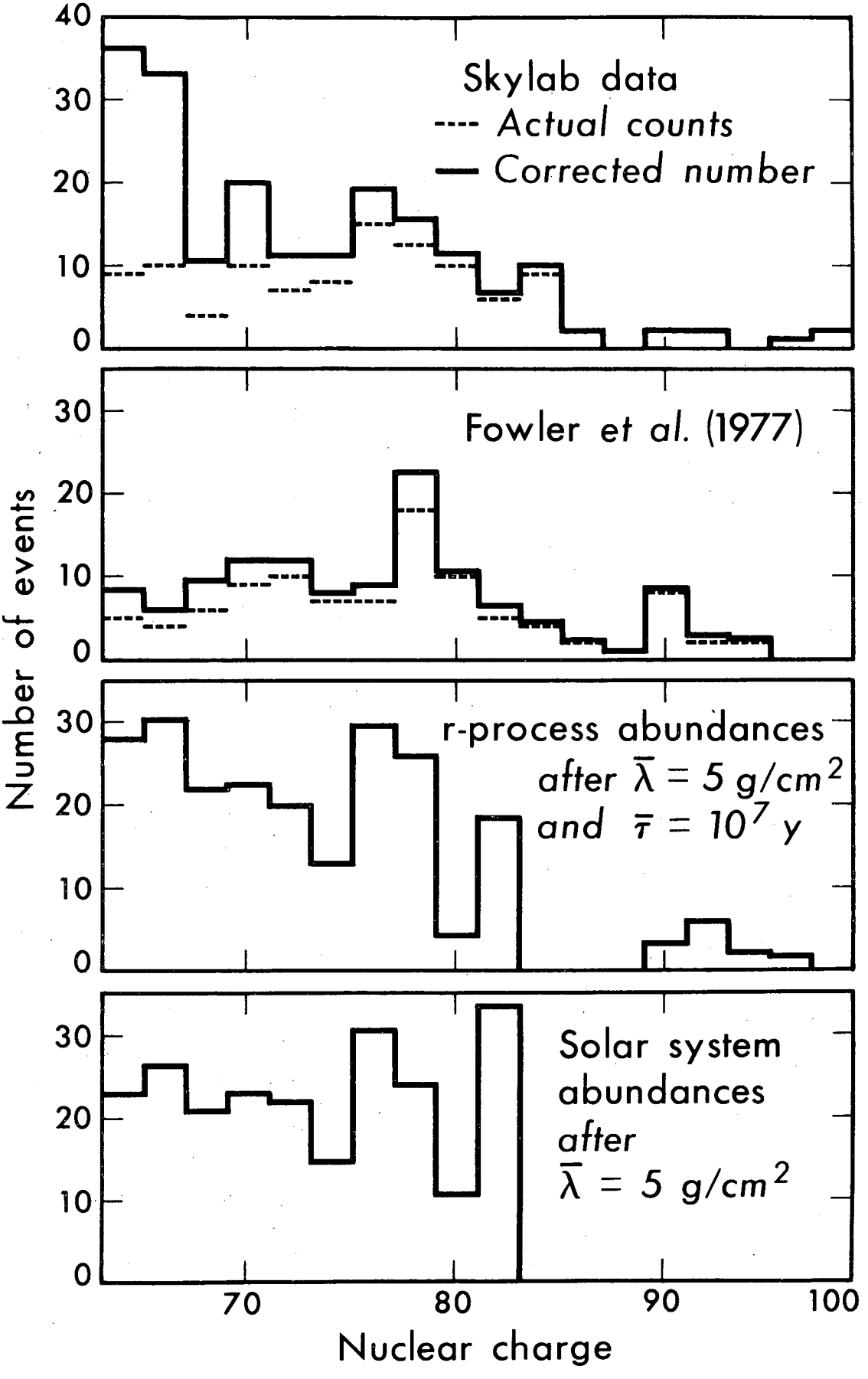

Fig. 2

XBL 784-8312

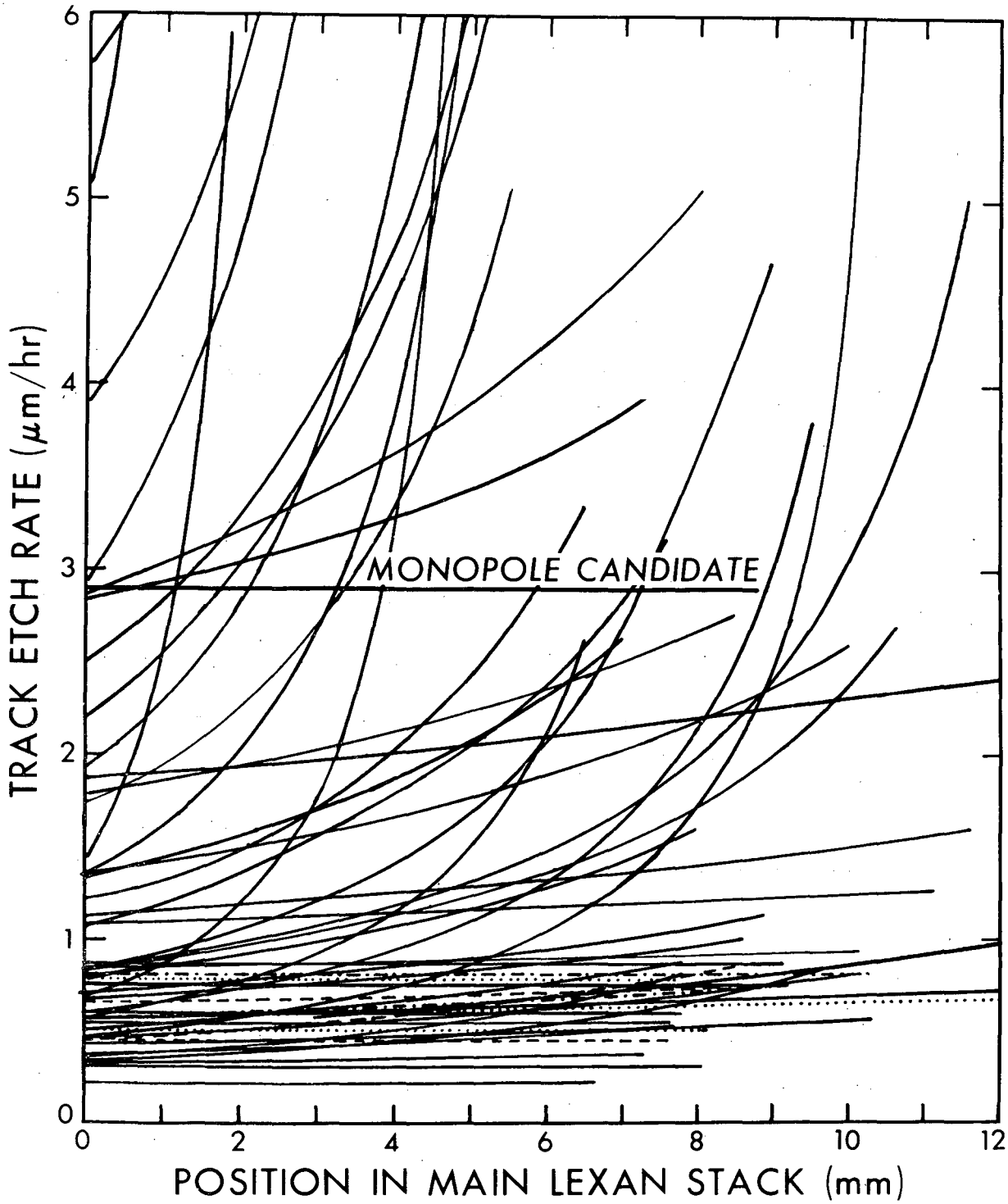

Fig. 3

XBL 784-8299

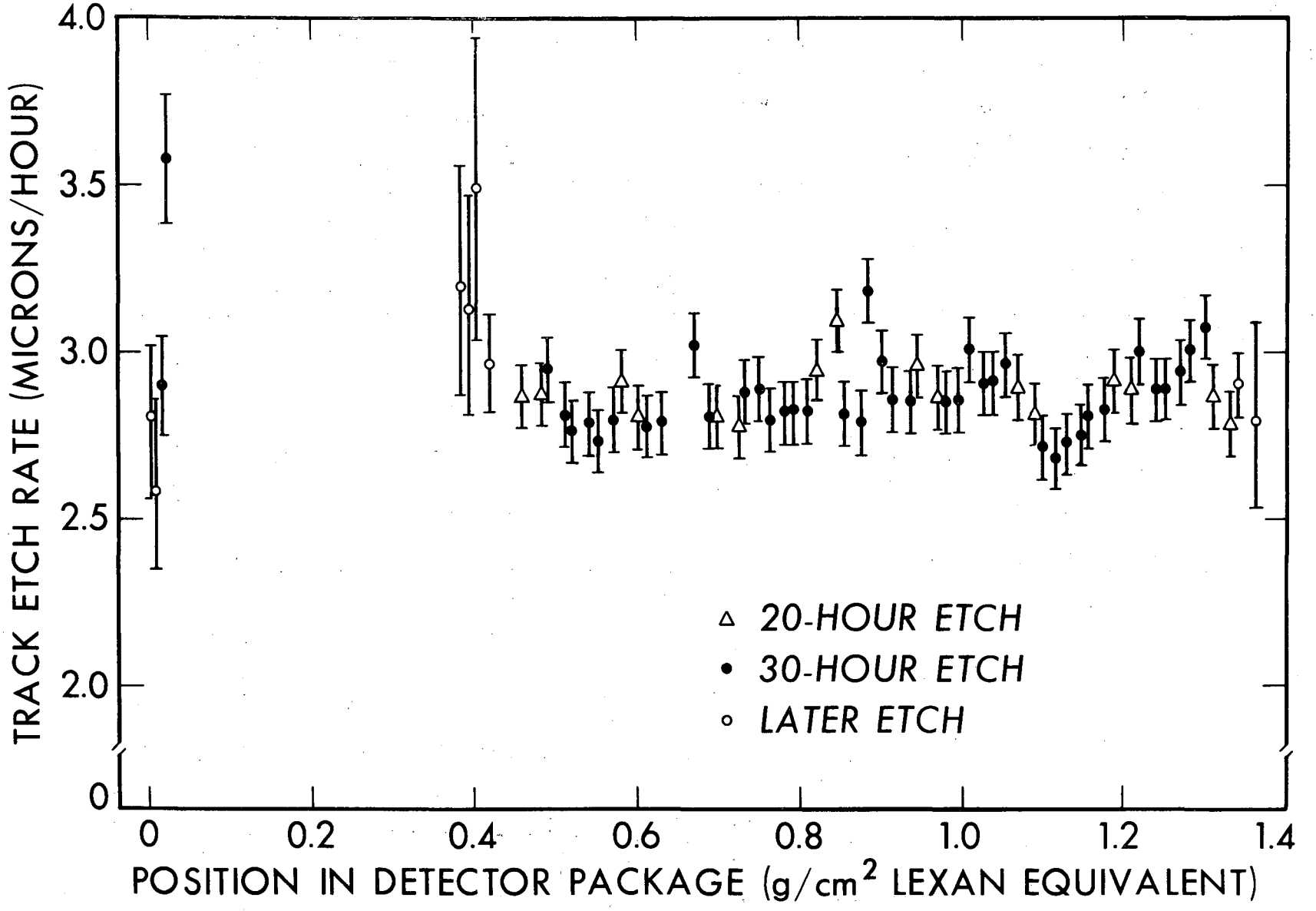

XBL 784-8305

Fig. 4

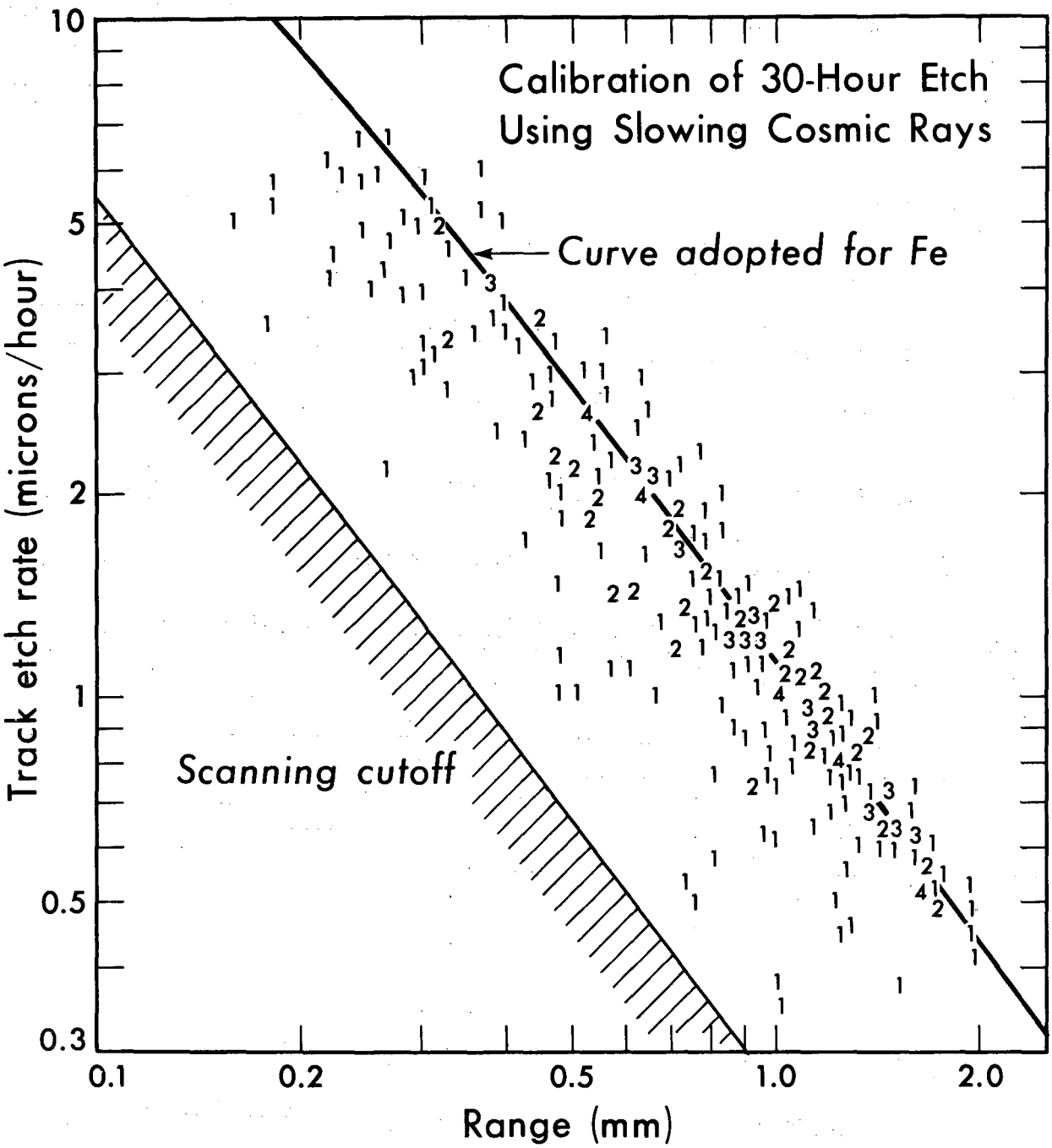

XBL 784-8300

Fig. 5

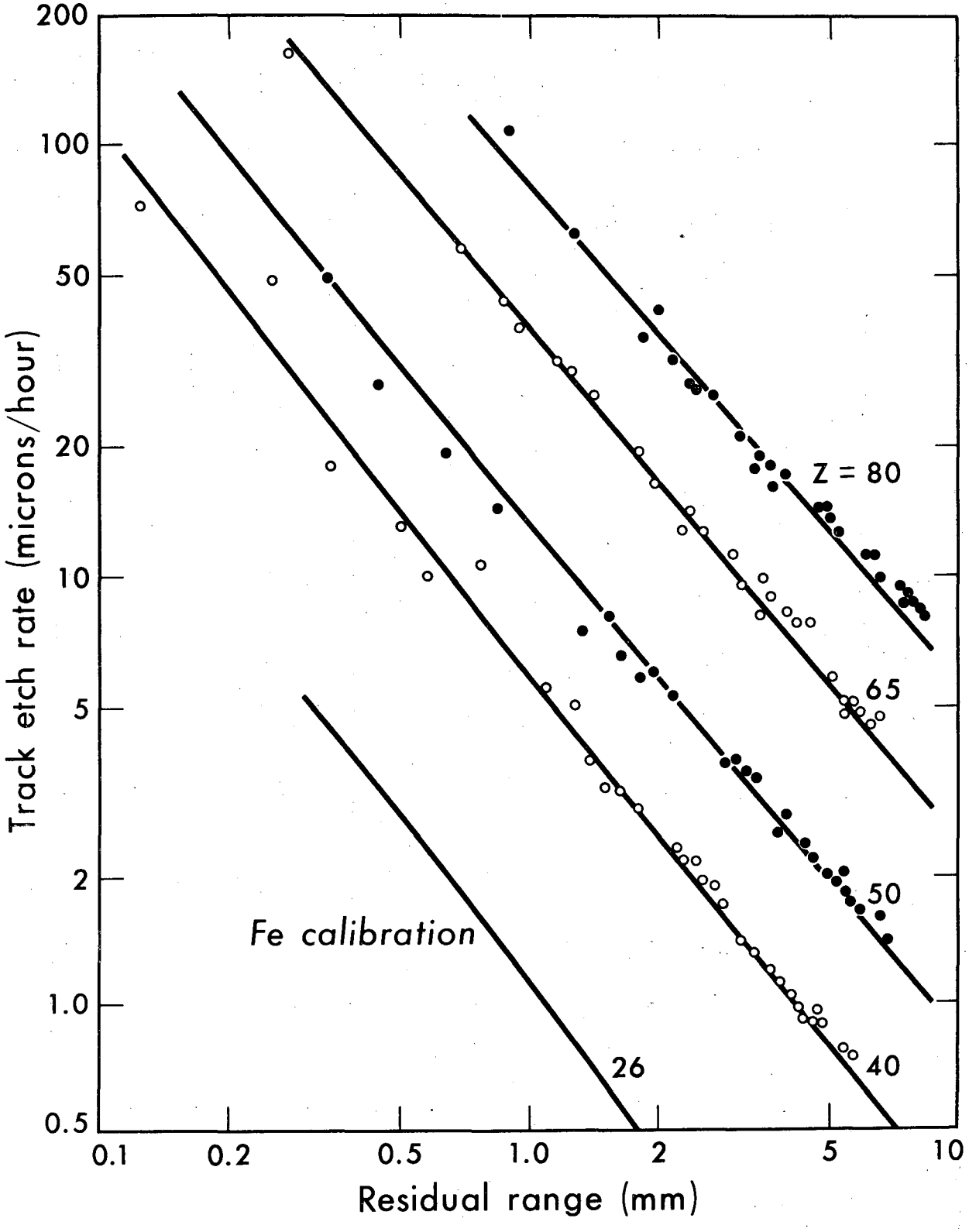

Fig. 6

XBL 784-8304

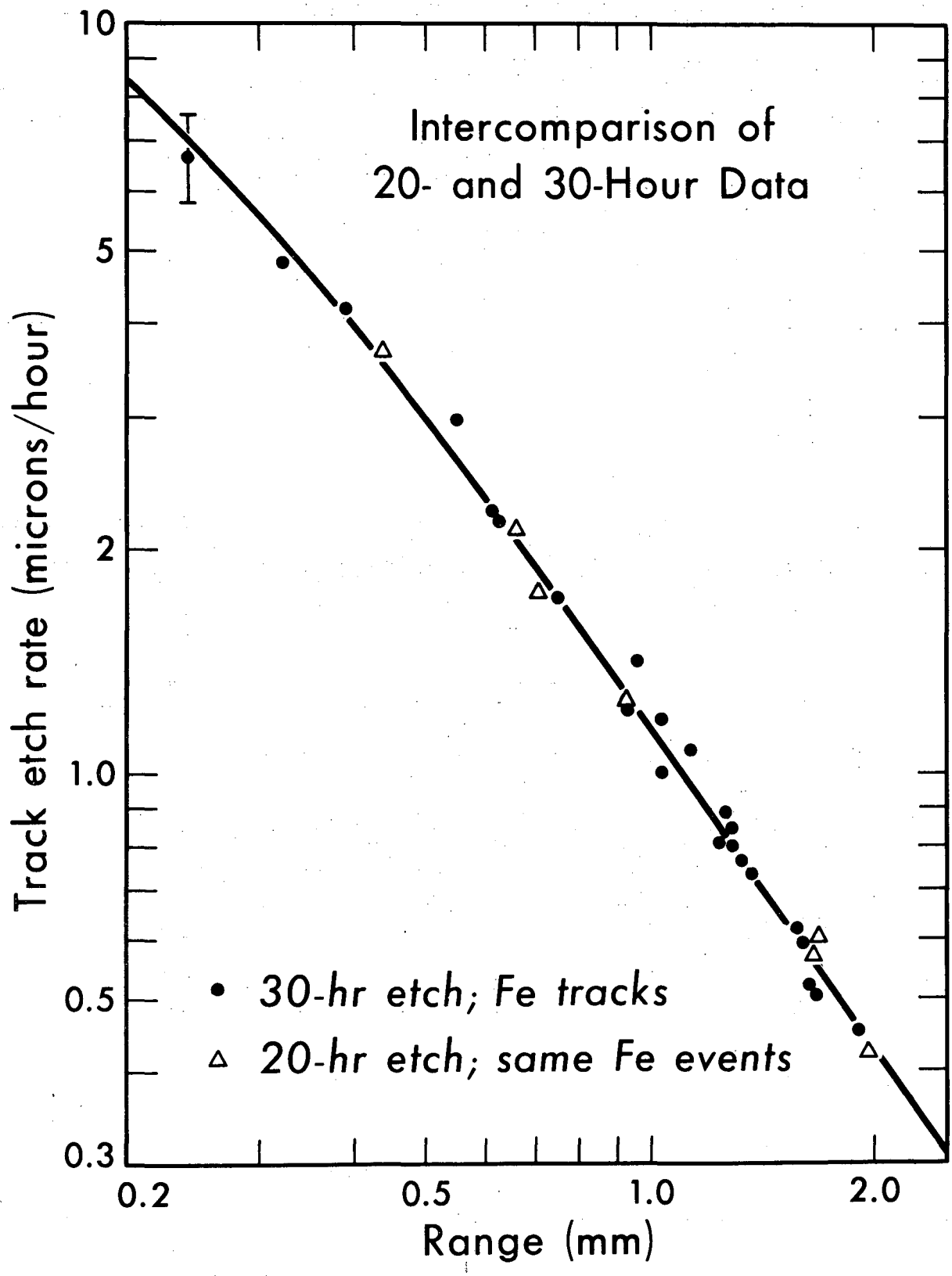

Fig. 7

XBL 784-8311

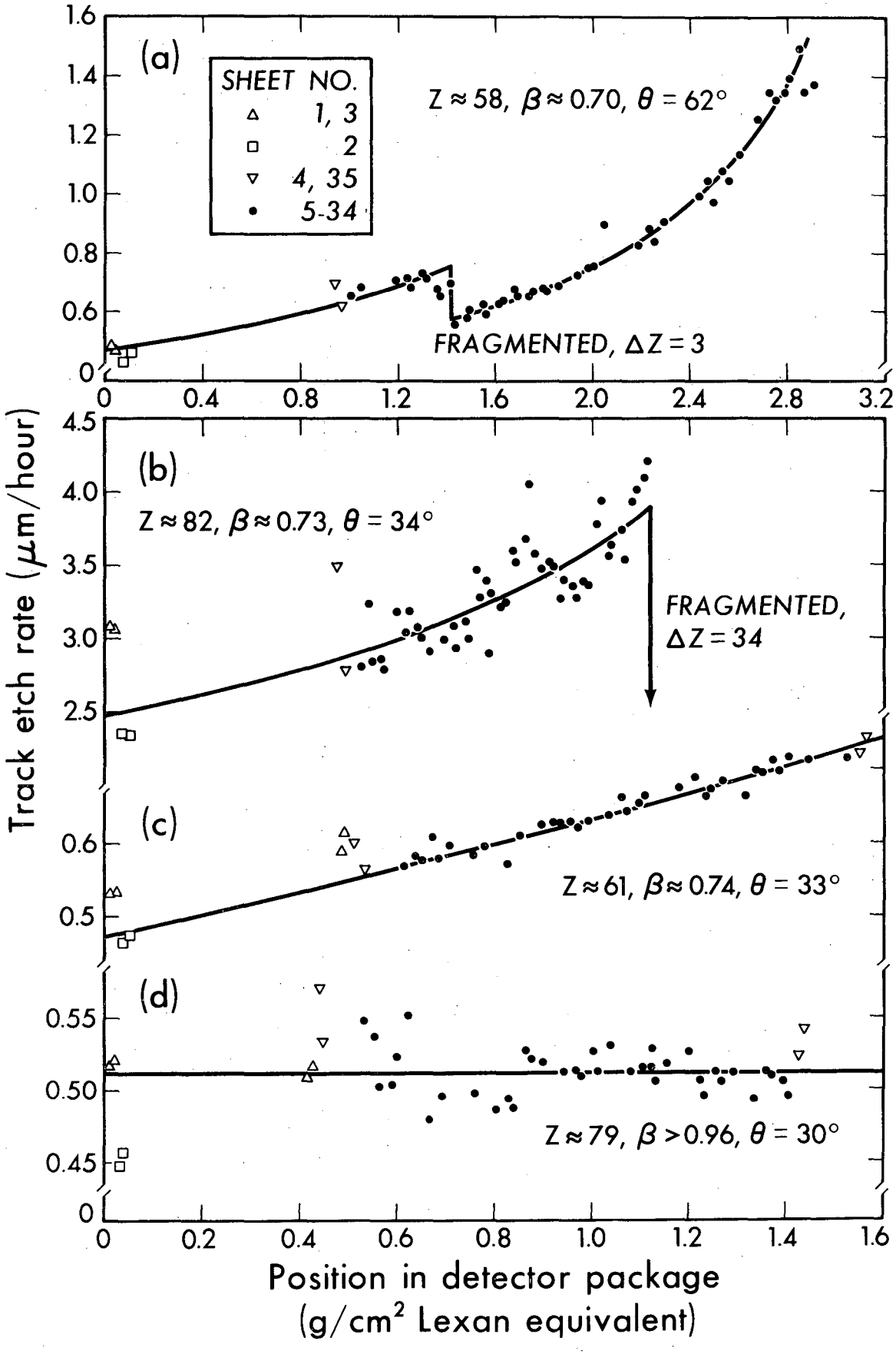

Fig. 8

XBL 784-8308

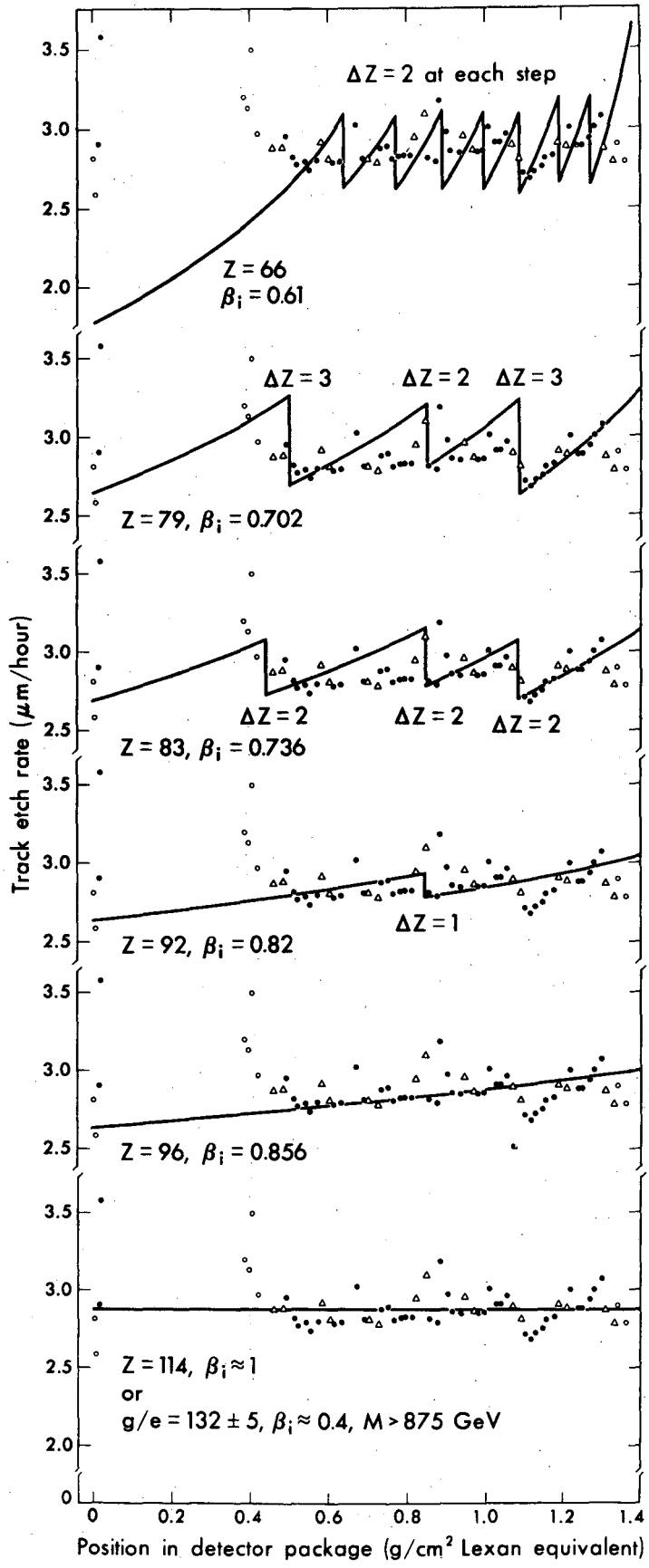

Fig. 9 XBL 784-8301

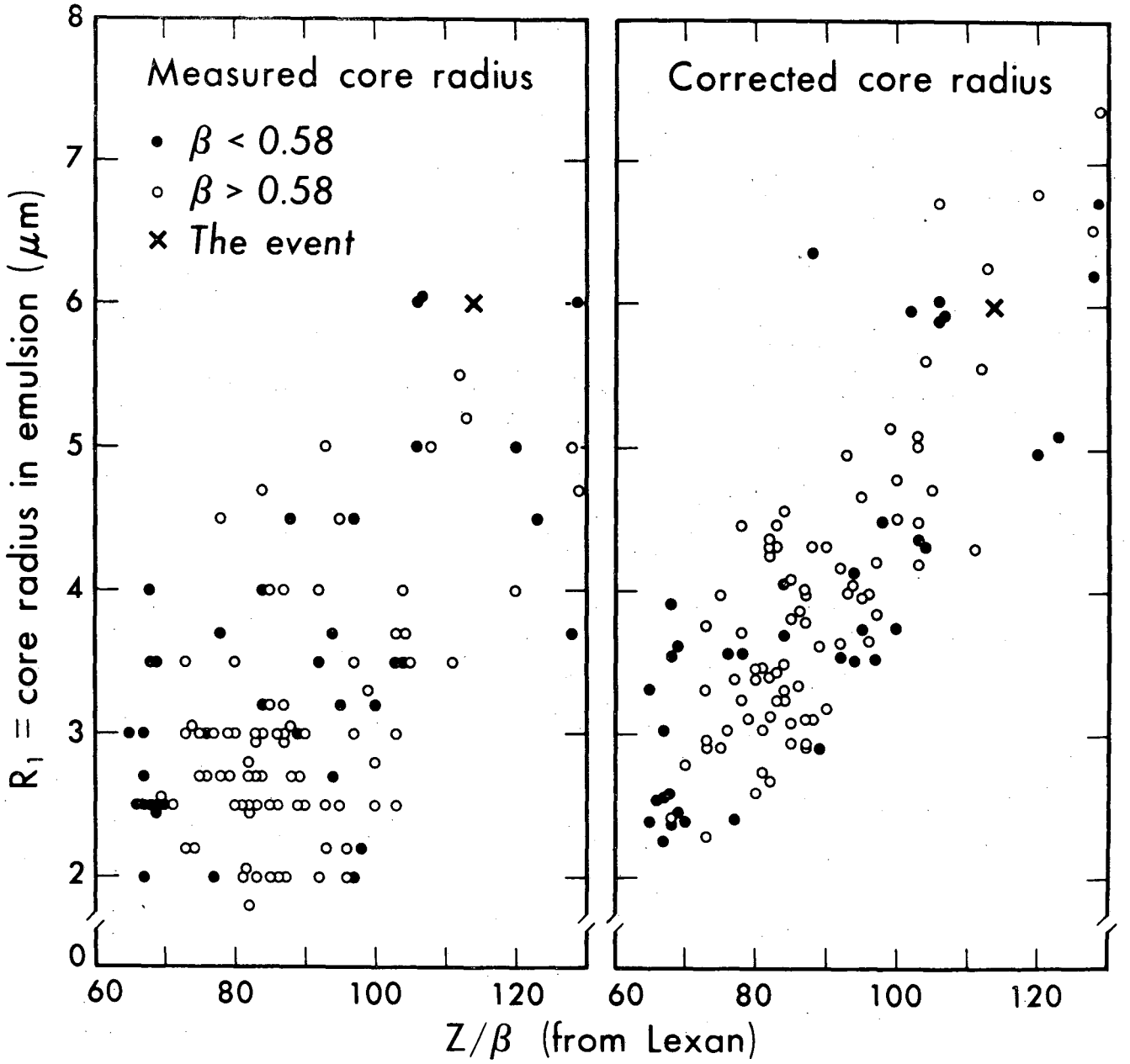

XBL 784-8309

Fig. 10

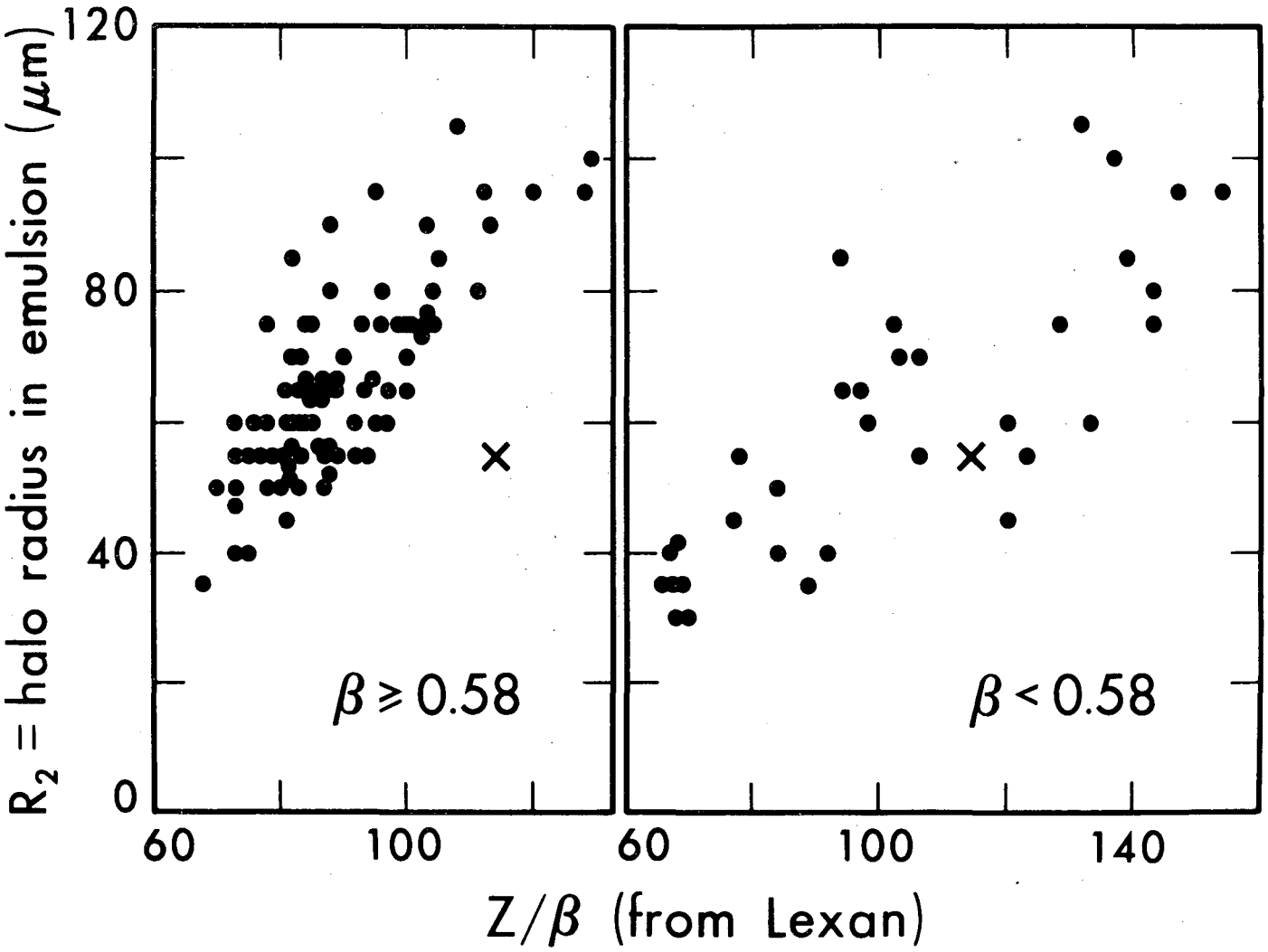

XBL 784-8307

Fig. 11

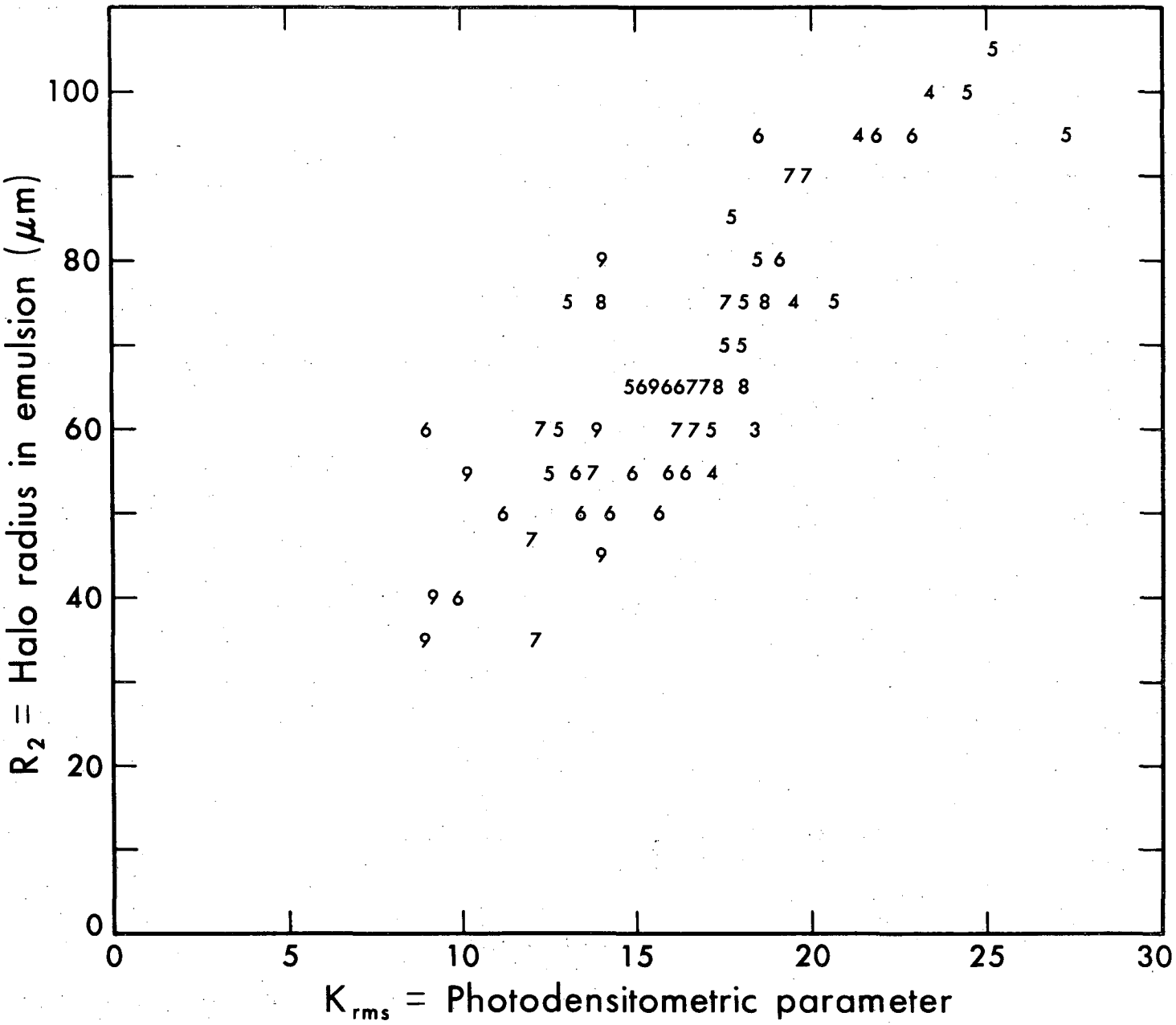

XBL 784-8310

Fig. 12

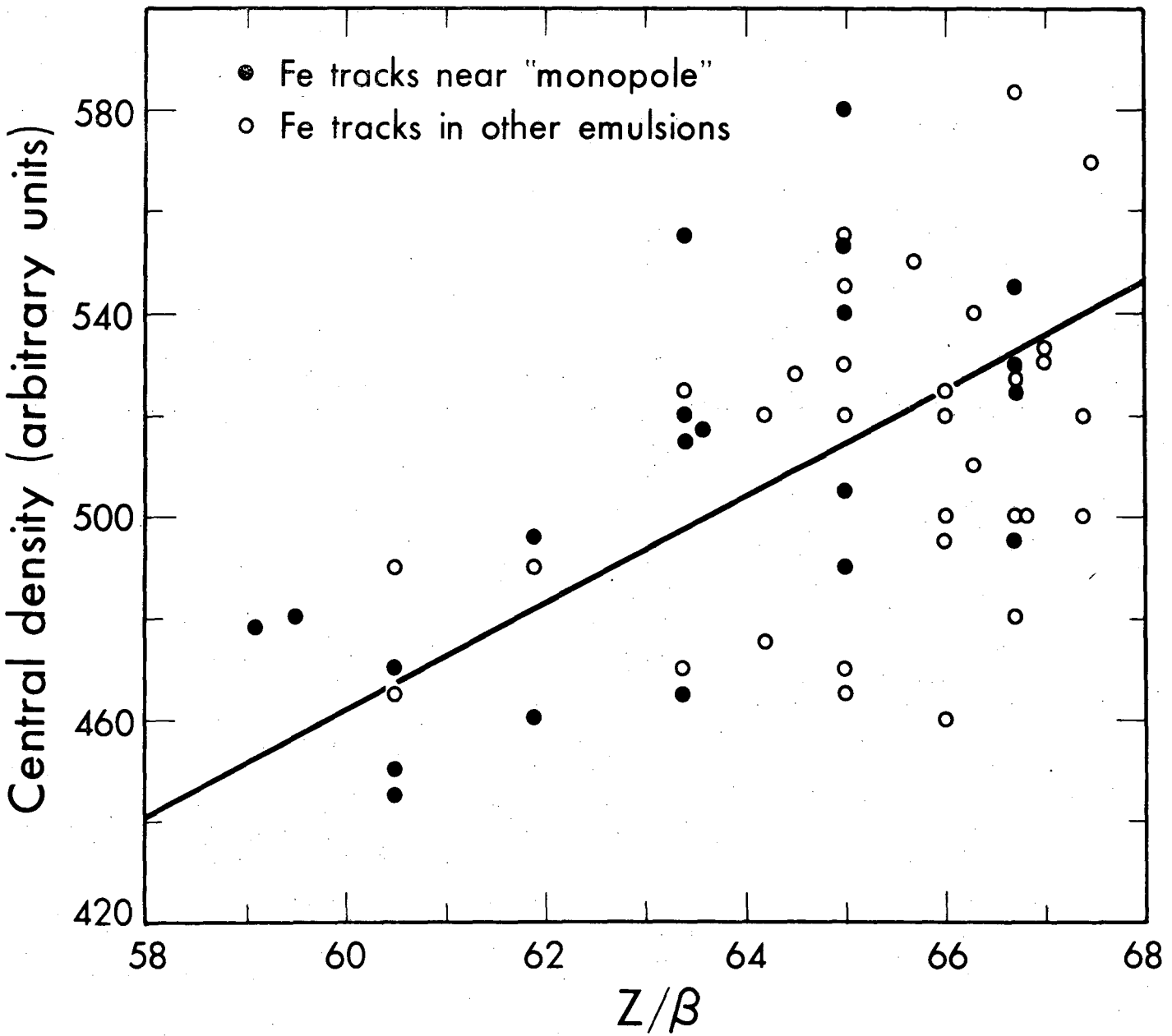
Fe tracks near "monopole"
Fe tracks in other emulsions
Central density (arbitrary units)
580
540
500
460
420
58
60
62
64
66
68
Z/β
XBL 784-8303

Fig. 13

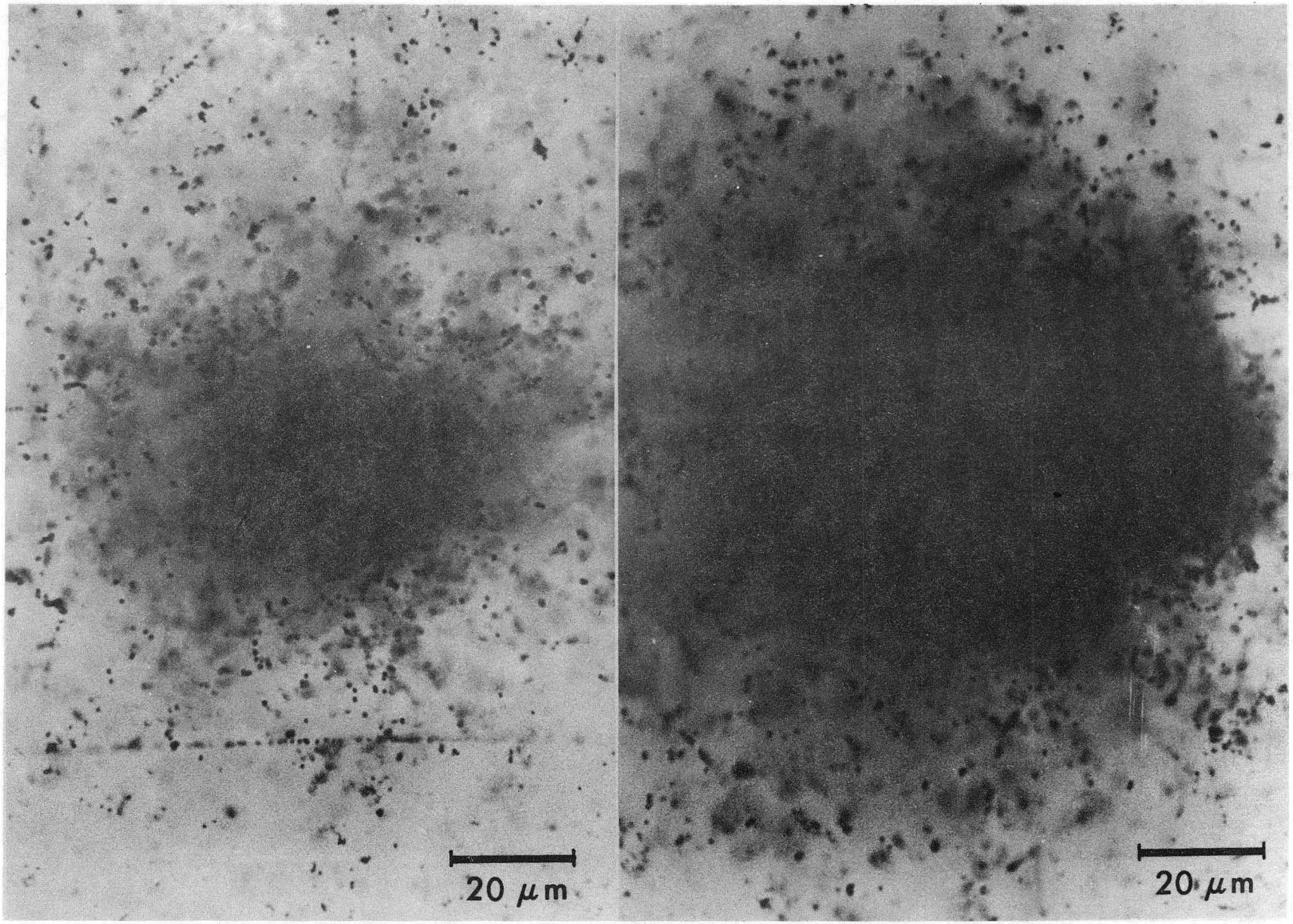

XBB 783-3218

Fig. 14

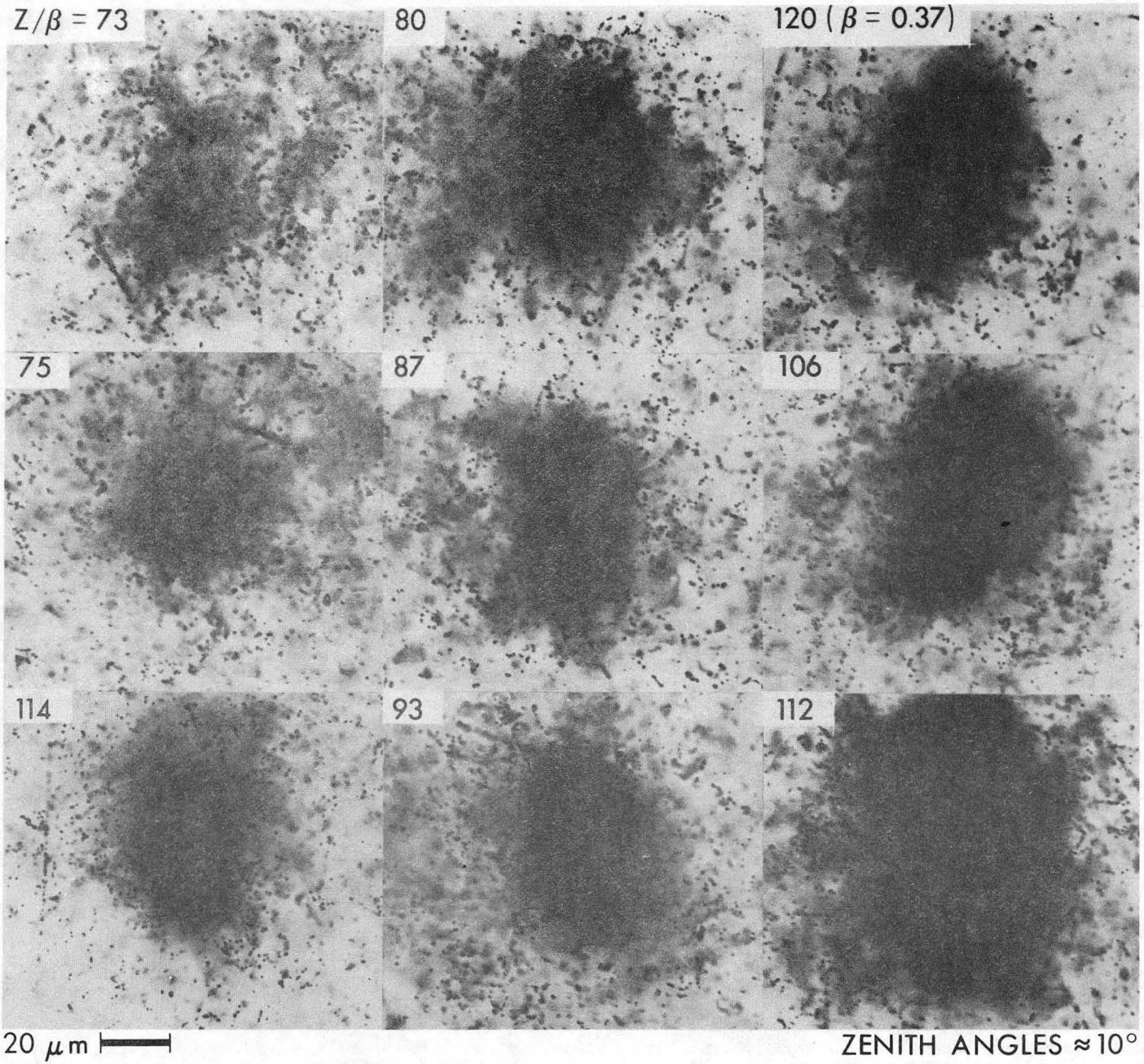

XBB 783-3216

Fig. 15

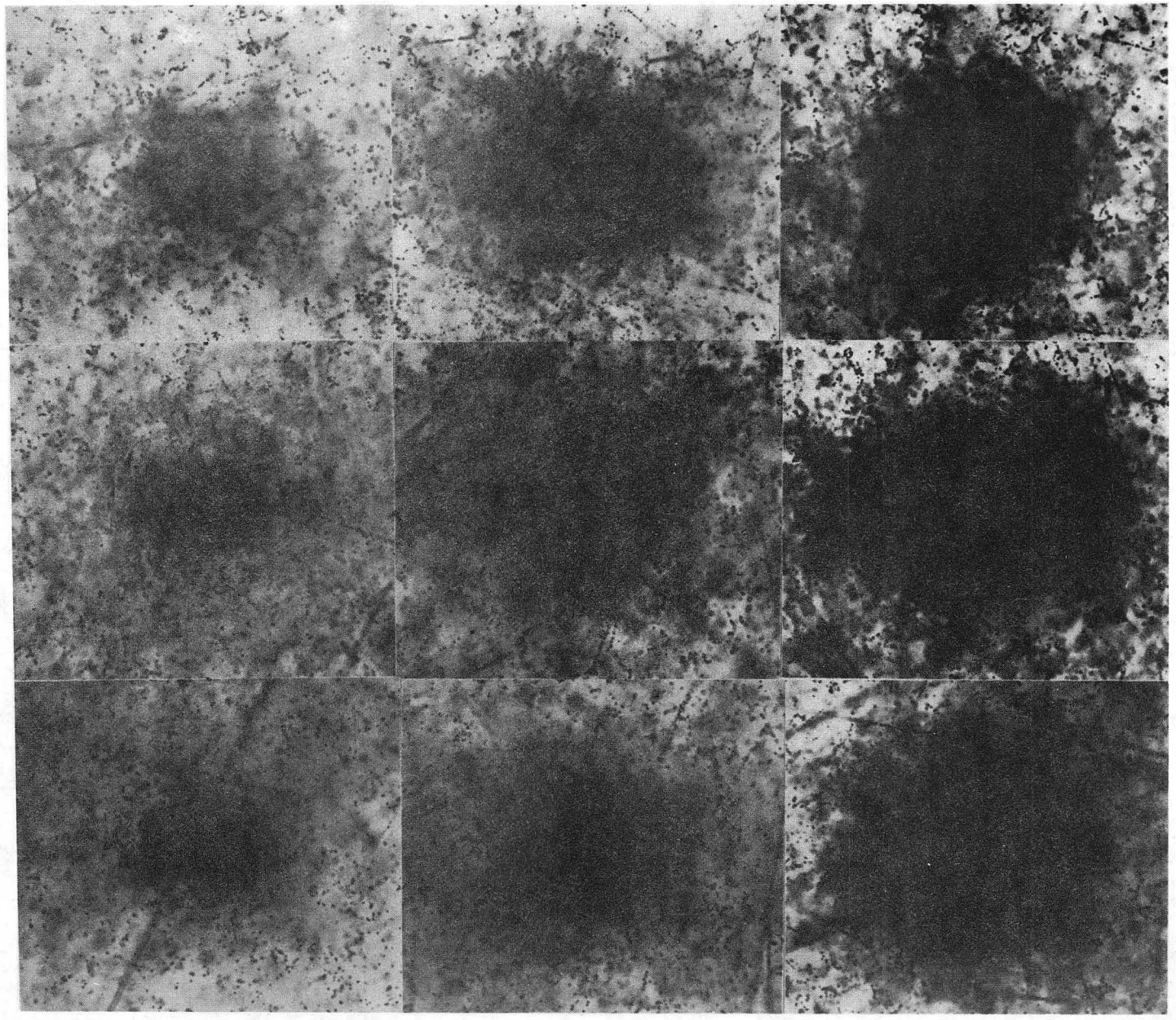

XBB 783-3217

Fig. 16

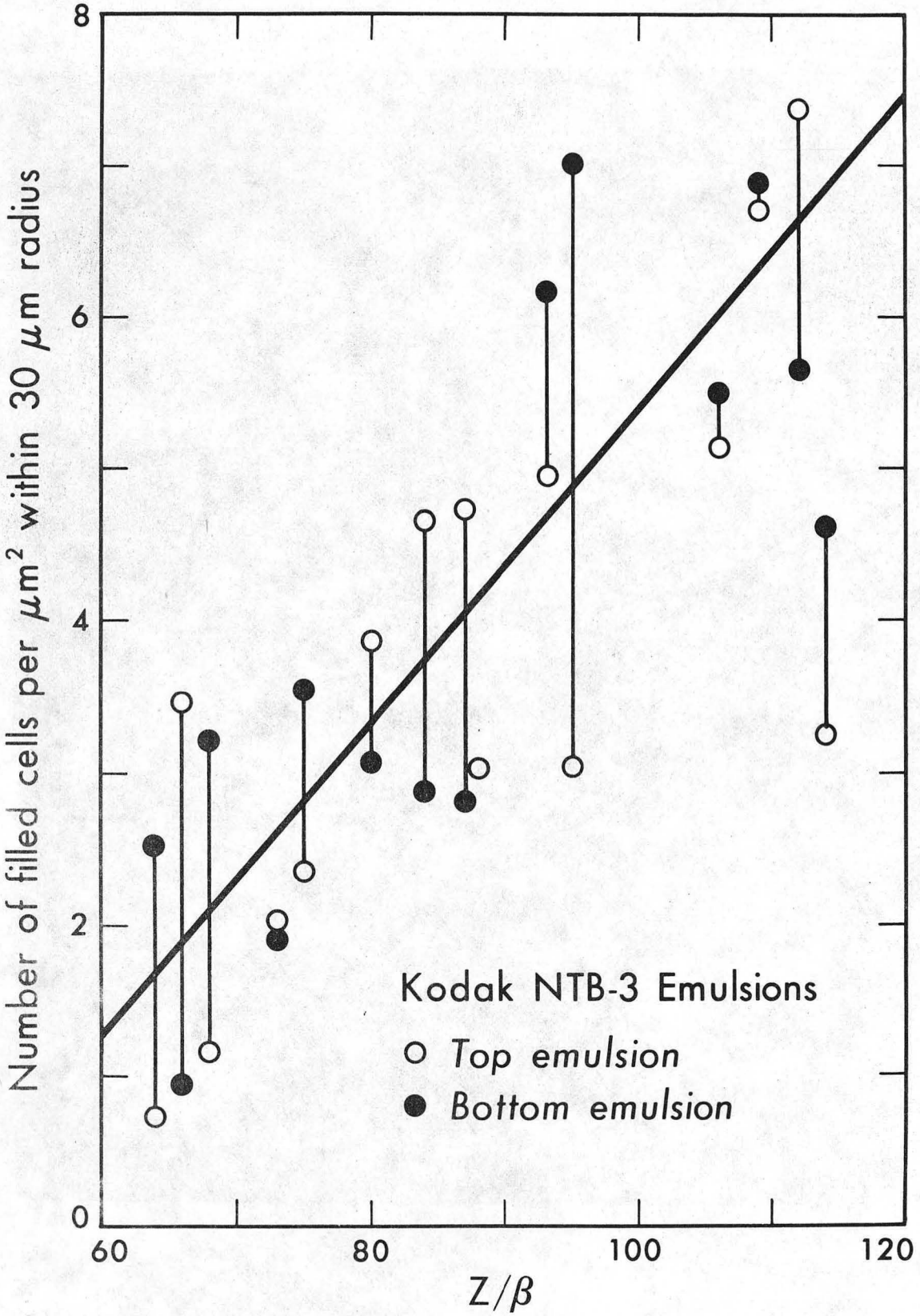

Fig. 17

XBL 784-8306

This report was done with support from the Department of Energy. Any conclusions or opinions expressed in this report represent solely those of the author(s) and not necessarily those of The Regents of the University of California, the Lawrence Berkeley Laboratory or the Department of Energy.

TECHNICAL INFORMATION DEPARTMENT
LAWRENCE BERKELEY LABORATORY
UNIVERSITY OF CALIFORNIA
BERKELEY, CALIFORNIA 94720